Figure 63: The 36-ft Parabola being lifted by crane into the transit mounting (Courtesy of ATNF Historical Photographic Archive: B2975-19 Image Date: 14 January 1953).

Figure 64 shows the aerial undergoing final assembly in its mount. The central track support is also visible in this photograph.

Figure 64: The 36-ft Transit Parabola in final assembly in its mounting (Courtesy of ATNF Historical Photographic Archive: 2975-21 Image Date: 14 January 1953).

In this configuration, and with the operating frequency of 1,420 MHz, the beamwidth of the aerial was theoretically 2º at the full width half-power points, but this was later measured using the Sun as a reference source to be 2.8º (Kerr et al., 1959). Figure 65 shows the measured radiation pattern of the main lobe compared to a Gaussian curve with the same width between half power points. The Gaussian curve is indicated by the solid line and the open circles show the actual measurements.

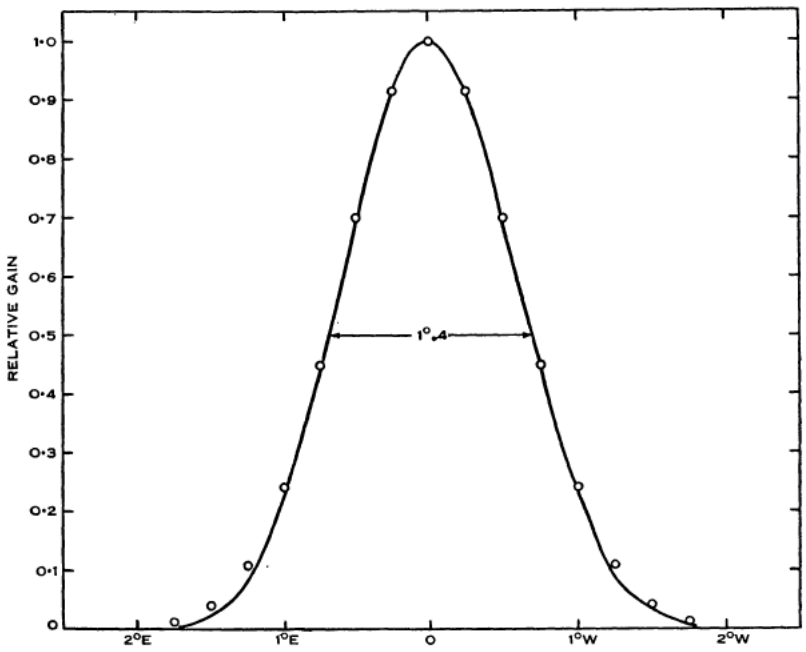

Figure 65: The measured shape (open circles) of the main lobe radiation pattern of the 36-ft parabola at 1,400 MHz compared to a Gaussian curve (solid line) (after Hindman and Wade, 1959: 260).

Despite the very robust mounting structure, structural distortions in the aerial framework and in the prime focus mounting could result in pointing errors of up to 1º and hence it was necessary to carefully measure the distortions at various aerial delineations so that corrections could be applied to position measurements. To do this, a small optical telescope was fixed to the aerial framework and the transit of stars at various declinations was observed. Direct measurements were also made using a sighting telescope. The original single pole prime focus mount proved too flexible and it was soon replaced by a tripod mount. The finished instrument ready for H-line observation is shown in Figure 66.

Figure 66: The 36-ft Transit Parabola ready for H-line observations (Courtesy of ATNF Historical Photographic Archive: 3170-2 Image Date: 14 January 1953).

The receiving equipment that had been used for the initial H-line detection and the first surveys was based on a receiver that was swept across a narrowband while rapidly switching between two adjacent frequencies (refer to Section 10.4.7 for a more detailed description of this equipment). This produced a modulated signal that was independent of the background signal; however, the modulated signal itself was very weak. This meant that long integration times were necessary to reach the required sensitivity and hence the frequency band in which the H-line was present could only be swept very slowly. To overcome this limitation, Pawsey proposed the construction of a new type of receiver (Kerr et al., 1954), the world's first multi-channel receiver (Kerr, 1984). Instead of sweeping the frequency band in which the H-line could be detected, Pawsey proposed the use of a fixed-frequency system. In this system a broad-band output covering the frequency band to be analysed was filtered into a number of parallel narrow-band channels which could all be displayed simultaneously. By comparing the mean noise levels in each narrow-band channel with the overall broadband it was possible to remove background noise from the signal. This allowed the whole frequency band covered by the broad-band input to be analysed and the line profiles

determined in a single integration period and meant that observations of the same sensitivity could be made much more rapidly that with the previous receiver.

The initial tests of the multi-channel receiver were made using only a limited number of channels. The first paper published based on observations using the new receiver design used only a single channel of 40KHz bandwidth (Kerr et al., 1954). A Superheterodyne design with double frequency change was used for the receiver. A local oscillator at 1,390 MHz was coupled to a high frequency mixer which then fed the first stage intermediate-frequency channel of 30 MHz. Both of these components were mounted at the aerial feed point at the aerial's prime focus where a flanged horn acted as the primary feed. In this configuration the aerial was horizontally polarised parallel to its east-west axis. A low frequency mixer, coupled to a 23 MHz oscillator, was then fed to the next intermediate-frequency channel of 7 MHz. At this point the overall bandwidth was 1.7 MHz. From this a 40 KHz section was selected for examination by a narrowband filter. By adjusting the two oscillators and the narrowband filter, which operated at 7 MHz, the receiver could be tuned to the zero beat frequency point, which corresponded to a receiver frequency of 1,420.405 MHz. In this way the receiver output provided a direct measure of the Doppler frequency components, either positive or negative, around the 'at rest' frequency of the H-line. These Doppler components were due to the radial velocity of the hydrogen producing the emission. This velocity was then manually corrected to take account of the Earth's rotation and orbit around the Sun, as well as the motion due to the Sun's orbit in the Galaxy, to arrive at a local standard of rest. Figure 67 shows a block diagram of the 'single channel' multi-channel receiver that was used in the initial observations and trials of the receiver.

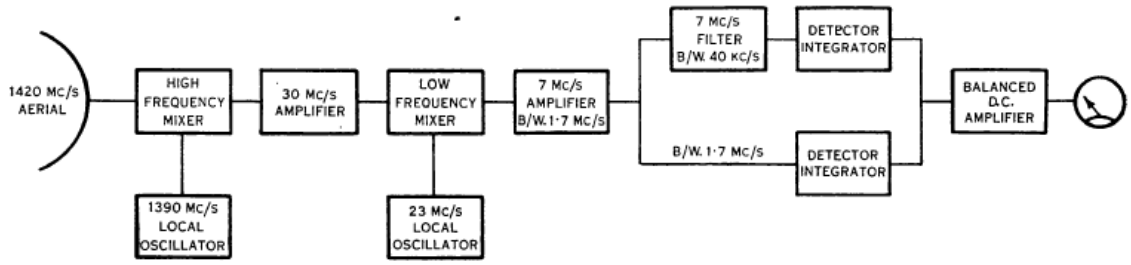

Figure 67: A block diagram of the "single-channel" multi-channel receiver prototype (after Kerr et al., 1954: 301).

In the original construction the single pole prime focus mounting had been replaced by three arms that were used to support the prime focus equipment, but this was modified in December 1953 to an even more rigid four arm system as shown in Figure 68.

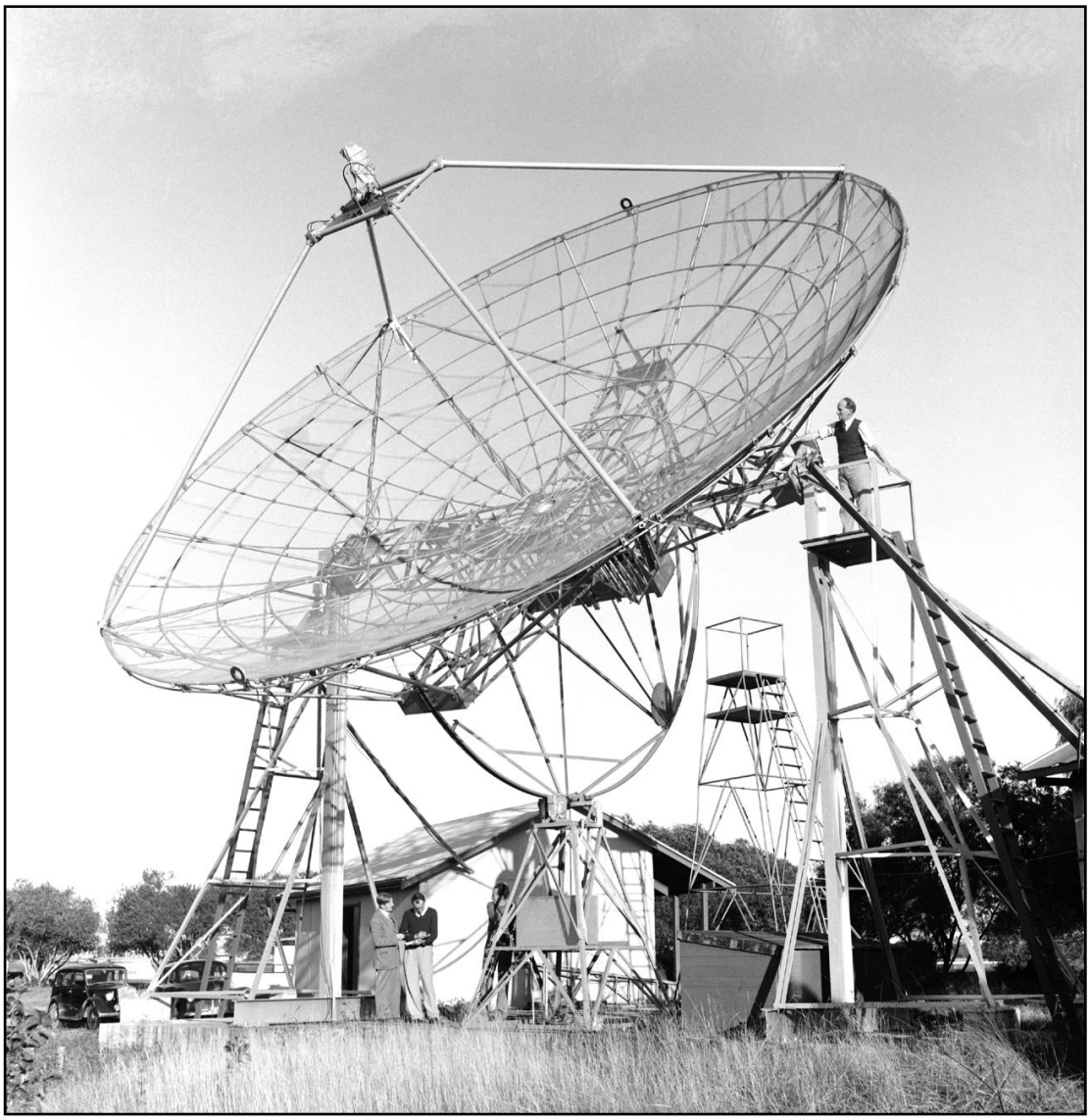

Figure 68: The 36-ft aerial showing the four-arm prime focus supports (Courtesy of ATNF Historical Photographic Archive: 3679-1 Image Date: 1 June 1955).

As part of the modifications, the prime focus feed was shifted outward by about 1-ft to its correct focus point. This improved the gain of the aerial by nearly 20% and virtually eliminated the side-lobes (Kerr, 1954b).

The new receiver also required a different type of observing technique to that used in the earlier H-line studies. The aerial was positioned at a fixed declination and then the sources were allowed to drift through the aerial beam courtesy of the Earth's rotation. A continuous recording was made in the multiple frequency channels and the H-line profiles derived by fitting together a series of these recordings. For the early observations using the 'single' channel prototype receiver these observations needed to be repeated for each different frequency channel so that the line profile could be derived. By using multiple channels

that gave sufficient frequency coverage to encompass the observed radial velocities, a 1º strip of the sky could be scanned and the line profile to be directly derived as a function of right ascension and declination.

Figure 69 shows an example of the H-line profile produced by the receiver. The receiver was tuned to the rest frequency of the Hydrogen emission, so the frequency shift from the central frequency was a direct function of radial velocity. Figure 69 shows the measurement at the multiple frequency channels (dots). These are fitted by two Gaussian curves to produce the profile.

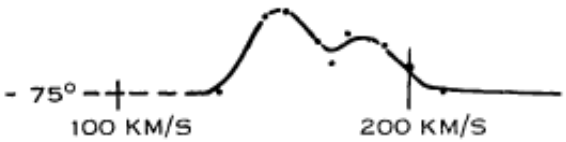

Figure 69: Example of the H-line profiles produced by the prototype multi-channel receiver (after Kerr et al., 1954: Adapted from Figure 3: 303).

The prototype receiver was used to perform a survey of neutral hydrogen in both the Large and Small Magellanic Clouds. These were the first observations of neutral hydrogen from extragalactic sources. Getting the original receiver to work effectively across multiple channels had proved to be extremely difficult. In mid 1953, J.D. Murray was asked by Pawsey to see what could be done with the receiver design. Murray recalled that this was not a happy task and after 6-7 weeks work determined that the original receiver design would never work and would need to be changed to a switched design (Murray, 2007). At this point Murray returned to the laboratory and began work on an entirely new receiver design that would become the 48-channel receiver used at the Murraybank field station.

Hindman and Kerr persisted with their receiver and ultimately modified its design significantly. Instead of switching between two frequencies a continuous comparison approach was used whereby two channels were connected to opposite sides of a differential D.C. amplifier. Figure 70 shows a block diagram of the modified later stages of the multi-channel receiver. The channels could be stepped across the desired frequency band allowing a one channel overlap to produce a continuous line profile. To produce full coverage of a broad profile in the Galaxy required eight to ten observing days (Kerr, 1984).

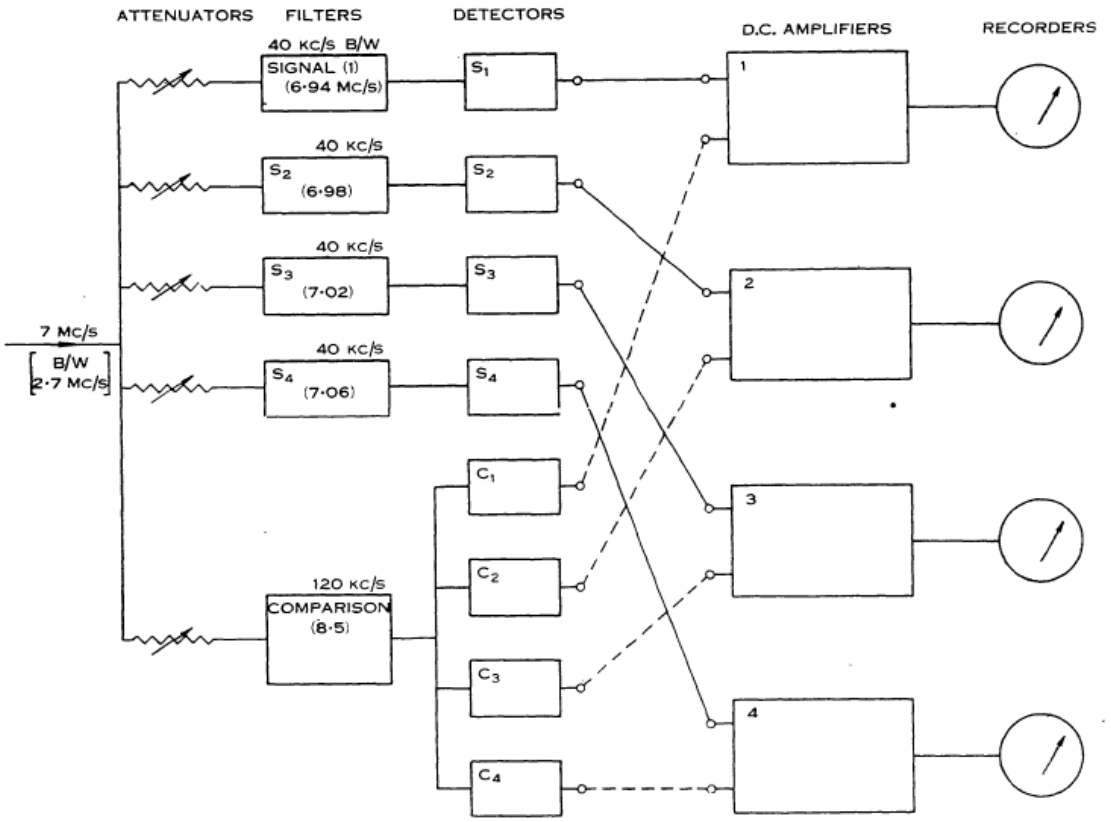

Figure 70: The modified late stages of the four-channel receiver (after Kerr et al., 1959: 274).

These receiver modifications overcame the issues inherent in the swept and switched type of receivers, namely the difficultly of maintaining a flat baseline while tuning over a wide frequency band and the precise equalisation of the local oscillator and the front end performance in the two switch positions. However, the new design introduced a new issue. Because the signal comparisons used different parts of the band-pass for comparison, they could be subject to differential gain drift. This required very careful stabilisation of the components. To check for drift and to establish a zero level, the aerial was pointed at a 'cold' part of the sky, in this case the South Celestial Pole, after each scan across the Milky Way. The output signal produced was of the 'picket fence' type reminiscent of the early solar measurement made using the 16-ft × 18-ft Paraboloid at Georges Heights (see Figure 30 for an example of the output signal). Figure 71 shows an example of the four-channel output along three constant-declination tracks across the Milky Way. The 'P' symbol indicates where the aerial was pointed at the South Celestial Pole.

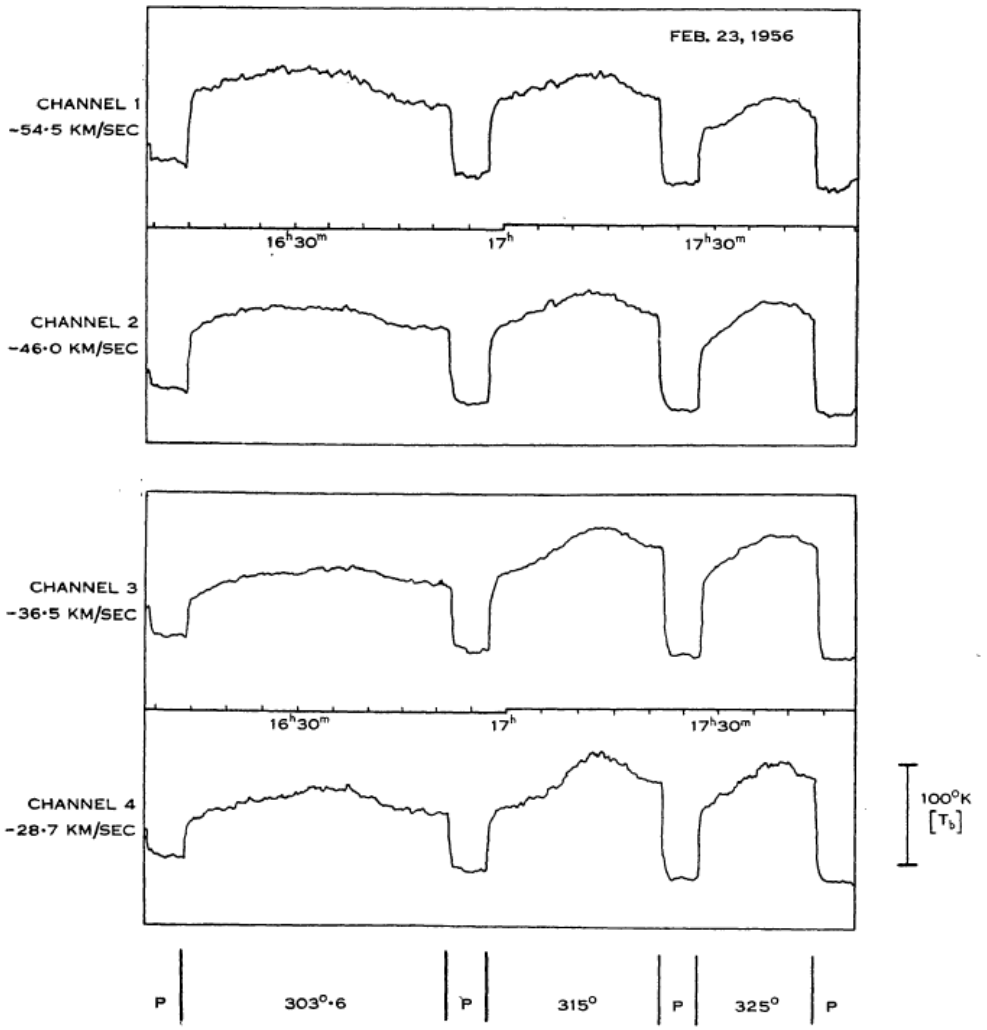

Figure 71: Example of the "Picket Fence" effect where the 36-ft aerial was pointed at the south celestial pole between declination track scans (after Kerr et al., 1959: 280).

In 1955 Piddington and Trent, in a departure from H-line work, used the 36-ft Parabola to conduct a survey at 600 MHz between declination 90º South and 51º North (Piddington and Trent, 1956b). They replaced the multi-channel receiver with a 600 MHz receiver which was fed by a single dipole and reflector plate mounted at the prime focus. The receiver was essentially identical to that used by Piddington and Minnett for their earlier survey work at 1,210 MHz using the 16-ft×18-ft Paraboloid (see section 10.4.1 and Figure 33 for detailed description). A 6-ft parabolic aerial directed at the south celestial pole was used to provide the reference source for the main aerial and is shown in the right foreground of Figure 72. This was a major undertaking as the beam width of the aerial at the half power points at this frequency was just over 3º. Observations were made by setting the aerial at a fixed declination and then allowing the beam to drift in right ascension as the Earth rotated. The declination was then stepped by 1¼ degrees and the next scan taken. The whole process was then repeated at least twice to remove instrument effects and external interference and this achieved almost full sky coverage from -90º to +51º. The results of this survey were published in 1956 (Piddington and Trent, 1956b).

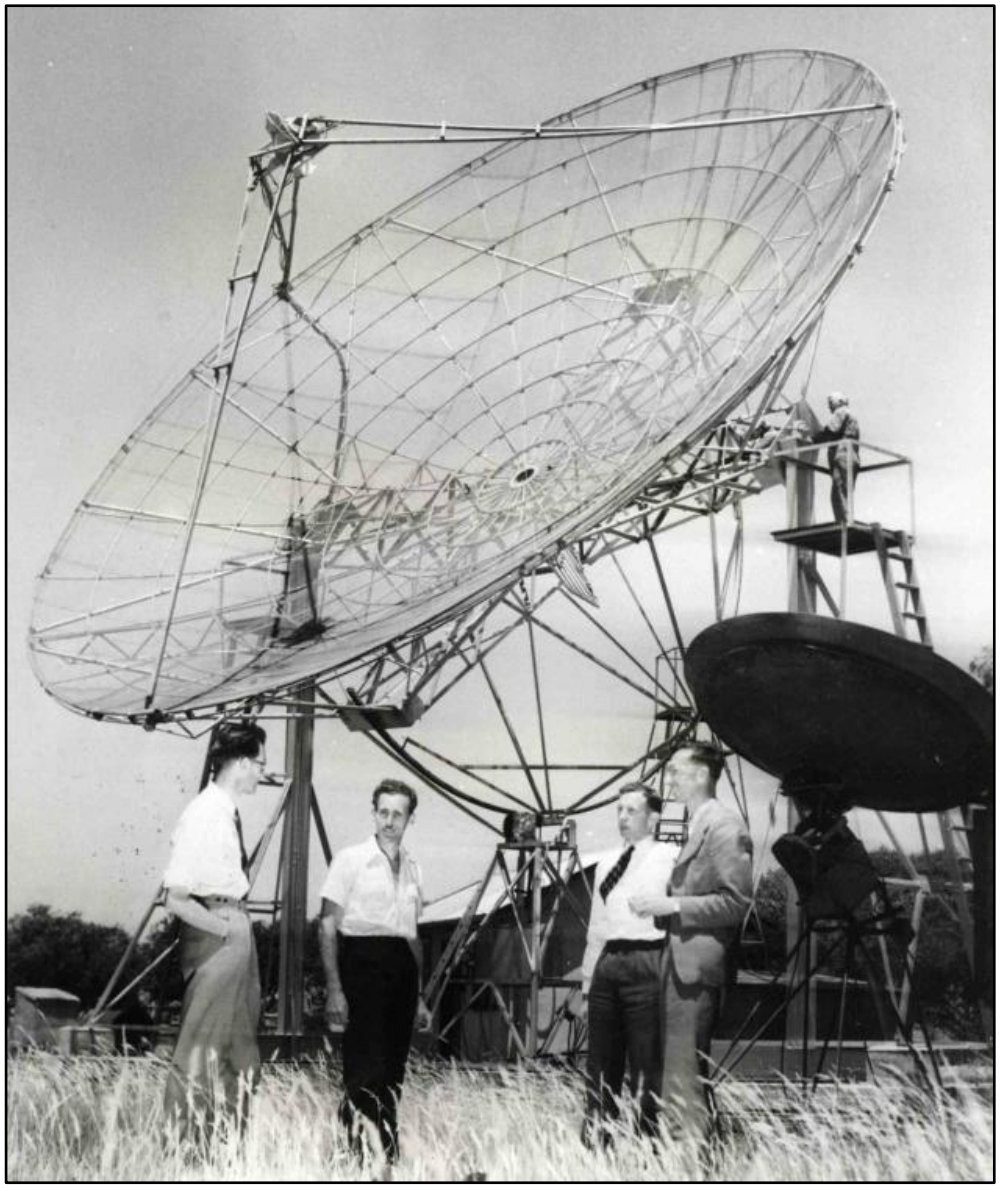

Figure 72: The 36-ft transit parabola with the 6-ft reference aerial in the right foreground. The people in the image are from left to right Kerr, Hindman, Robinson and Pawsey (Courtesy of ATNF Historical Photographic Archive)

Having got the multi-channel receiver working, Hindman and Kerr began work on the survey of the southern Milky Way. This survey work led to collaboration with the Dutch Leiden Observatory to produce a composite diagram of the spiral arm structure of our galaxy (Kerr et al., 1957). The work also was a major component of the data used to determine a new system of galactic co-ordinates based on a newly agreed centre and plane for the galaxy that was adopted by the IAU General Assembly in 1958.

With the completion of observations for the southern H-line survey, Hindman and Wade adapted the modified receiver to allow broadband detection of radiation around 1,400 MHz. They did this by modifying the receiver so that it accepted two bands, each 30 MHz away from the first stage oscillator

frequency of 1,393 MHz. This way they could exclude the H-line emission signal from investigation of the broadband continuum. Figure 73 shows a block diagram of the modified receiver.

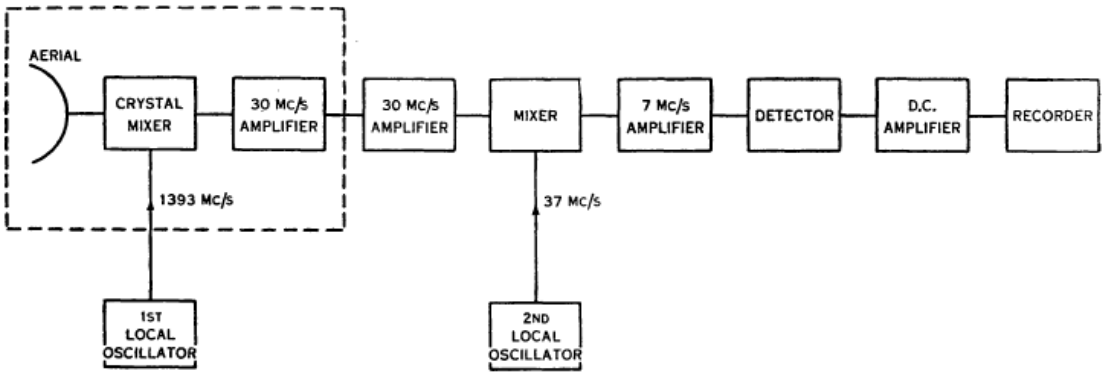

Figure 73: Block diagram of the modified receiver to allow broadband detection around 1,400 MHz (after Hindman and Wade, 1959: 261).

The modified receiver was used to investigate the Eta Carine Nebula and Centaurus A.

In 1956 a new field station was opened at Murraybank and the ongoing Radiophysics H-line research was transferred to this field station (Orchiston and Slee, 2005a). At Murraybank a fully-steerable 21-ft Parabola (Figure 74) was installed overcoming the issues with operating a transit instrument for the survey work. The Murraybank aerial was a modified design of the "Chris-Cross" aerial with increased rigidity and an increase in diameter (Pawsey, 1955b).

In a report on the projected future programme for the Radio Astronomy Group on 29 June 1959 it was noted that as the southern Milky Way H-line survey was now completed, the 36-ft Parabola and associated hut would be held in reserve as a test bed for receiver testing until such time as the new equipment facility being developed at the new Radiophysics Headquarter at Epping was completed (Pawsey, 1959a).

In the Annual Report for the Division for the year ended 30 June 1958 it was noted that the development of masers (Microwave Amplification by Stimulated Emission of Radiation) was underway in the U.S. (Bowen, 1958). It also noted that this type of receiver would be most useful for 21-cm research and therefore a small group had been organised to investigate. This group consisted of F.F. Gardner, D.K. Milne and G. Bogle. Masers were considered an offshoot of work in the field of low-temperature paramagnetic resonance in which the Division of Physics had a large body of experience and the maser development had revived an interest in 'parametric' amplification which offered low noise amplification without the engineering complexities of the maser. The report also noted that an Officer [B. Robinson] had been stationed at Leiden where work on masers for radio astronomy was underway. In 1958, an operational maser receiver was constructed and tested at Potts Hill using the 36-ft Transit Parabola (Milne

and Whiteoak, 2005: 33). This was one of the first operational masers in the world. The maser used liquid helium for cooling and this proved to be impracticable for operations at Parkes and so further development was abandoned in favour of using a 20-cm nitrogen-cooled parametric amplifier (ibid.). The maser trials were the last experiments performed using the 36-ft Parabola at Potts Hill.

Figure 74: The 21-ft Parabola at the Murraybank field station (Courtesy of ATNF Historical Photographic Archive).

10.4.8. Mills Cross Prototype (H)

After his experiences in using two-element and three-element interferometers, initially at Potts Hill and then more extensively at Badgerys Creek field station during 1950 to 1952, Mills was looking for a way in which he could overcome some of the limitations inherent in this type of interferometer. Clearly a traditional parabola pencil beam instrument of sufficient size to produce high resolution would be suitable, but this would have been prohibitively expensive to construct.

One of the main issues Mills had been dealing with at Badgerys Creek was the problem that the small spacing of the interferometer aerials required long periods of integration and therefore the measurements suffered from gain fluctuation in the receiver. It was while exploring a solution to overcome this problem that Mills recalled:

> "I had begun to look for a better alternative when I received some unintended assistance from Cambridge. News came through the grapevine that a revolutionary system had been introduced there but it was all very hush-hush and no details were known; It was believed that it involved a modulation of the interference pattern. This seemed to be just what was needed. A little thought suggested modulation by interchanging maxima and minima on the interference pattern by switching phase and using a synchronous detector, as in the Dicke system. The necessary equipment was built and it worked very well. Later I found that this was precisely the system used at Cambridge, the only difference being their use of a hardware switch in the antenna feed lines whereas I had used an electronic switch following the preamplifier." (Mills, 1984: 149).

Using the new phase switched interferometer at Badgerys Creek Mills soon discovered another major issue with using spaced interferometers for survey work. Many of the sources resolved at the short spacing bore no resemblance to those detected at the longer spacing. Mills determined that this was most likely caused by the sources being extended in nature rather than being point sources. He determined that this was causing the confusion of the interference patterns.

Mills believed that sensitivity was not the issue for the source survey work; rather, high resolution was the key requirement. As he has stated:

> "By then, I knew that collecting area was relatively unimportant, the important thing was a large overall size to give high resolution. As a filled array seemed wasteful, I first looked at various passive configurations such as crosses and rings, but these all suffered from high side-lobe levels. Suddenly it occurred to me that by combining the phase-switch, which I had used on the interferometer, with a crossed array the side-lobe problem would be substantially reduced." (Mills, 1984: 151).

Mills (1984) has commented that there was a degree of scepticism within Radiophysics that the idea of the phase switched cross array would actually work. This was an example of some of the rivalry that was beginning to emerge between researchers at the major field stations. When asked if there was actually some opposition to building the cross array, Mills later commented:

> "Oh, well, that I think this was part of the Pawsey-Bowen camp division. When I put it [the cross array] up Bolton was very antagonistic and thought it wouldn't work at all. In fact, he convinced Bowen of this, who I remember told me quite clearly and unequivocally that it couldn't possibly work. However, Pawsey was

behind me and so we had to build a small experimental model first, just to show that it would work, which it did." (Bhathal, 1996a).

Ultimately it was determined that a prototype of the new array should first be constructed at Potts Hill to test the concept before moving to a full scale deployment. In hindsight this proved to be a useful undertaking as considerable experience was gained that was later applied to construction of the full-scale cross at the Fleurs field station.

The prototype array was built by Little in consultation with Mills. Govind Swarup also spent three months working with Little and Mills on the development of a phase shifter for the array (Swarup, 2006: 24). The array was designed to operate at a frequency of 97 MHz and as such used an array of 24 folded dipoles. These were arranged in two arms which were oriented north-south and east west as shown in Figure 75.

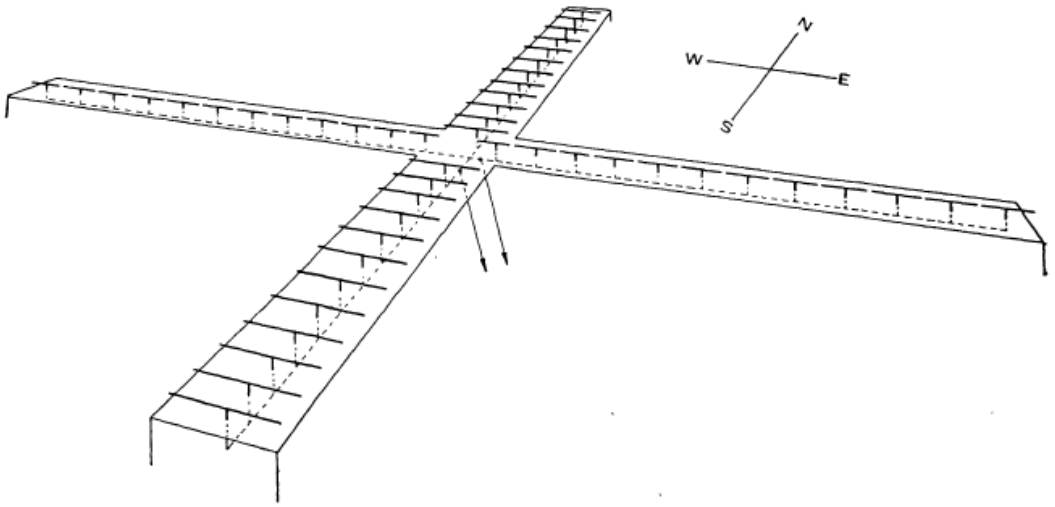

Figure 75: Diagram of the dipole arrangement of the prototype Mills Cross array (after Mills and Little, 1953: 275).

Each arm of the cross was 120-ft in length. The response of the combined arms produced a pencil beam with a beamwidth of 8º. The dipoles were backed by wire mesh suspended below the dipoles to act as a reflective surface as shown in Figure 76.

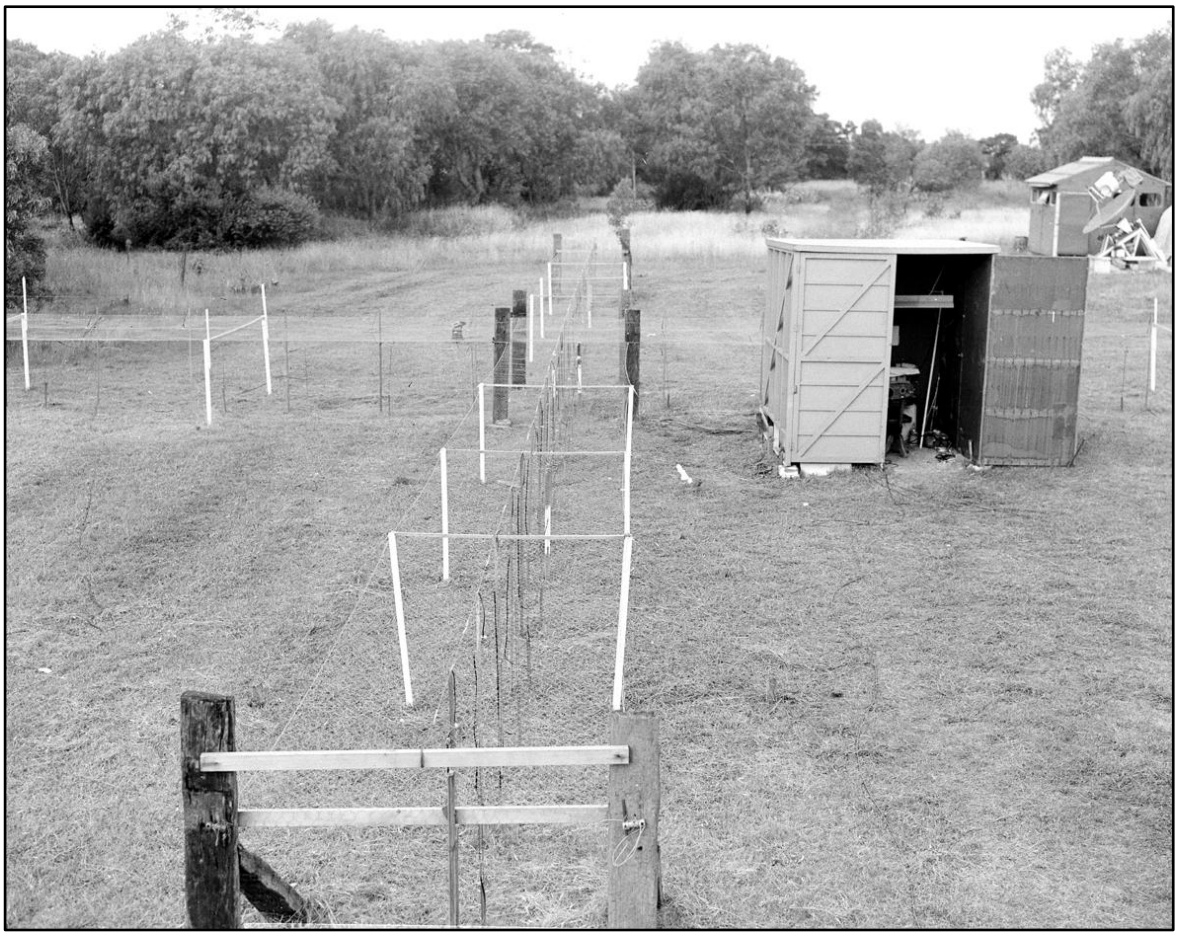

Figure 76: A close up view of the prototype Mill Cross at Potts Hill (ATNF Historical Photographic Archive: B3064-3 Image Date: 21 April 1953).

The line feeds for the dipole consisted of a two-wire transmission line that ran the length of each array, terminated at one end by matching resistors and the other leading to the common centre of the array. Figure 77 shows the arrangement of the dipole feeds.

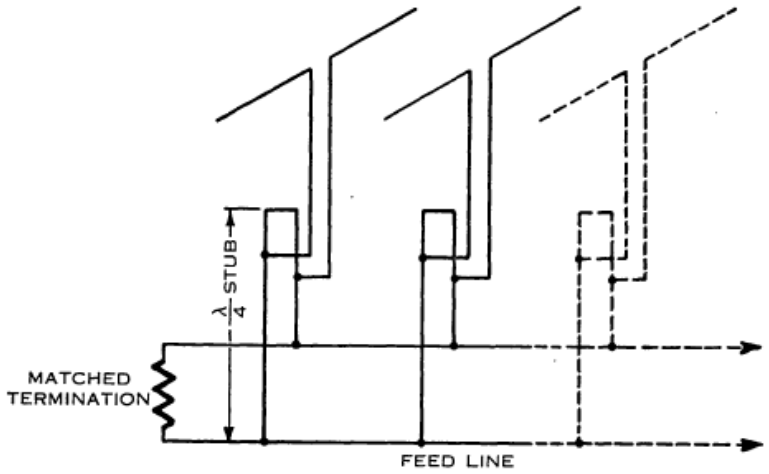

Figure 77: The line feed arrangement used on the prototype Mills Cross array (after Mills and Little, 1953: 276).

The pencil beam could be steered in declination by changing the relative phases of the currents in the dipole arms by changing the points of connection of the stubs to the line feeds. The output of each arm was first fed to a preamplifier and then combined through a phase switching arrangement; from there the signal was amplified, passed to a phase sensitive detector and then recorded. Two outputs were recorded, the phase-detected output and also the receiver output level. Calibration marks were inserted in the output record every twenty minutes by switching the preamplifiers to cold resistors for 1 minute. Figure 78 shows an example output recording of the Sun passing through the pencil beam of the array. The open dots in the figure show the computed polar diagram of the array.

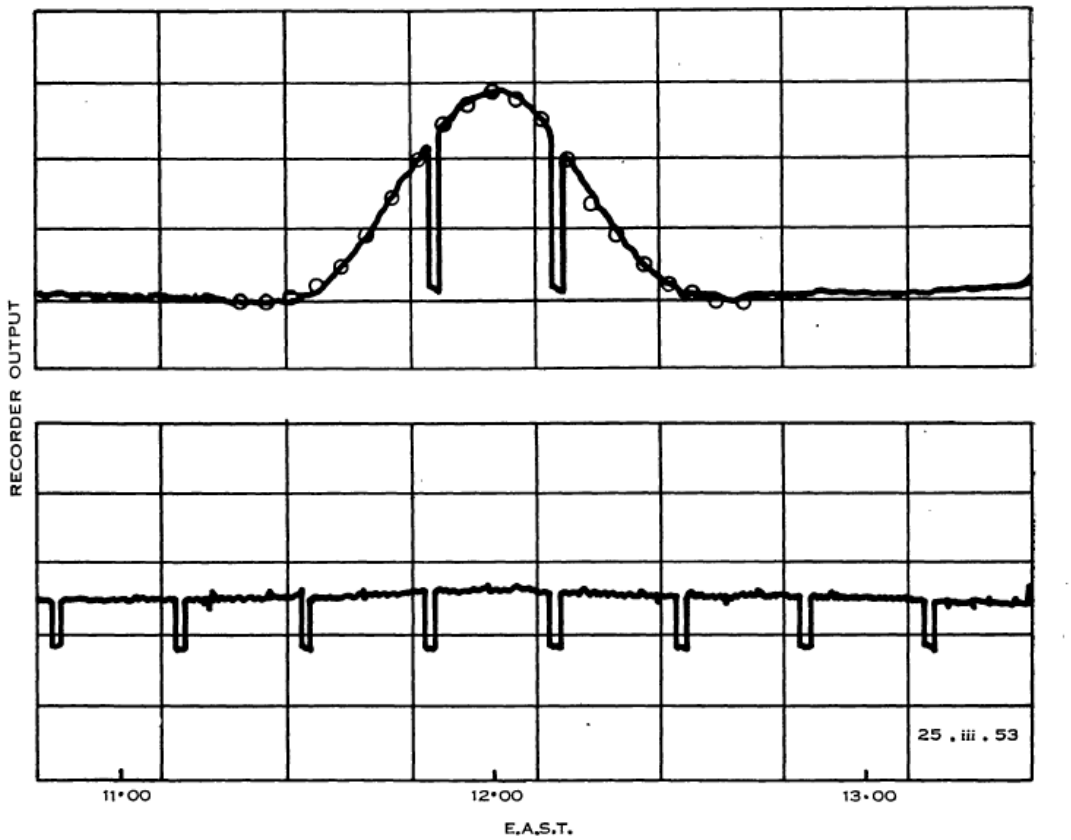

Figure 78: Example output recording of the Sun passing through the pencil beam of the prototype Mills Cross. The upper graph shows the phase-detected output while the lower graph show the receiver output level (after Mills and Little, 1953: 277).

Although the crossed array was constructed as a proof of the concept, it did produce the first radio detection of the Large Magellanic Cloud. Figure 79 shows the prototype array at Potts Hill looking west. In the background are the 16-ft × 18-ft Paraboloid and the 36-ft Transit Parabola.

Figure 79: The Mills Cross Prototype at Potts Hill. In the background is the 16-ft×18-ft Paraboloid and the 36-ft Transit Parabola (Courtesy of ATNF Historical Photographic Archive: B3171-4 Image Date: 7 October 1953).

It is interesting to note that in reply to a letter which Pawsey had written to Lovell at Jodrell Bank describing the concept of the Mills Cross, Lovell wrote:

> "Hanbury Brown must have heard something about your new aerial because he was talking to me about it the other day. As a matter of fact, Jennison put up a similar scheme for investigating the fine structure of the Cygnus and Cassiopeia sources but we were unable to proceed with it owing to financial difficulties." (Lovell, 1953).

Hanbury-Brown also noted:

> "We considered exactly the same scheme before deciding to go ahead with the big parabola, but came to the conclusion that we wanted the large gain as well as the narrow beam width especially for work at high

frequencies. I have recently re-examined the technical problems of phasing an array of this type for a wavelength of 2 metres, however in view of our programme on the 250 ft dish we shall not attempt to build it." (Hanbury-Brown, 1953).

10.4.9. Miscellaneous Instruments

This section describes some of the other instruments that were used at Potts Hill.

10.4.9.1. Yagi Arrays (I)

One of the first instruments to be used when the field station was established at Potts Hill in 1948 was a simple Yagi antenna. This was used by Little for daily solar measurements at 62 MHz and was located at the northern side of the reservoir (Orchiston and Slee, 2005a). Several different Yagi configurations were used at Potts Hill as part of the solar monitoring program. Figure 80 shows an example of a four-element Yagi used for solar observations at Potts Hill. While no individual results were published from observations from this instrument, data collected from these observations were incorporated in the multi-frequency observation and statistical research papers.

Figure 80: A four-element Yagi array at Potts Hill (Courtesy of ATNF Historical Photographic Archive: P12205-1)

10.4.9.2. Suspended Dipole (J)

The last instrument to be constructed at Potts Hill was a simple dipole antenna suspended between two poles using the ground as a reflector. It operated at 19.6 MHz and was erected in early 1956 (Orchiston and Slee, 2005a). It was used as part of a spaced aerial experiment by Gardner and Shain to examine scintillations in radio emissions from Jupiter to determine if these were inherent in the source or caused by

the ionosphere (Gardner and Shain, 1958). The main instruments in the experiment were located at Fleurs field station some 25 km to the west. Simultaneous recordings were taken at both sites so that burst arrival time could be compared.

Gardner and Shain noted in their 1958 paper that there was considerable local interference at the Potts Hill site. Mills also noted that part of his reason for moving to Fleurs was the increasing levels of radio interference at Potts Hill (Mills, 1984).

10.4.9.3. Spectrohelioscope

The installation of a spectrohelioscope or spectroheliograph at Potts Hill to support the optical correlation to the solar radio observations was first proposed by Payne-Scott (1947). In her original proposal Payne-Scott (ibid.) noted that she had discussed the construction with R. Giovanelli and W. Steel from the Physics Division of the CSIR and they had offered their assistance should the proposal proceed.

Over a number of years Radiophysics considered purchasing a spectrohelioscope, however, despite a great deal of investigation no purchase was made. In October 1951, Woolley wrote to Pawsey stating that with the departure of C. Allen from Mount Stromlo, they were having a great deal of difficulty maintaining their solar program. In fact he noted that if it were not for Radiophysics' interest they would suspend the program in January 1952 (Woolley, 1951). Pawsey replied to Woolley suggesting that in view of the difficulties perhaps Stromlo's spectrohelioscope could be loaned to Radiophysics and be supervised and maintained by Giovanelli (Pawsey, 1951e).

In July 1952 Woolley wrote to Pawsey agreeing to the loan of the spectrohelioscope for a period of one year, with the possibility of extension dependent on the needs of the Ionospheric Prediction Service (Woolley, 1952).

The spectrohelioscope was ultimately installed at Potts Hill by Giovanelli in late 1952 and was employed to make regular images of the Sun using a Hα filter so comparisons could be made with the radio frequency observations. The instrument was operated by Radiophysics staff as noted by Davies:

> "…on clear days I made maps of the features of the H-alpha Sun and used Stonyhurst discs to present the data. The features included sunspots, bright plagues, and prominences (which were visible in emission on the limb or in absorption as dark filaments on the disk)."(Davies, 2005: 95).

Figure 81 is taken from a newspaper article on the overall solar program of the Radiophysics group in 1956 and shows Giovanelli and the spectrohelioscope.

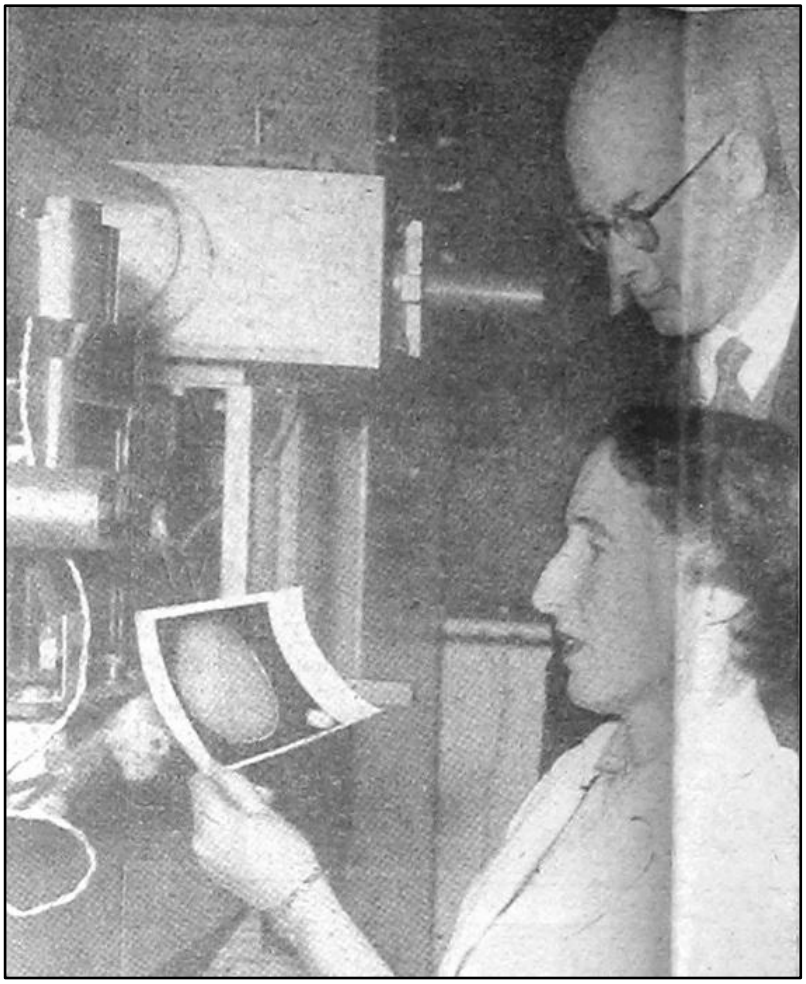

Figure 81: Dr. Giovanelli and Miss Marie McCabe examining a spectroheliograph photograph (Courtesy of Sun-Herald, Sydney 16 September 1956).

10.4.10. Fate of Instruments

While the fate of many of the instruments from Potts Hill remains unclear, it appears that at least some of the aerials were either transferred or donated to universities within Australia. In March of 1961, Professor G.R.A. Ellis of the Department of Physics, University of Tasmania enquired if it was possible to obtain any old aerials from Radiophysics. Pawsey replied indicating that "some time ago we gave one or several (old dishes) to Reg Smith [Dr. R.A. Smith, Department of Physics, University of New England, Armidale]." (Pawsey, 1961b). Dr. Smith was conducting ionospheric research at this time, although the results of his research with the ex-Radiophysics instruments were never published.

As we have already seen, the E-W Solar Grating Array was permanently loaned to India and went on to become the Kalyan Radio Telescope operational from April 1956.

At one stage consideration was given to recycling the equatorial mount of the 16-ft × 18-ft Paraboloid for use with a new larger aerial; however this was abandoned with the construction of the Murraybank aerial. The fates of both the 36-ft Parabola and the 16-ft × 18-ft Paraboloid are unknown.

Unfortunately it is likely that many of the instruments were sold for scrap metal as the research efforts of the Division were consolidated on the Parkes Radio Telescope. Figure 82 shows a 10-ft Parabola in a state of disrepair at Potts Hill in the late 1950s. Given the condition of this aerial it is likely that it would have been scrapped.

Figure 82: A 10-ft Parabola showing damage to one of its eight sections at Potts Hill in the 1950s (Adapted of the ATNF Historical Photographic Archive: B2639 Image Date: 28 November 1951).

10.5. Major Research Contributions

The research contributions at Potts Hill from 1948 to 1962 were wide ranging. At the outset the work was heavily weighted towards solar research. However, the investigation of cosmic noise sources grew steadily during the life of the field station and would dominate its later years with Potts Hill being the home of the original 21-cm H-line confirmation and then surveys of the Magellanic Clouds and southern Milky Way.

This Section examines in detail the research contributions of solar, cosmic and the Jupiter radio emission research in which the Potts Hill field station was involved. The section concludes with a brief discussion of the 1952 U.S.R.I General Assembly which was held in Sydney.

10.5.1. Solar Research

Prior to the establishment of the Potts Hill field station in 1948, solar research had been occurring at a number of the Radiophysics field stations scattered across the Sydney district (Orchiston et al., 2006). One of the key challenges of this early work had been the limitations inherent in determining positions of source radiation due to the low angular resolution of the types of instruments being used. Some early progress had been made using interferometry techniques (McCready et al., 1947). However, the opportunity to accurately determine source positions and the disk distribution of solar emission through the use of solar eclipses soon became apparent. In 1946 Covington, working in Canada, had used the opportunity presented by an earlier partial solar eclipse to accurately measure the time, and hence position, on the solar disk when radio emission was masked by the passage of the Moon's disk in front of a source (Covington, 1947). Sander (1947) also used this same eclipse to examine the Sun at the higher frequency of 9,428 MHz. The first use of a solar eclipse in radio astronomy was by Dicke (1946b), but it was Covington who was the first to show that strong emission was associated with a sunspot group that was occulted by the Moon's disk. A similar partial solar eclipse was scheduled to be observable from Australia on 1 November 1948. This opportunity turned out to be the catalyst for consolidating the majority of the Radiophysics solar research program at the new field station at Potts Hill.

10.5.1.1. 1948 Eclipse Observations

In anticipation of the 1 November 1948 eclipse, a range of instruments was relocated to the Potts Hill field station so that multi-frequency observations could be obtained. The 16-ft × 18-ft Paraboloid was relocated from the Georges Heights field station and was used as the lead instrument for observations at 600 MHz (Christiansen et al., 1949b). These observations were made in conjunction with two portable 10-ft parabolas that were located at the remote sites of Rockbank in Victoria and Strahan in Tasmania. This was the first time that radio astronomical observations were conducted in these two Australian states (e.g. see Orchiston, 2004a). A 68-in Parabola was used for observations at 3,000 MHz (Piddington and Hindman,

1949) and the 44-in ex-Searchlight Parabola was relocated from the Radiophysics headquarters at Sydney University to be used for observations at 9,428 MHz (Minnett and Labrum, 1950). Christiansen had originally considered making the observations of the eclipse from Adelaide as it was considered that the Sun in Sydney may have been too close to the horizon at the time of the eclipse for useful observations (McCready, 1948c).

The primary goals of the observations at 600 MHz were:

(1) to determine the accurate distribution of radio brightness over the solar disk;
(2) to pin point the location of localised radio emitting regions, and
(3) to look for possible polarisation effects that were predicted to be associated with the Sun's magnetic fields.

By conducting observations at three dispersed sites it was possible to triangulate position estimates of discrete sources on the solar disk. The three sites gave six possible intersecting arc solutions for any observation, three on entry and three on exit from the eclipse. Both Strahan and Rockbank had full visibility of the eclipse. At Potts Hill, sunset occurred before the last contact of the Moon's disk (i.e. the 4th contact point). Figure 83 shows the situation for the eclipse as observed from Potts Hill.

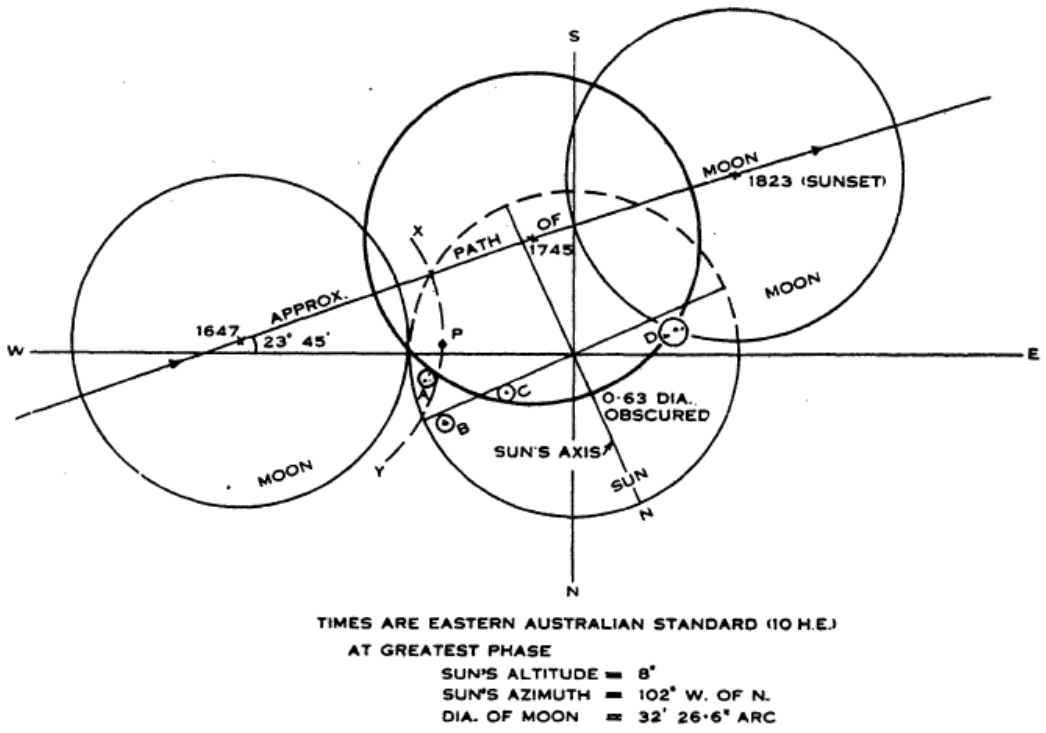

Figure 83: Circumstances of the partial solar eclipse of November 1, 1948 as observed from Potts Hill (after Piddington and Hindman, 1949: 529).

Prior research had suggested that the radio emission at these frequencies could be divided into two main components. The first was believed to be the thermal component associated with the 'quiet' Sun. The second was a slowly-varying component that had been correlated with total area of sunspots on the solar disk. Figure 84 shows a scatter plot correlating sunspot area with apparent temperature. This data was taken from earlier observations at 600 MHz (λ = 50cm) and indicates the 'quiet' background level when no sunspots are present on the solar disk.

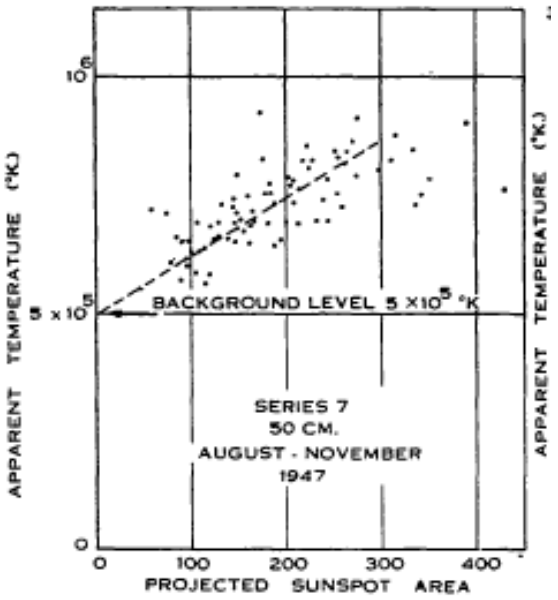

Figure 84: Correlation diagram between apparent temperature and sunspot area given as units of 10^{-5} of solar disk (after Pawsey and Yabsley, 1949: 208)

Martyn's theoretical model (Martyn, 1946b) and observations (Pawsey, 1946) had suggested a temperature for the solar corona in the order of 10^6 K at 200 MHz. This indicated that with the increase in temperature as a function of distance from the solar disk, limb-brightening should be observed as the edges of the disk would expose a greater depth of the higher temperature coronal atmosphere than face-on observations.

The orientation of the eclipse also provided an opportunity to test the prediction that the general magnetic field of the Sun should lead to inequality in the circularly polarised components from the northern and southern hemispheres of the Sun. The passage of the Moon effectively covered the southern hemisphere during the eclipse thus allowing the emission from the northern hemisphere to be compared with overall emission. To try and measure this effect, the two remote field stations aerials were configured to measure left and right-polarisation components of the solar radiation. The main aerial located at Potts Hill was linearly polarised.

On the day of the eclipse there were six small sunspot groups visible with a total area of 85×10^{-5} (0.085%) of the solar disk (Figure 85).

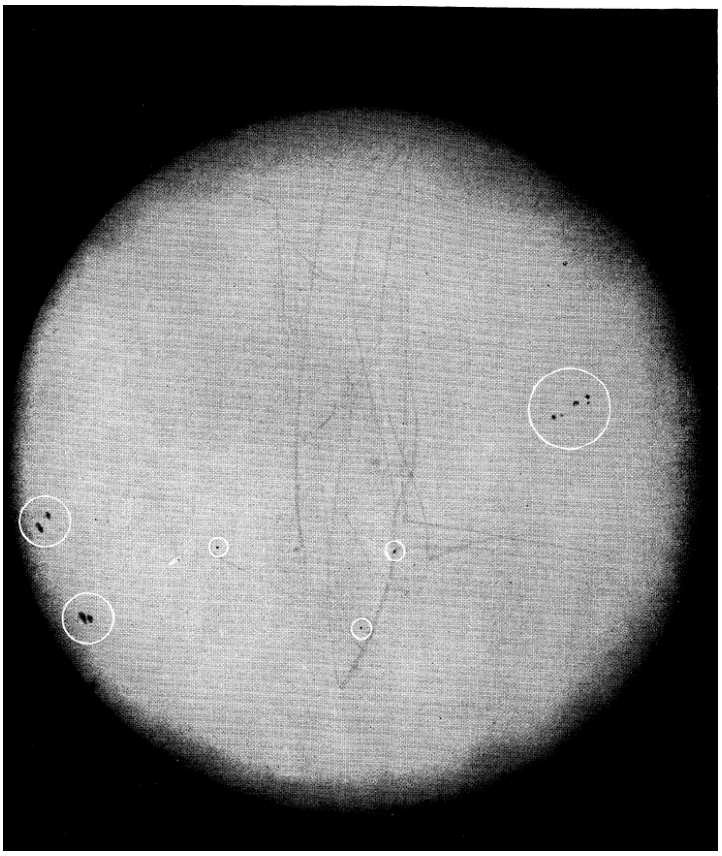

Figure 85: Sunspot groups visible on the solar disk immediately prior to the partial solar eclipse of 1 November 1948 (Christiansen et al., 1949b: Plate 2).

The Commonwealth Solar Observatory at Mount Stromlo provided eclipse predictions and optical observations during the eclipse. These contributions are acknowledged in the published observations. Optical observations were also made using a telescope located at Sydney Technical College and shown in Figure 86 (Orchiston et al., 2006: 45). However, this contribution was not acknowledged other than recording:

> "…the circumstances of the eclipse at Sydney were checked by means of a series of accurately timed photographs" (Christiansen et al., 1949b: 512).

To support the Rockbank observations a single photograph was taken at Melbourne Observatory (Clapham, 1948).

Figure 86: The Sydney Technical College telescope used for solar imaging during the eclipse observations. Photographs were taken using the 15 cm (6-in) guide-scope attached to the 46 cm (18-in) reflector (Courtesy of the ATNF Historic Photographic Archive: B1899-7).

All three of the radio observation sites made successful observations of the partial solar eclipse at 600 MHz. The eclipse record from Potts Hill is shown in Figure 87. The record for Rockbank is shown in Figure 88 and Figure 89 shows the record for Strahan.

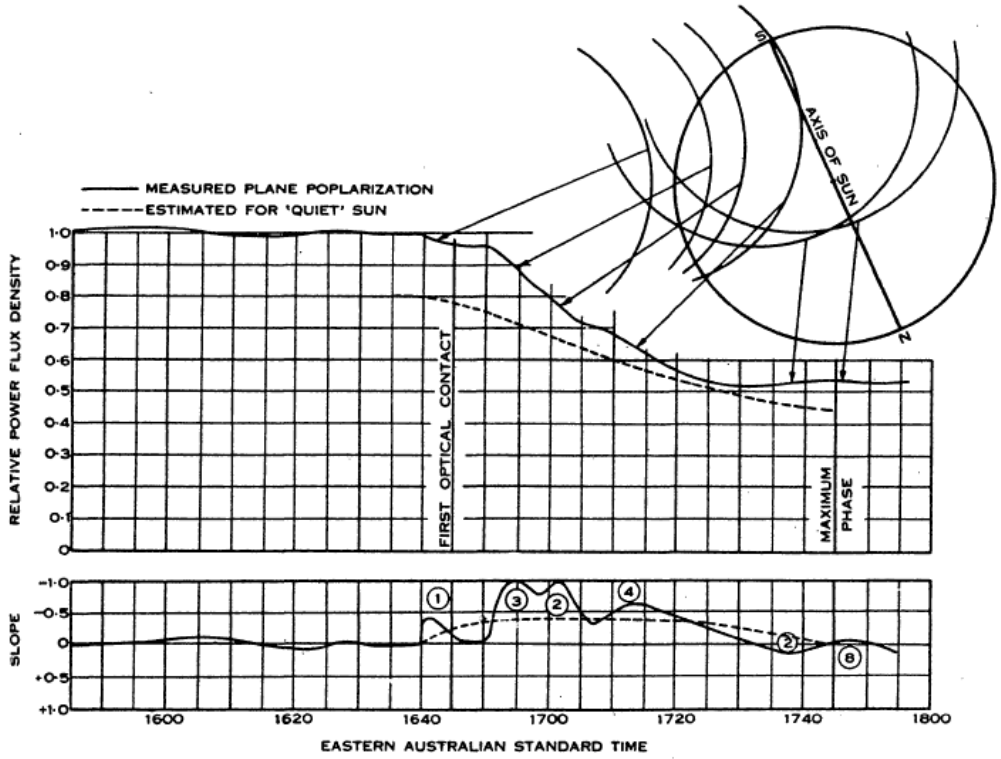

Figure 87: Eclipse record taken at Potts Hill at 600 MHz (after Christiansen et al., 1949b: 510).

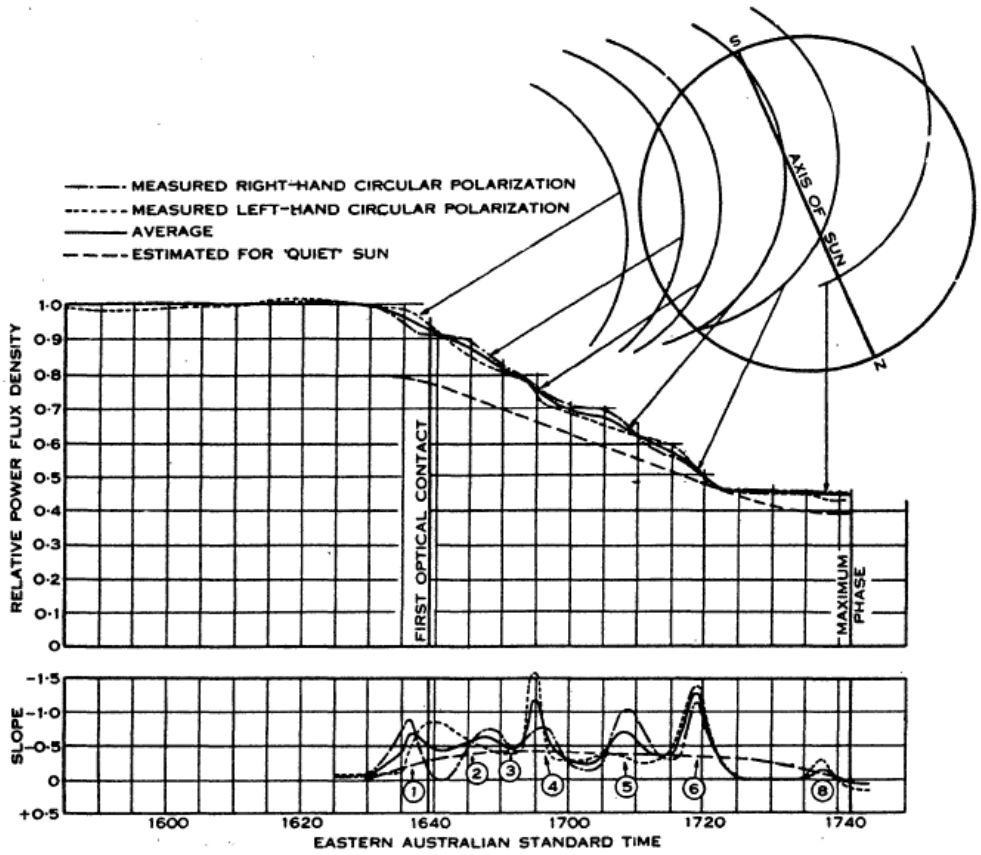

Figure 88: Eclipse record taken at Rockbank in Victoria at 600 MHz (after Christiansen et al., 1949b: 511).

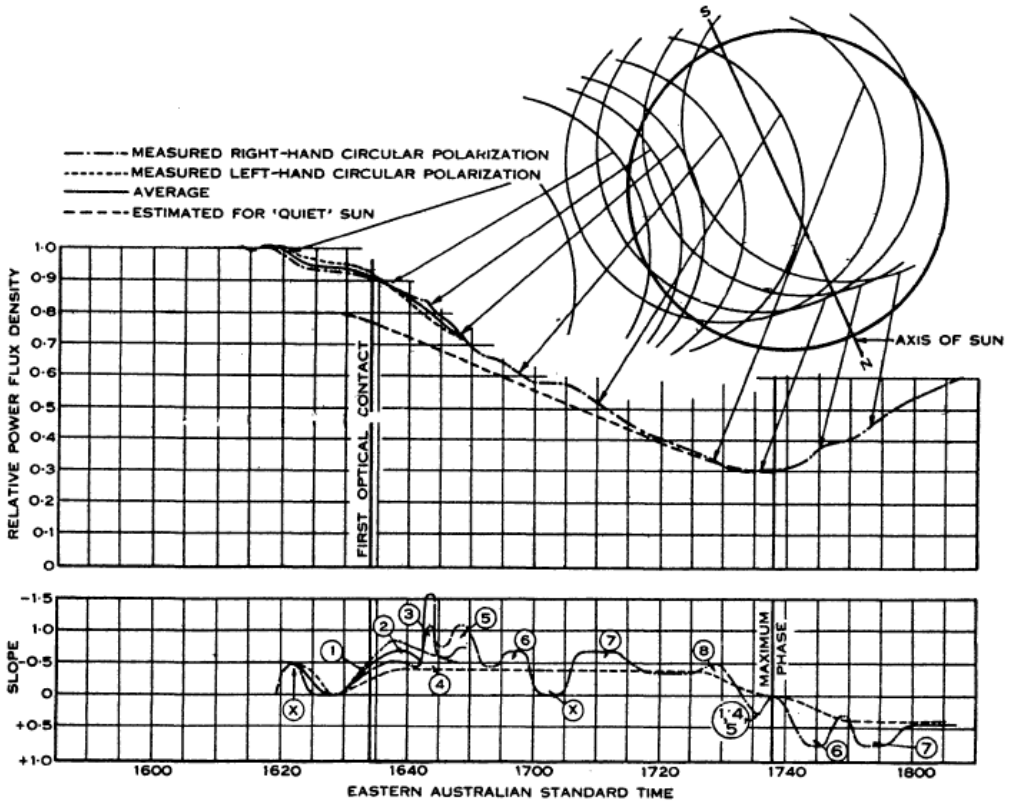

Figure 89: Eclipse record taken at Strahan in Tasmania at 600 MHz (after Christiansen et al., 1949b: 512).

As the eclipse occurred near sunset, the Sun was low on the horizon and therefore the full records of the eclipse were affected and the major focus of the analysis was on the first 2/3rd of the eclipse record. Eight prominent discrete radio sources were observed at all three sites and these are marked in the recordings as the circled numbers 1-8. A simplified illustration is also shown in Figure 94. It can clearly be seen that the radio emission began to decline well before the first optical contact of the Moon's disk and it was estimated that 40% of the radiation at 600 MHz originated outside the visible disk of the Sun, with an average effective temperature of 5×10^6 K. The effective temperature of some of the eight bright areas was estimated to exceed 10^7 K. The equivalent blackbody temperature of the Sun (T_s) was calculated from the following relationship with aerial temperature (T_a):

$$T_s = \frac{4\pi}{G\Omega_s} . T_a \qquad (7)$$

where,

G is the maximum gain power of the aerial compared to an isotropic radiator; and

Ω_s is the solid angle subtended by the visible Sun's disk.

The triangulation of the positions of the bright sources from the three observation sites indicated that seven of the eight sources appeared to be associated with optical features that were visible on the solar disk. Three of these were close to visible sunspot groups, three were close to the positions of sunspot groups from the previous rotation of the Sun (27 days earlier), and one was located close to a solar prominence that appeared on the south-western limb of the Sun. It should also be noted that sources were not associated with all of the visible sunspot groups or prominences. Figure 90 **s**hows the location of the radio sources on the solar disk.

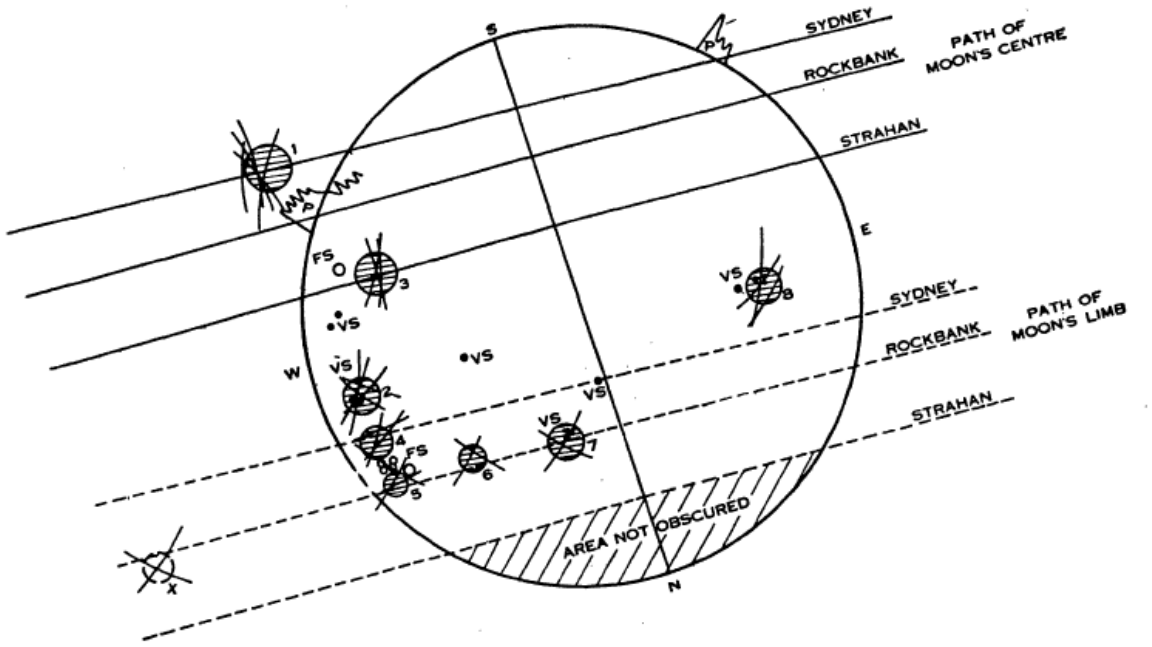

Figure 90: The location of the discrete radio sources on the solar disk. VS = Visible sunspot, FS = Position of a visible 27 days earlier sunspot, P = Solar prominence (after Christiansen et al., 1949b: 513).

It was estimated that the eight discrete sources made up ~20% of the radiation generated at 600 MHz and the remainder was generated by an approximately symmetrical source 1.4 times larger than the visible disk of the Sun (i.e. the solar corona). This result was consistent with the earlier results of Pawsey and Yabsley (1949) and shown in Figure 84. Although the measurements were consistent with the theoretical models for limb-brightening, they did not provide definitive proof of its existence at 600 MHz. However, these observations provided the most detailed evidence at the time that the bright discrete emissions were associated with sunspots and made up the slowly-varying component of the solar radiation at 600 MHz.

The polarisation measurements made during the eclipse provided less than definitive results. The measurements were made at both of the remote sites using the portable 10-ft Parabolas. A mechanical problem with the telescopic coaxial transmission feed-line was encountered at Strahan early in the observations. This prevented the aerial from being switched between polarisation senses. Consequently only right-hand polarisation could be measured at this site. The existence of a general magnetic field for

the Sun had been proposed since at least 1918 (Hale et al., 1918) after optical detection of the Zeeman effect, which results in splitting of spectral emission lines. The theoretical prediction at the time was for the Sun to have a general magnetic field intensity of ~50 Gauss (Smerd, 1950a). Circular polarisation was detected associated with the bright regions. The expected differences between the north and south hemispheres were not detected and apart from when a bright area was eclipsed, the measurements quickly returned to equilibrium. The maximum change that was observed was a peak of ~2%, while the experimental accuracy would have allowed changes of 3% to be detected. This suggested that the general field must be significantly weaker than 8 Gauss assuming a 3% difference. While this did not match the theoretical model, it is actually consistent with modern measurements. Current measurements of solar magnetic fields give values ranging from 0 to 1800 Gauss while the general field for the Sun is in the order of ~1-2 Gauss (Cerdena et al., 2006). Smerd later conducted a detailed analysis of the observational results and concluded that the Sun's general magnetic field could not be greater than 11 gauss based on the observational results (Smerd, 1950a).

The detailed results of the 600 MHz observations were published in 1949 in the *Australian Journal of Scientific Research* (Christiansen et al., 1949b) and also in a summary paper sent to *Nature* (Christiansen et al., 1949a).

The observations at 3,000 MHz (λ = 10 cm) were made using the 68-in Paraboloid at Potts Hill. By measuring the eclipse at different wavelengths it was hoped to provide data on the temperature gradient of the solar atmosphere. The earlier work had indicated a very steep rise in temperature from the photosphere through the chromosphere to the corona. Piddington and Hindman made observations over an extended period before and after the eclipse to provide a baseline for comparison to the eclipse observations. Figure 91 shows the close correlation between sunspot area and the equivalent disk temperature derived from measurement of radiation at 3,000 MHz from October 1948 to March 1949.

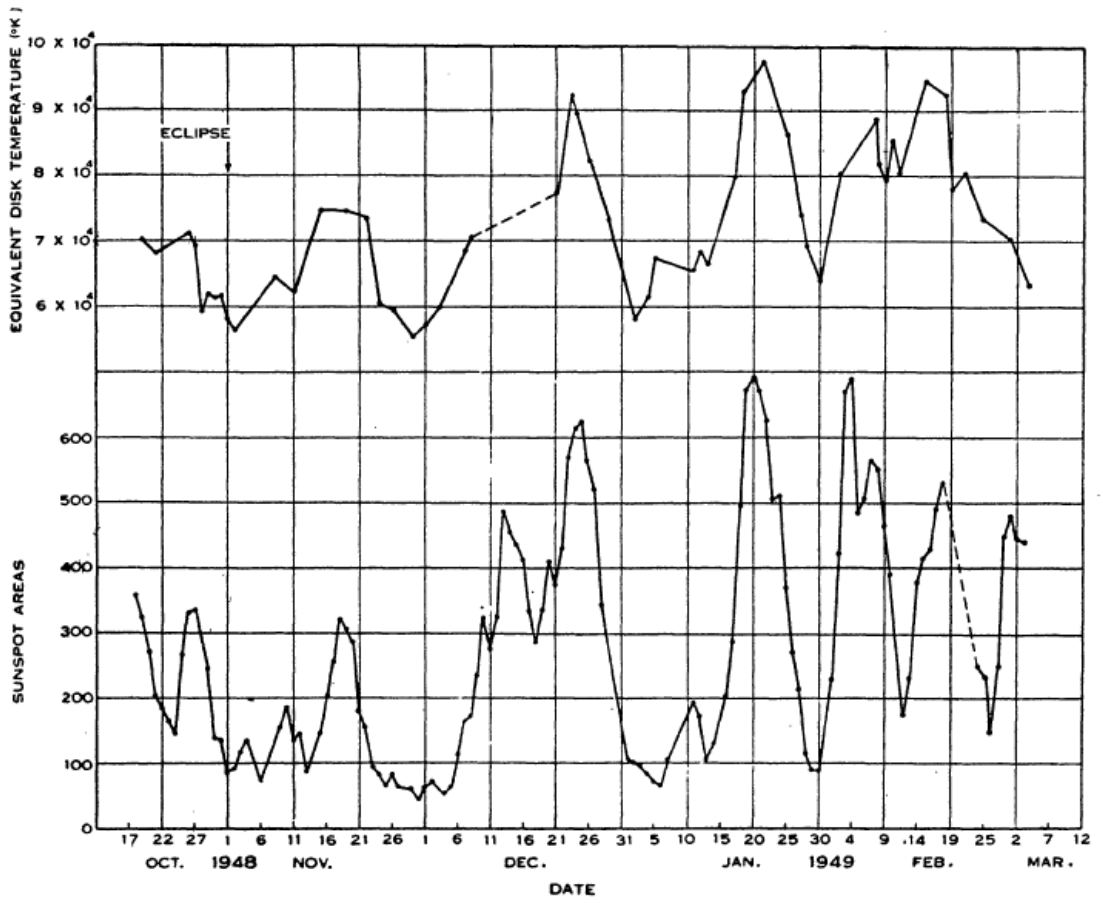

Figure 91: Correlation of sunspot area to 3,000 MHz radiation (after Piddington and Hindman, 1949: 527).

Using the method developed earlier by Pawsey and Yabsley and illustrated in Figure 84, Piddington and Minnett derived a baseline temperature for the quiet Sun of 5.4×10^4 K at 3,000 MHz. This compared to a temperature of 6.5×10^4 K derived from the analysis of Covington's earlier measurement at the slightly longer wavelength of 10.7 cm (2,800 MHz). The highest observed equivalent temperature over the period was 9.8×10^4 K. A reconstruction of the scatter plot based on the data in Figure 91 shows that the extrapolation to the zero sunspot area would yield a temperature of 5.9×10^4 K, which is slightly higher than the published value.

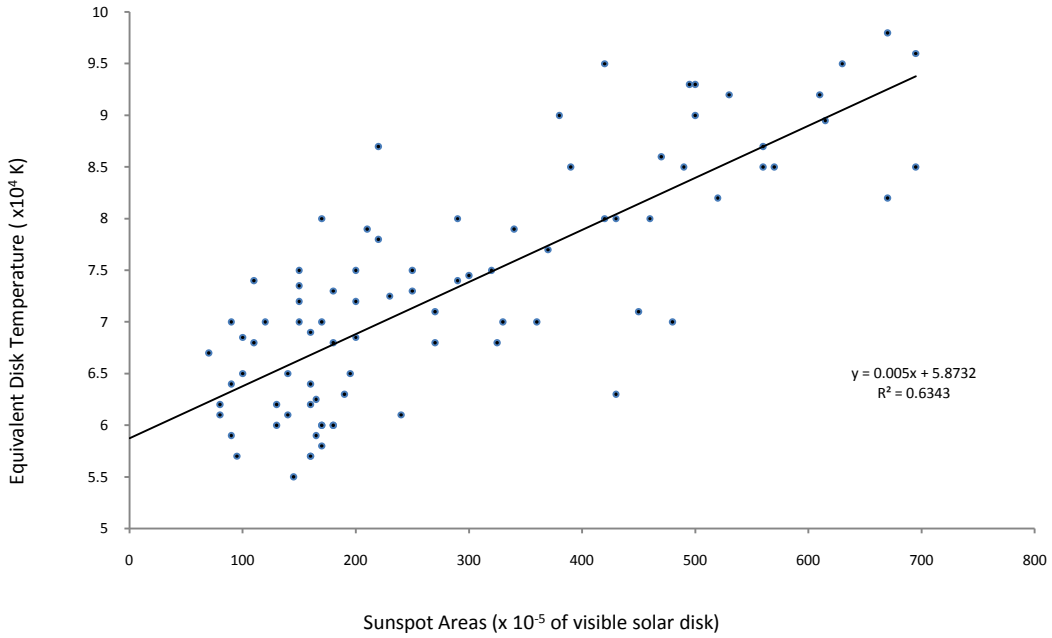

Figure 92: A reconstruction of the scatter plot used to determine the 'quiet' Sun temperature at 3,000 MHz. The graph is based on data used to produce Figure 91.

The main goal of the eclipse observation was to establish a distribution of the non-variable component of the solar radiation across the solar disk. Figure 93 shows the record of the eclipse observation.

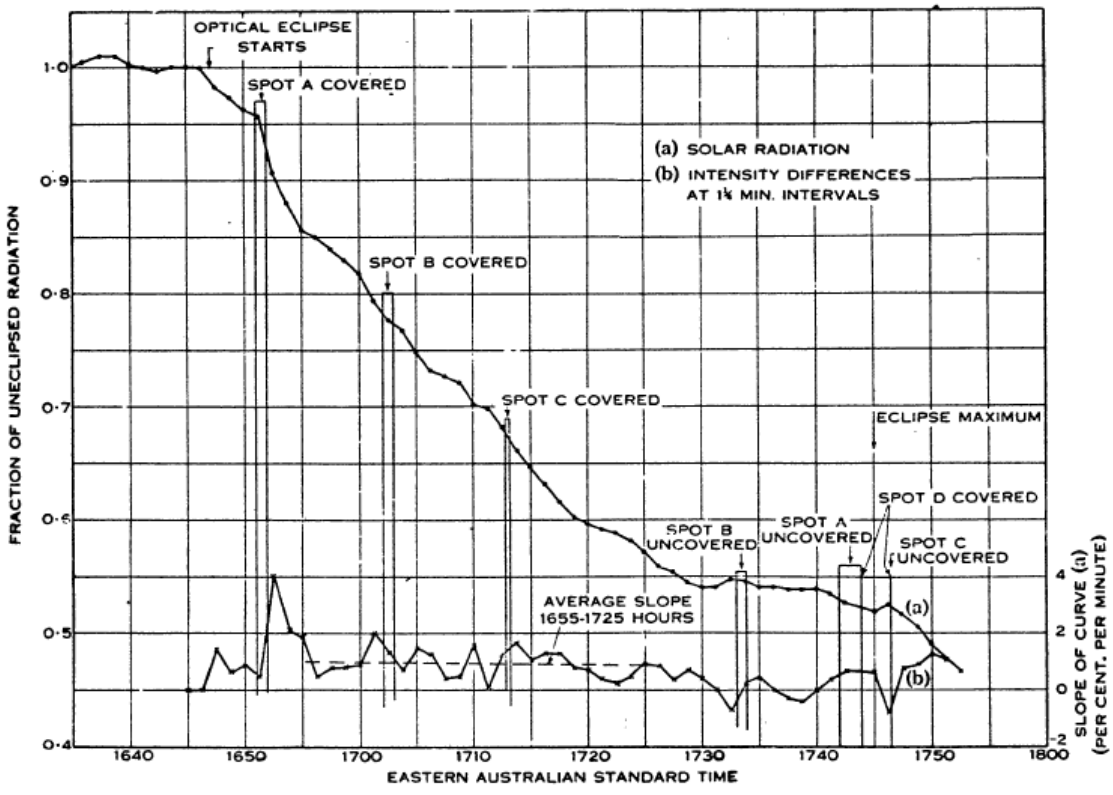

Figure 93: Eclipse record taken at Potts Hill at 3,000 MHz (after Piddington and Hindman, 1949).

Unlike the 600 MHz observations, the decline in radiation levels at 3,000 MHz almost coincided with the optical first contact. At best, the eclipse began some 30 seconds earlier. This was in contrast to Covington's earlier observations which showed the radio eclipse starting some 3 minutes prior to the optical eclipse. It was speculated that this may have been due to the fact that the Sun was in a much quieter period than the previous eclipse observation. In 1946 Covington had observed a marked drop in radiation when a large sunspot group was eclipsed, but the occultation of the sunspots at 3,000 MHz during the 1948 eclipse produced little response; again this was unlike the 600 MHz measurements. At best two weak hot-spots may have been detected with a temperature of the order of 10^6 K. One of these radio hot-spots may have been associated with one of the bright areas (No. 3 in Figure 94) seen during the 600 MHz measurements. There appeared to be no association of the hot-spots with optical features. The overall profile attained appeared to be most consistent with a model of the Sun having 68% of the radiation distributed uniformly over the disk and 32% being concentrated in a ring near the limb, thus indicating limb brightening.

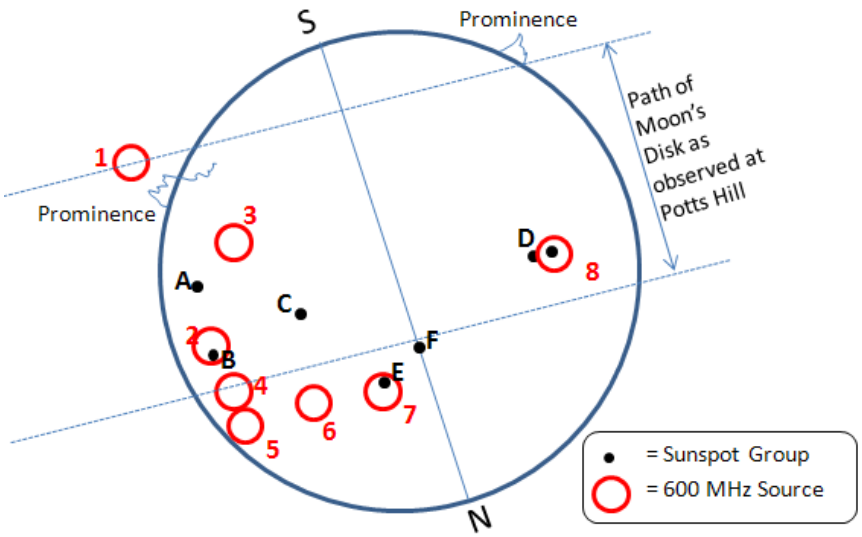

Figure 94: A simplified diagram of the eclipse showing the eight 600 MHz sources (1 to 8) and the six visible sunspot groups (A to D). Source 3 was also detected at 3,000 MHz.

Polarisation measurements at 3,000 MHz were made by fitting a screen to the 68-in Parabola just prior to the eclipse, and three times during the eclipse. Circular polarisation was detected and was believed to be associated with a discrete source. However, like the 600 MHz observations, there was no evidence of a differential between hemispheres (i.e. a change between of polarisation between left to right or vice versa) that might have indicated a strong general magnetic field.

The third team at Potts Hill, led by Minnett and Labrum, observed the eclipse at 9,428 MZ (λ = 3.18 cm). Like Piddington and Hindman, Minnett and Labrum observed the Sun for an extended period of three

months to establish a 'quiet' Sun baseline. Both Piddington and Hindman had been instrumental in assisting Minnett and Labrum in setting up their experiment and their contribution is acknowledged in the published results. Figure 95 shows the correlation of apparent disk temperature to sunspot area as measured over the three month period.

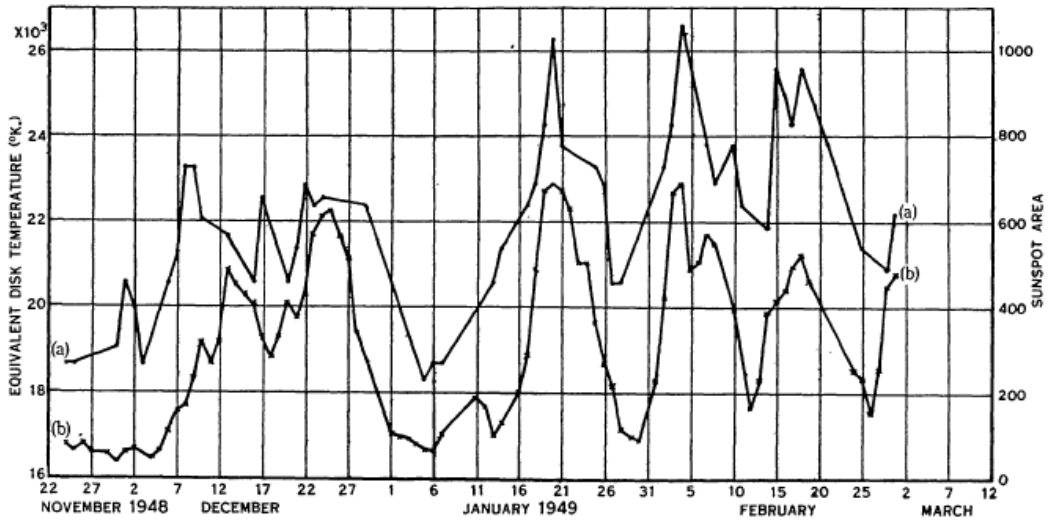

Figure 95: Correlation of sunspot area and radiation at 9,428 MHz (after Minnett and Labrum, 1950: 65).

The correlation at 9,428 MHz was much stronger than that seen in the 3,000 MHz measurements and is readily apparent from comparison with Figure 91. Based on the scatter plot analysis, the correlation at 9,428 MHz was r = 0.79 (r^2 = 0.89) compared to r^2 = 0.63 for the 3,000 MHz observations. The zero sunspot area baseline temperature for the Sun at 9,428 MHz was estimated to be 19,300 K as shown in Figure 96.

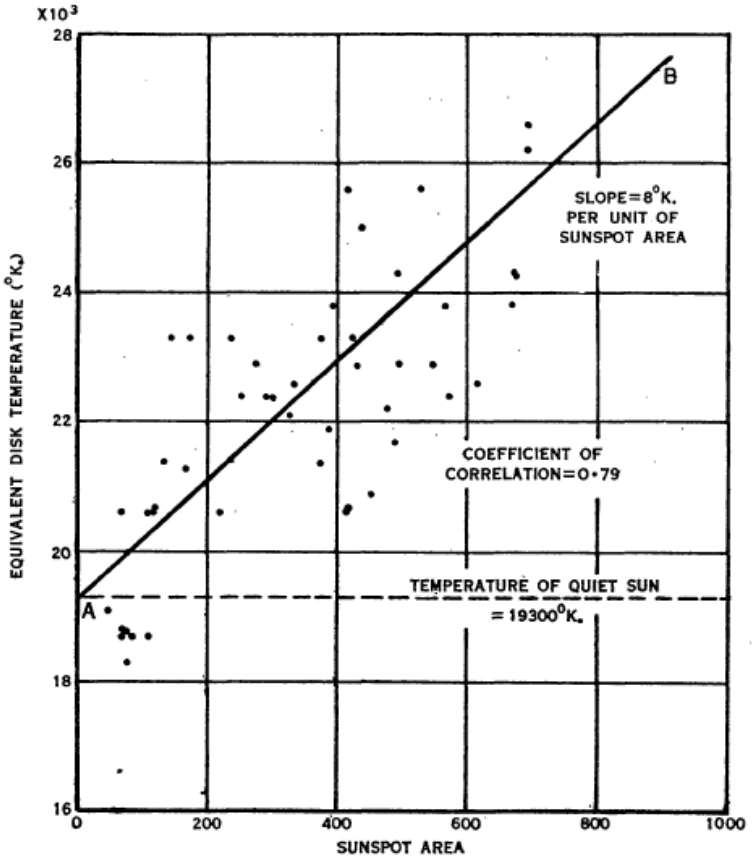

Figure 96: Scatter plot showing the correlation between sunspot area and equivalent solar disk temperature and used to establish the temperature of the 'quiet' Sun at 9,428 MHz (after Minnett and Labrum, 1950: 66).

This estimate of equivalent disk temperature was in general accord with earlier measurements for similar wavelengths. The slope of the best fit line indicated an 8 K increase per unit of sunspot area. This compares with a slope of 50 K at 3,000 MHz given by Figure 92. This showed that the variation of temperature as a function of sunspot area was very much lower at the higher frequency.

Figure 97 shows the record of the partial eclipse at 9,428 MHz.

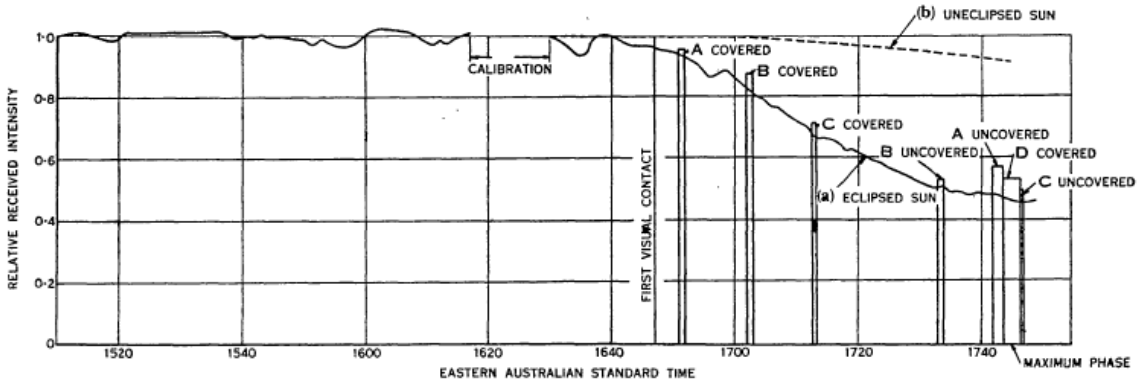

Figure 97: Eclipse record taken at Potts Hill at 9,428 MHz (after Minnett and Labrum, 1950: 69).

The sunspot groups that were in the eclipse path are labelled A to D and correspond to the labelling in Figure 94. No effect, outside of possible instrumental variation, was observed during the passage of the Moon's disk over the solar disk. Given that only an 8 K increase per unit of sunspot area would be expected based on the slope of the scatter plot analysis, any change would have been outside the sensitivity of the instrument to detect. There was some indication that the decline in radiation levels began before the optical eclipse although instrumental variations cannot be excluded. Examining the rate of temperature change during the eclipse, Minnett and Labrum concluded that two possible alternate models would fit the experimental results; either a uniform distribution with a radius 1.1 times that of the visible disk or a distribution with 74% of radiation uniformly distributed and 26% concentrated in a ring around the limb.

In summary, the 1948 eclipse observations provided key data relating to the quiet Sun and the slowly-varying component. While optical emission is strongest in the lowest layer of the solar atmosphere, the photosphere, it was becoming clear that the radio quiet component of the radiation had a very different origin. Much higher temperatures than the 5,800 K photospheric temperature were being observed and these ranged from ~10^4 K levels of the chromosphere to 10^6 K in the corona. At the time of the observations the radiation was thought to be thermal in nature, although a non-thermal origin had not been ruled out. It was also clear that at 600 MHz the source extended well beyond the visible disk of the Sun, correlating with an origin in the corona. The extended source was not clear at the higher frequencies, nor was the limb-brightening effect definitively observed. Correlation of the variable component with sunspot area appeared clear at all frequencies and the position measurements at 600 MHz clearly associated emission with existing and old sunspot groups. Circular polarisation was also detected related to the different sources and ultimately to some of the sunspot groups. The observations found no evidence of the existence of a general solar magnetic field.

A second partial solar eclipse visible in Australia occurred on 21 October 1949. This eclipse was also observed at Potts Hill and at two remote sites; one at Eaglehawk Neck in Tasmania and the other at a new

site near Bairnsdale aerodrome in Victoria. The results of these observations were never published, but are discussed in Wendt et al. (2008).

10.5.1.2. Multi-Year Solar Observations

Following the success of the observations of the 1948 partial solar eclipse, Christiansen and Hindman (1951) collaborated to write up findings of the longer-term solar monitoring that had been occurring at the other field stations, and from 1948 onwards, at Potts Hill. Since 1947, daily observations had been made at 600 MHz (λ = 50 cm) and 1,200 MHz (λ = 25cm). From 1948, these were supplemented by daily observations at 3,000 MHz (λ = 10cm) and 9,400 MHz (λ = 3cm). Drawing on optical data from Mount Stromlo, daily sunspot area records could be used for comparison with the effective temperatures observed at each frequency. This allowed Christiansen and Hindman to look for longer-term trends.

In an earlier analysis, Pawsey and Yabsley (1949) had indicated that the thermal emission associated with the quiet Sun may be subject to longer-term variation in the course of the sunspot cycle. This type of change had been predicted by van de Hulst (1949) based on observations of a decrease in electron density of the corona toward the minimum in the sunspot cycle. The sunspot cycle had peaked in 1947, as indicated in Figure 98. This change in the cycle provided an ideal opportunity to examine if there were associated changes during the decline in the solar cycle.

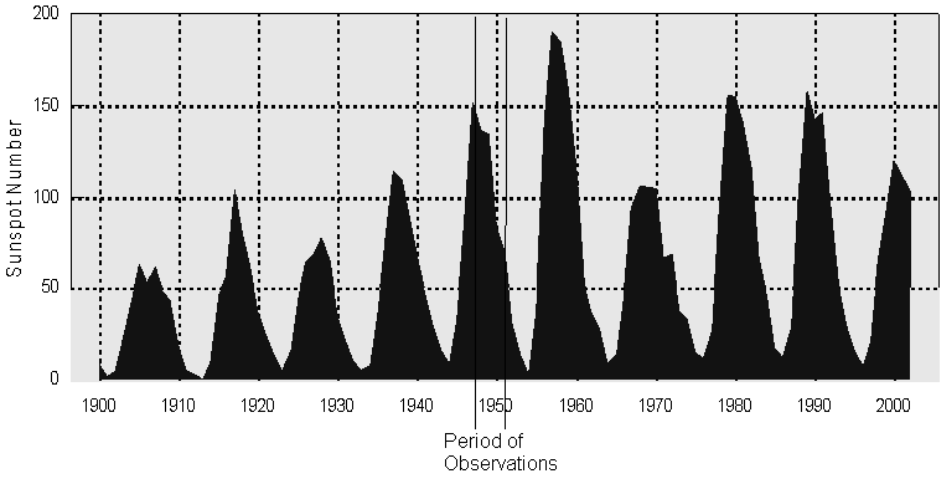

Figure 98: Sunspot numbers showing the period 1947 to 1951 (Based on data from the National Geophysical Data Centre).

During the period 1947 to 1950 there was an almost 50% decline in sunspot numbers as the cycle moved past its peak. Leading up to 1950, while the average sunspot areas declined, there appeared to be no significant decline in the base level temperature as measured in the scatter plots. There was, however, a significant decline in the slope of the line of best-fit indicating that the rate of temperature changes with sunspot area had significantly declined. This is shown in Figure 99.

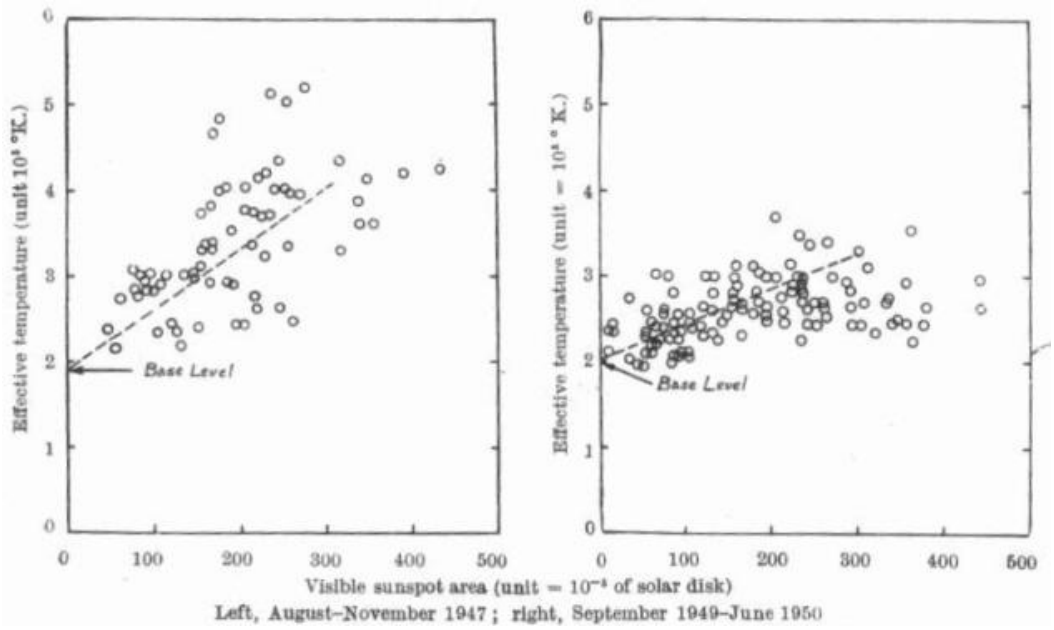

Figure 99: Correlation of sunspot area with effective solar temperature during 1947 and during 1949-50 at 1,200 MHz (after Christiansen and Hindman, 1951: 636).

This decline in the rate of change of temperature with sunspot area was observed across all frequencies (i.e. 600, 1,200, 3,000 and 9,428 MHz).

At the 1950 URSI Conference, Covington had reported that he had observed a 20% drop in the base level temperature at 600 MHz between 1947 and 1950. This same decline had not been observed in Australia. However, during 1950 a marked drop became apparent at 600, 1,200 and 3,000 MHz. No change was apparent at either 9,428 MHz or at 200 MHz (that was being observed on a daily basis at Mount Stromlo). The decline was most pronounced at 1,200 MHz. Figure 100 is a reconstruction of the observations at 1,200 MHz for three periods in 1950.

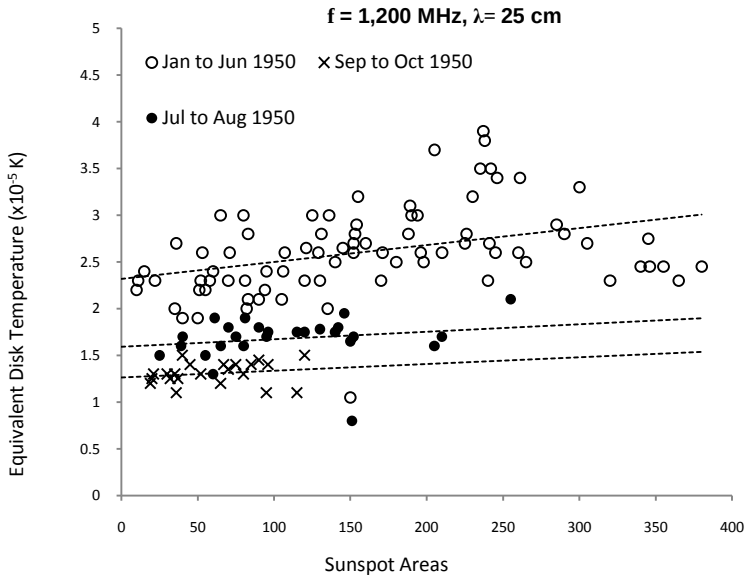

Figure 100: Plot of 1,200 MHz sunspot area versus apparent temperature correlation showing line of best fit and base temperature change for three different periods in 1950.

This shows the decline in the base level from an average of 2.3×10^5 K to 1.4×10^5 K, a decrease of nearly 40%. Christiansen and Hindman (1951) noted that these observations were consistent with van de Hulst's predictions.

Arguably, the definitive theoretical paper on the quiet Sun produced immediately after the 1948 eclipse was by Smerd (1950b). Smerd addressed some of the short-comings of earlier models proposed by Martyn, Ginsberg, and Waldmeier and Müller. In particular, he removed the need to rely on an arbitrary assumption on the size of the radiating radio disk in relation to the optical disk. In 1950 very little was known about the temperature distribution in the solar atmosphere. Temperatures in the order of 10^4 K had been inferred in the chromosphere below a height of ~6×10^3 km and temperatures of 10^6 K had been inferred in the corona above ~2×10^4 km. Somewhere in between these heights was a region of transition between these temperatures. Smerd proposed a model that was in good agreement with the observations. For frequencies above 10,000 MHz the corona was assumed to be practically transparent and therefore he referred to these as chromospheric frequencies. For frequencies below ~200 MHz it was calculated that the radiation would not penetrate the chromosphere and hence these were referred to as coronal frequencies. Frequencies between these were referred to as intermediate frequencies. The model made clear predictions on limb-brightening characteristics across the frequency range. Figure 101 shows the predicted distributions of radiation across the solar disk at a variety of frequencies assuming a coronal temperature of 10^6 K and a chromospheric temperature of 3×10^4 K. All of these predictions were subsequently confirmed by observation (Wild, 1980:9).

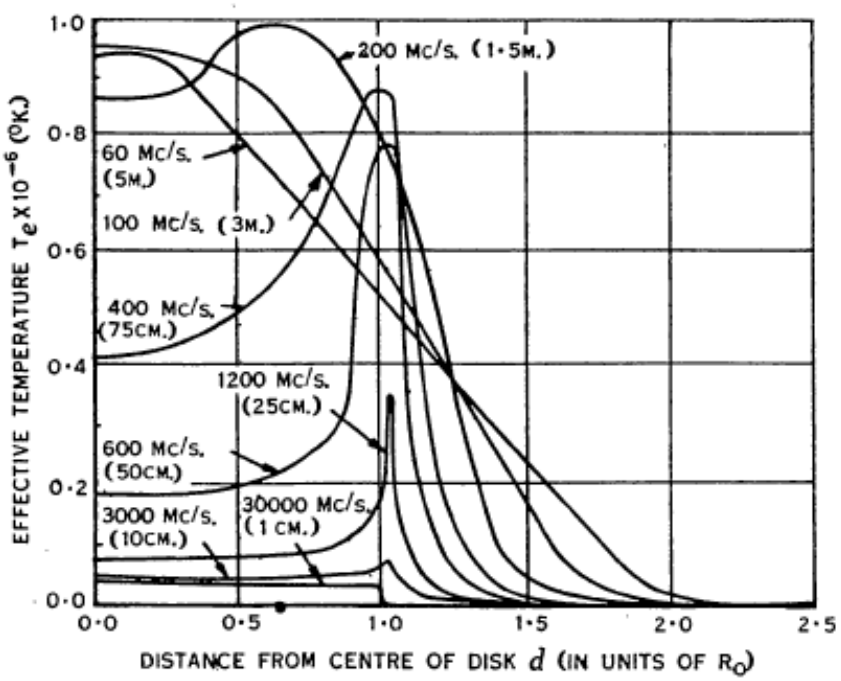

Figure 101: The theoretical distribution of temperature as a function of distance from the centre of the solar disk. Temperatures of 3×10^4 K and 10^6 K are assumed for the chromosphere and corona respectively (after Smerd, 1950b: 46).

Piddington and Minnett (1951b) also published a theoretical paper drawing on the eclipse observations and the longer-term studies. They proposed a model whereby the slowly-varying component of the solar radiation was due to thermal radiation from localised areas of temperature in the solar atmosphere of ~10^7 °K. These areas were believed to be often in the vicinity of sunspots, but not necessarily always associated with them. Piddington and Minnett's analysis showed that previous conclusions about the origin of radiation being at a lower level in the atmosphere were likely invalid. They identified three conditions where the refractive index of an emitted ray would be zero (i.e. reflected) for transverse, oblique and longitudinal propagation. These conditions were defined by the relations $x = 1$ and $x = 1 \pm y$ and are illustrated in Figure 102.

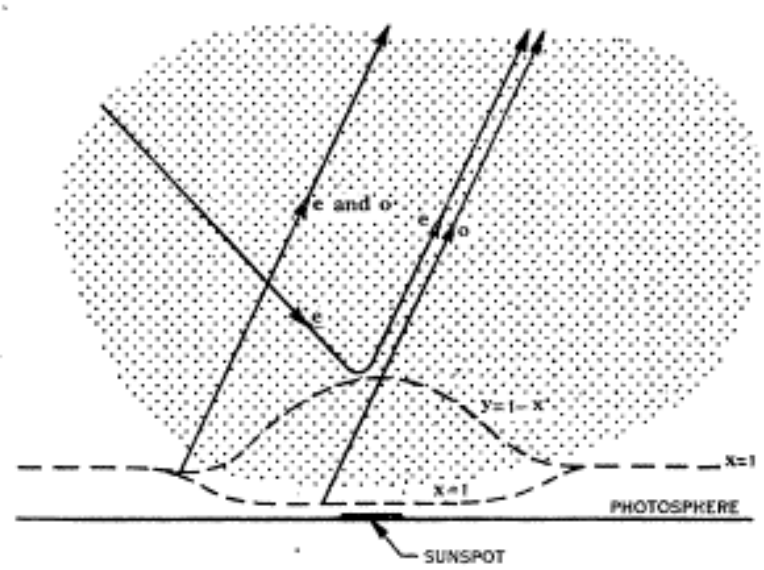

Figure 102: Illustration of the reflective levels and ray paths in a hot dense region above a uni-polar sunspot. *o* and *e* refer to the ordinary and extraordinary waves respectively (after Piddington and Minnett, 1951b: 146).

Their model also gave a reasonable account of the observed levels of circular polarisation.

In 1953, Piddington and Davies published a re-examination of the earlier statistical analysis of sunspot areas and apparent temperatures and drew on the continued daily observation of records from Potts Hill. This analysis attempted to describe the origin of the solar corona (Piddington and Davies, 1953a). The paper built on the notion of hot high-density regions being the source of the slowly-varying component above 600 MHz. Piddington and Davies observed that the sunspot component diminished less rapidly than the visible sunspots and remained in an elevated state for more than a month after visible sunspot activity had ceased. Therefore, it appeared that the earlier scatter plot analysis would overstate the base temperature level for the quiet Sun. Correcting the plots by using a composite of spot areas based on solar rotations showed a much lower base temperature for the quiet Sun, as indicated in Figure 103.

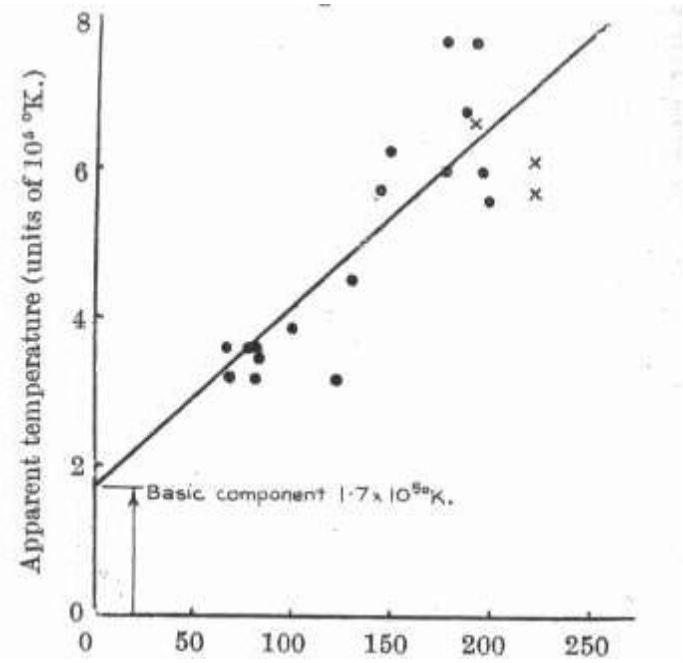

Figure 103: Corrected correlation of apparent temperature at 600 MHz to composite rotational average sunspot area based on observations from December 1949 to April 1951 (after Piddington and Davies, 1953b: 629).

This suggested that the earlier falls that had been seen in the base level of the quiet Sun, particularly in 1950, were simply the result of the longer term decline in the sunspot activity to the true base level. As the very hot gas formed in association with a sunspot it then remained after the spot disappeared and gradually spread and merged with the cooler surrounding atmosphere over the following months. Piddington and Davies calculated that this energy source was capable of maintaining the 10^6 K temperatures observed in the solar corona over the period 1949 to 1951. This analysis provided an important early step in understanding the mechanisms related to coronal heating. A summary paper was published in *Nature* and a more detailed analysis appeared in the *Monthly Notices of the Royal Astronomical Society* (Piddington and Davies, 1953b).

10.5.1.3. Solar Brightness Distributions

As discussed in the previous Section, the distribution of radio emission across the solar radio source was of prime interest as it provided information on the structure, density and temperatures of the solar atmosphere. Obtaining high angular resolution in early observations had relied on the use of solar eclipses which were clearly not practical for collecting a large pool of observational data. It was for this reason that Christiansen had decided to build a high-resolution radio telescope that could perform daily monitoring of the Sun. This was the first Solar Grating Array, which was described in section 10.4.6.

Christiansen had been temporarily diverted from solar research while he was involved in the confirmation of the H-line detection and some preliminary survey work. The first Solar Grating Array was

completed in early 1952 and Christiansen then began a program of daily observations. The high-resolution beams of the grating array produced a one-dimensional response scan across the solar disk at 1,410 MHz. Figure 54 shows an example of the output of the Sun passing through the individual aerial beams. Using a succession of daily scans it was possible to determine how the one-dimensional profile changed over a number of days as the Sun rotated. Figure 104 shows the one-dimension brightness distribution on different days in October 1952.

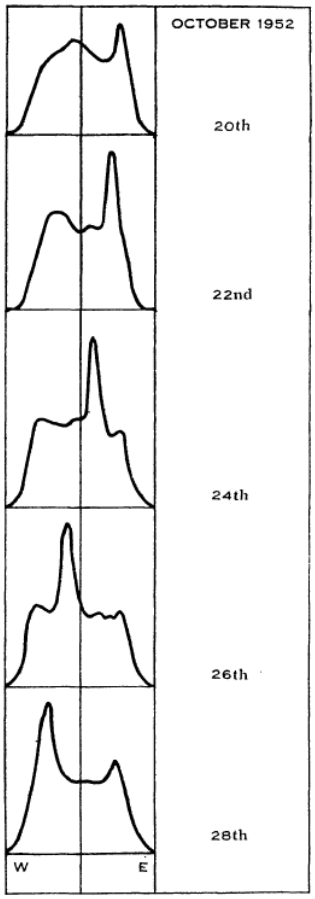

Figure 104: Daily records of one-dimensional brightness distributions across the solar disk from 20 to 28 October 1952 (after Christiansen and Warburton, 1953b: 198).

One early finding that greatly simplified the observational analysis task was that the centre of the radio record corresponded with the centre of visual solar disk, and that bright areas near the limb did not materially change the size of the radio disk. By superimposing the individual scans over an extended period a base level for the radiation became clearly evident. This independent method probably provided the final tipping point toward conclusive evidence that the base level in fact existed. Figure 105 shows an example of such a superimposition.

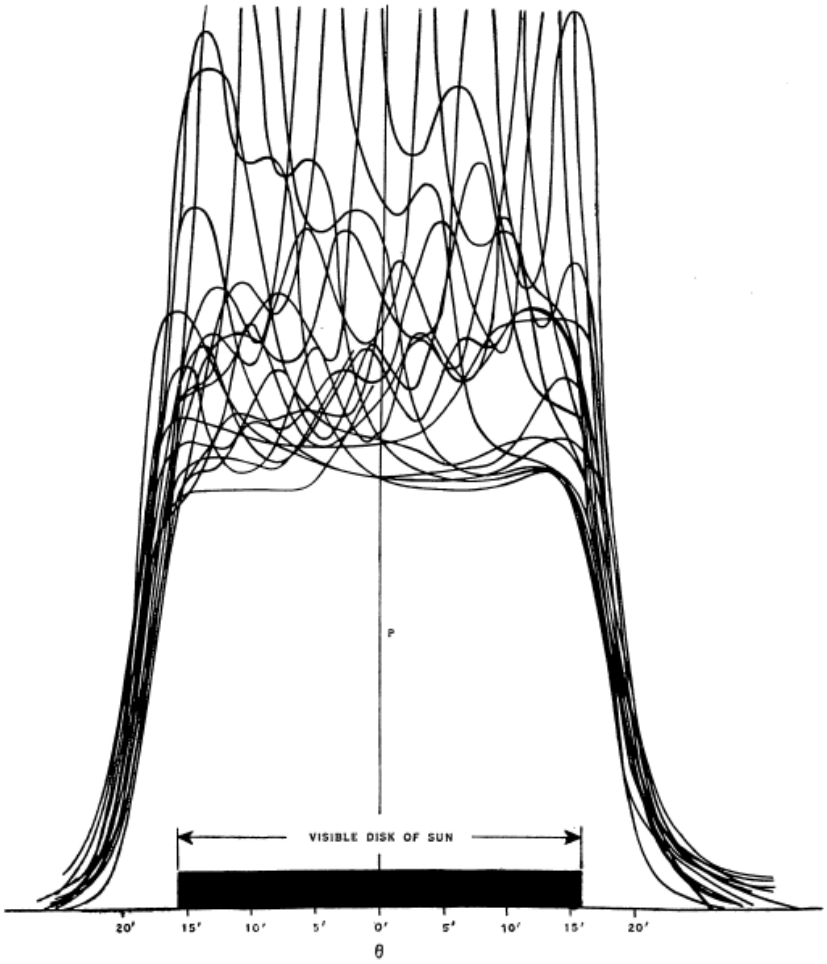

Figure 105: Twenty individual daily one-dimensional brightness distribution scans superimposed. The visual solar disk is indicated by the black bar on the x-axis (after Christiansen and Warburton, 1953b: 200).

Christiansen and Warburton (1953b) used the superimposition technique to determine that the base level temperature of the Sun at 1,420 MHz was 7×10^4 K during the period of observations. Another factor that was clearly evident from the distributions was that the source emission was larger than the optical solar disk. For simplicity a circular symmetry was assumed for the purposes of the analysis, although there were already indications that the distribution appeared more elliptical (as had already been determined from optical observations). Initially it was thought that the effect of this assumption would be small. However, it was fairly quickly recognised that taking into account the non-circular symmetry would be essential and this was to lead to the construction of the second (north-south) Solar Grating Array so as to allow two-dimensional scan (ibid.).

Even allowing for possible errors in the circular symmetry assumption, it was very clear from the observations that limb-brightening had been detected. Figure 106 shows the initial radial distributions based on the one-dimensional scans.

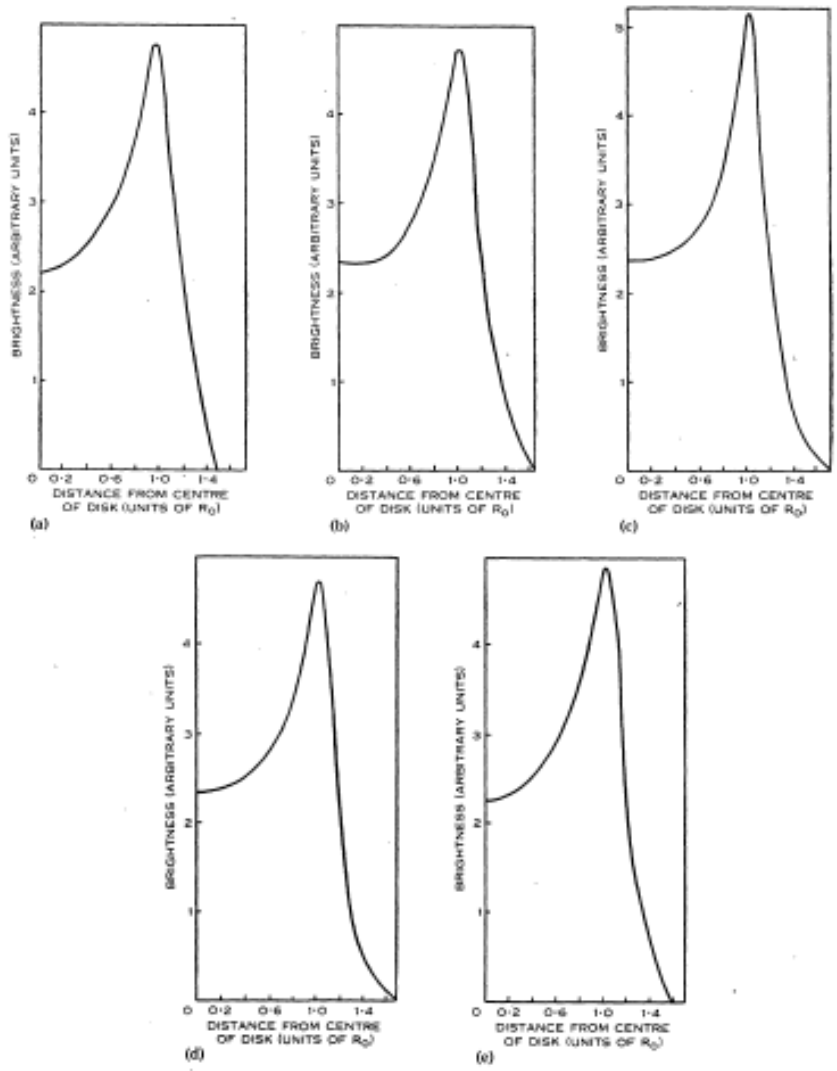

Figure 106: Radial distributions of brightness across the solar disk based on one-dimensional scan observations (after Christiansen and Warburton, 1953b: 268).

These distributions clearly show a limb-brightening effect as predicted in a number of different theoretical models, including one proposed by Smerd (1950b). Unfortunately, since the distributions were measured at only the one frequency it was not possible to determine exactly which parameters in the models best matched the observations, although they were consistent with Smerd's model for a 10^4 K chromosphere and a $0.3\text{-}3.0 \times 10^6$ K corona.

The North-South Solar Grating Array became operational in September 1953. This allowed the simultaneous scanning of the Sun by the east-west and north-south beam orientations as shown in Figure 107.

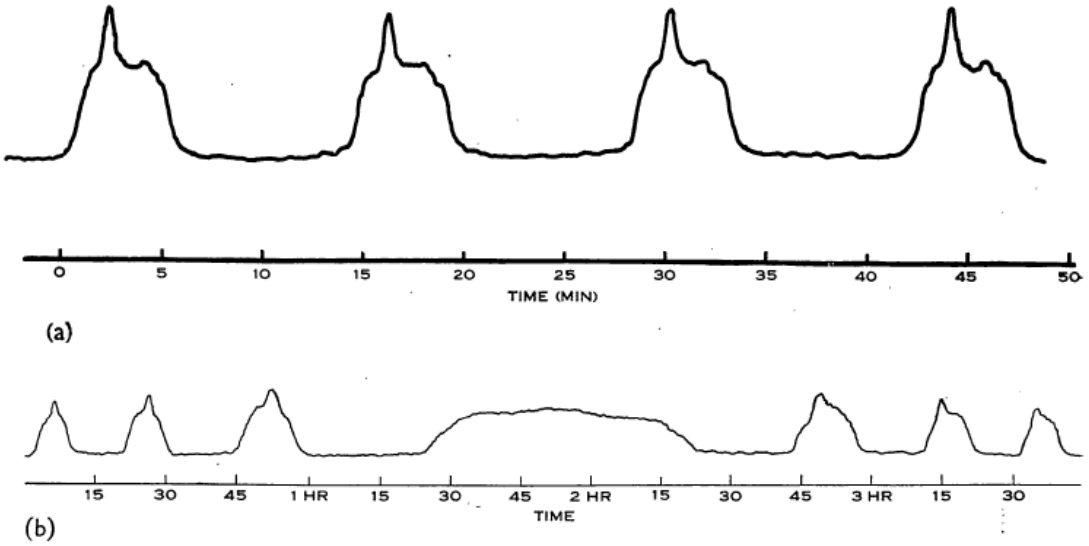

Figure 107: An example of the Sun passing through several of the beams of the east-west (a) and north-south (b) beams of the Grating Arrays (after Christiansen and Warburton, 1955a: 477).

Over the course of a day a wide variety of scan angles could be observed and these could be extended further by observation over a period of months. Figure 108 shows the result of a one-dimension scan taken at different times on a single day and thus achieving scans at different orientations relative to the Sun's axis of rotation.

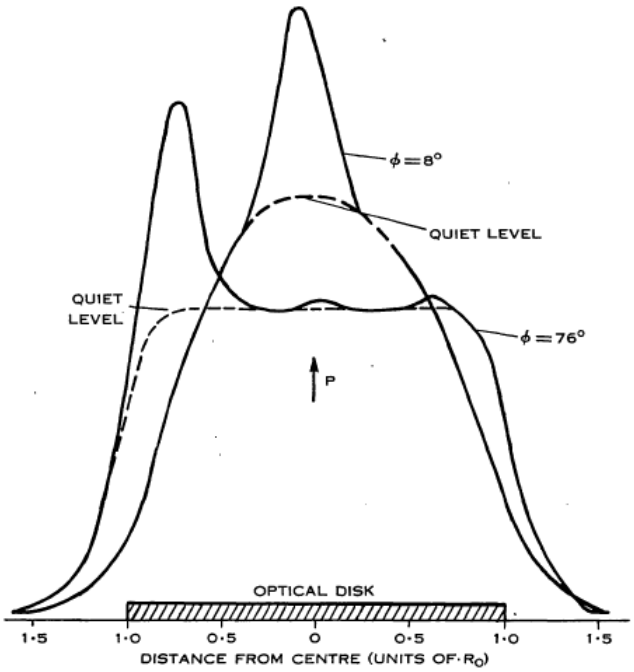

Figure 108: An example of a one-dimensional scan taken for two different scanning angles by observing at different times on the same day (after Christiansen and Warburton, 1955a: 478)

In order to produce a two dimensional image, a cosine Fourier analysis of the individual one-dimensional distributions for the different scanning angles was performed. It is important to note that by using the cosine Fourier analysis Christiansen assumed the Sun was symmetrical and phase was ignored. The numerical value for each scan was plotted radially corresponding to the direction of the scan and then strip integrated with the strip summations being perpendicular to the scan angle. The cosine Fourier transform of the strip integrals was then taken to give radial cross-sections of the brightness distribution. The final two-dimensional distribution was then constructed by plotting each of the radial cross sections and plotting contour lines joining points of equal intensity. This tedious process took months of calculation and plotting by hand to produce a single two-dimensional image as shown in Figure 109. For comparison, Figure 110 shows a photograph of the Sun taken during the total solar eclipse of 30 June 1954.

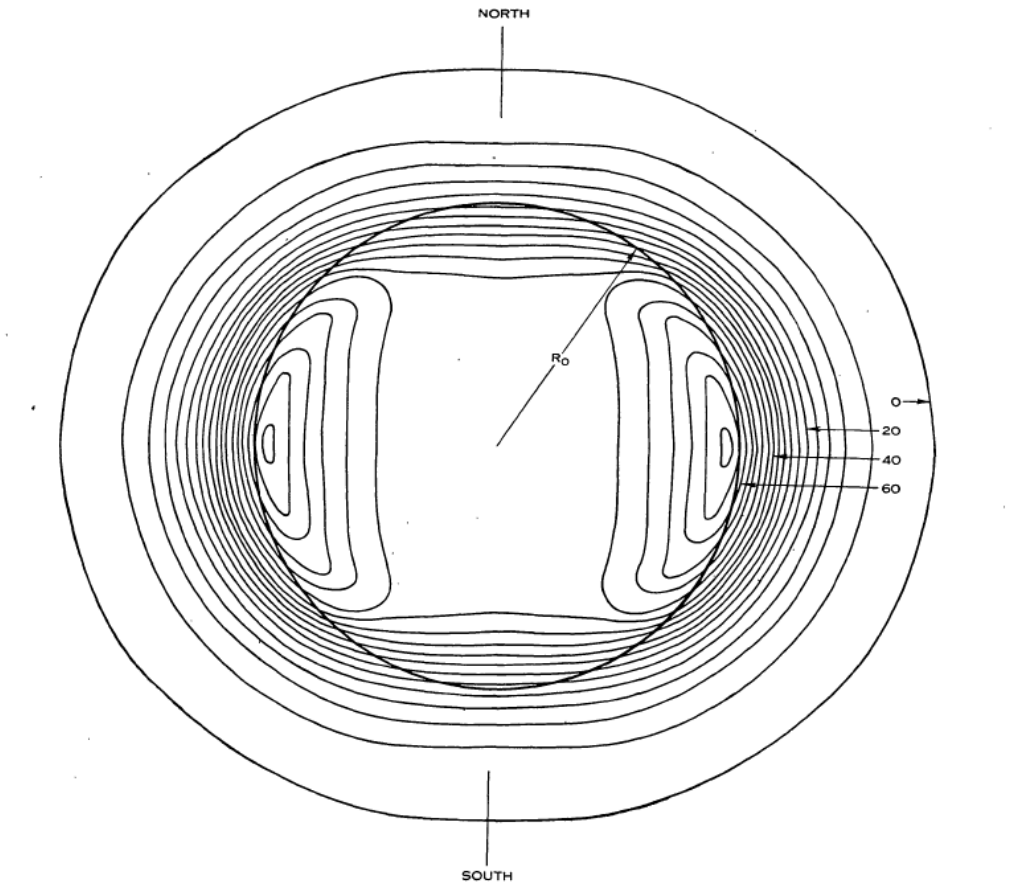

Figure 109: An example of the derived two-dimensional image of the radio brightness distribution across the Sun at 1,420 MHz. The central brightness temperature is 4.7×10^4 K and the maximum peak temperature is 6.8×10^4 K. Contours are spaced at equal intervals of 4×10^3 K (after Christiansen and Warburton, 1955a: 482).

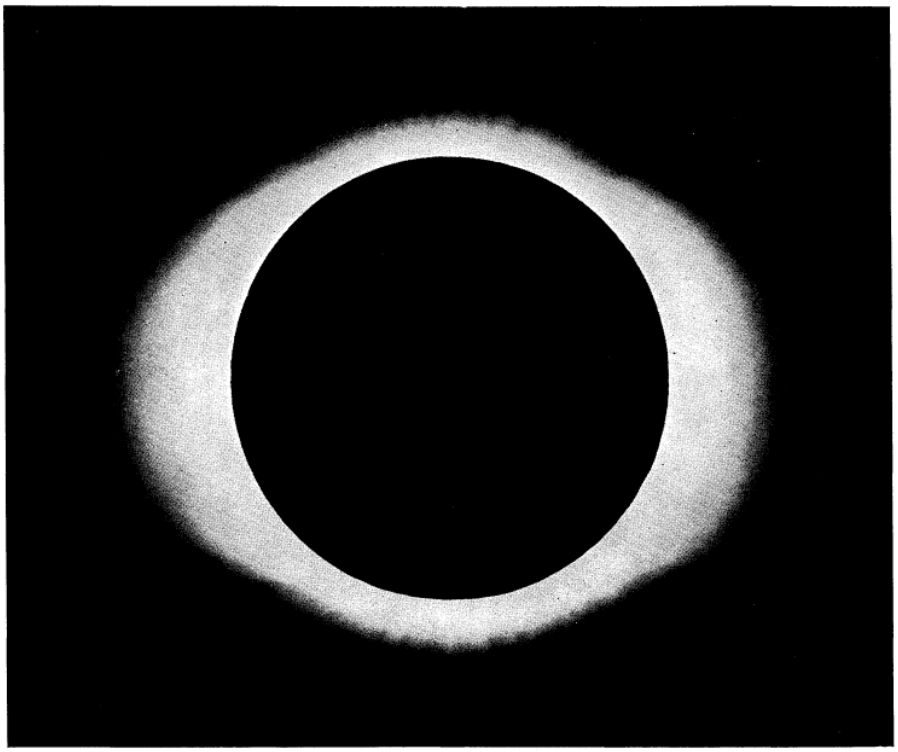

Photograph of the Sun at the total eclipse June 30, 1954 (M. Waldmeier).

Figure 110: Photograph of the Sun during the total solar eclipse of June 30, 1954 (after Christiansen and Warburton, 1955a: Plate 2).

The hand calculations were performed by Christiansen and Warburton with the assistance of Swarup using electronic calculators (but not computers!). Bracewell has stated (1984) that the graphical method that was used for this reconstruction was adopted from his method of cord construction, although his contribution was not acknowledged in the published paper.

Bracewell had been assigned by Pawsey to work on the issue of fan-beam reconstructions and he shared an office with Christiansen and Minnett during this period. In 1956 Bracewell published a paper on strip integration based on this work. The paper included a description of the use of projection-slice theorem which would be used to underpin modern imaging techniques including computerised tomography and medical imaging (see Bracewell, 1956, 2005).

Staff at Radiophysics developed Australia's first electronic computer, which was called CSIRAC (CSIR Automatic Computer). This was the fifth (or fourth depending on the definition of 'operational') electronic stored (digital) program computer developed in the world and ran its first program in November 1949 (McCann and Thorne, 2000). Figure 111 shows an image of CSIRAC.

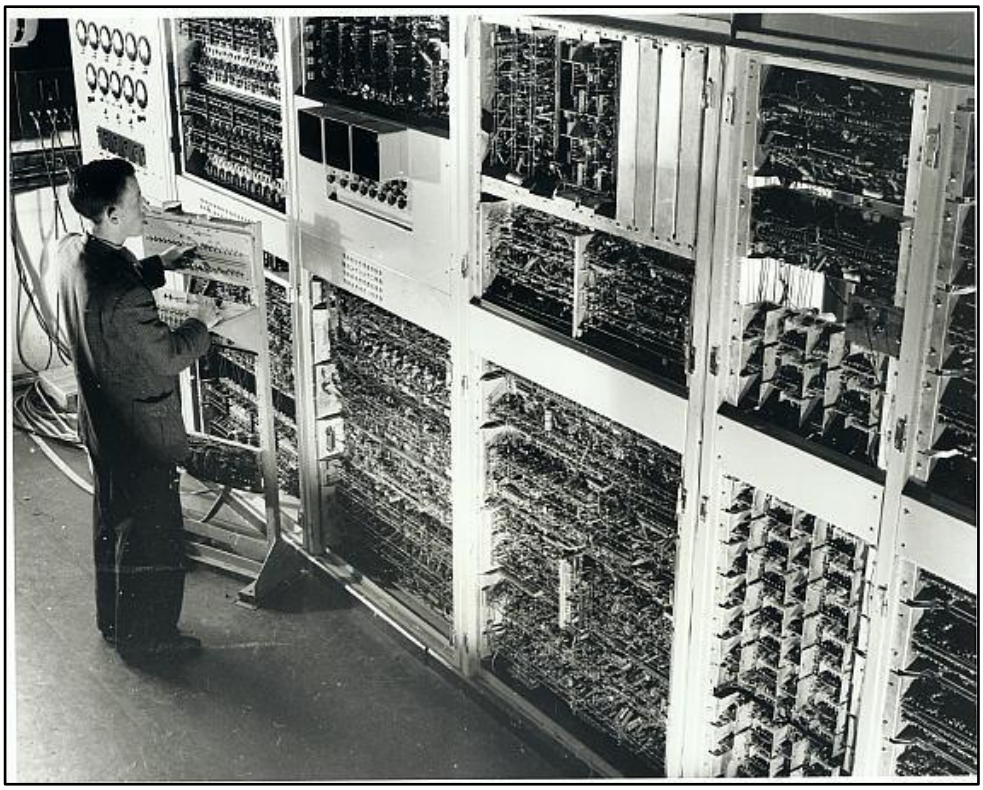

Figure 111: CSIRAC at the Radiophysics Laboratory in June 1952 (Courtesy of Geoff Hill).

CSIRAC was originally called CSIR Mk1 and was used for a variety of applications in the Division including astronomical table generation. However, the leap of imagination needed to apply this capability to the calculation of Fourier Transforms to produce imaging in radio astronomy was not made while the computer was operated by Radiophysics. Given the close proximity of the work on the computer and the repetitive nature of the manual calculations, it is surprising that this connection was not made. In 1955 it was decided not to pursue the further development of computers in the Division, and CSIRAC was transferred to Melbourne University in 1956. Some years later Cambridge made the inevitable connection by applying electronic computers to Fourier Transformations, and this went on to become the mainstay of imaging in radio astronomy. In fact, CSIRAC was eventually used for Fourier analysis after its transfer to the University of Melbourne. This application of Fourier techniques was however by Jim Morrison from the Chemical Physics section of the CSIRO who was measuring ionisation efficiency curves, and was based on his previous experiences in X-ray crystallography. Working with the programming team he implemented the equivalent of a Fast Fourier Transform routine to perform this analysis (see McCann and Thorne, 2000: 136).

Figure 109 reveals that the two-dimensional distribution of radiation at 1,420 MHz was not circularly symmetrical and showed a strong correlation with the optical form of the corona as seen at times of total solar eclipse. The elliptical source extended 1.6 times further at the equator than at the poles. The limb-brightening effect was also not evenly distributed, with the strongest brightening at the equator and

practically no effect at latitudes above 55°. Christiansen and Warburton (1955a) noted that this latitude corresponded to the latitude at which structural changes in the corona could be seen optically at times of sunspot minimum, and that comparing the outline of the 8,000 K contour to the photographic image showed a strong correlation. Christiansen and Warburton (ibid.) concluded that the majority of the radiation at the centre of the image emanated from the chromosphere, while the limb-brightening effect was due to the greater depth of view of the corona with its higher temperature gradient.

Observations during 1952, 1953 and 1954 showed no change in the shape or level of temperature of the quiet component of the solar radiation (Christiansen and Warburton, 1955a). This supported the assertion made by Piddington and Davies (1953b) that previous observation of changes in the base level were due to the lag effects of changes in sunspot activity.

During Christiansen's visit to Meudon Observatory in France during 1954, the East-West Solar Grating Array was modified by Swarup and Parthasarathy to operate at 500 MHz. From July 1954 to March 1955 they performed daily observations to obtain one-dimensional distributions across the solar disk. Figure 112 shows examples of superimposed observations over a period of several months.

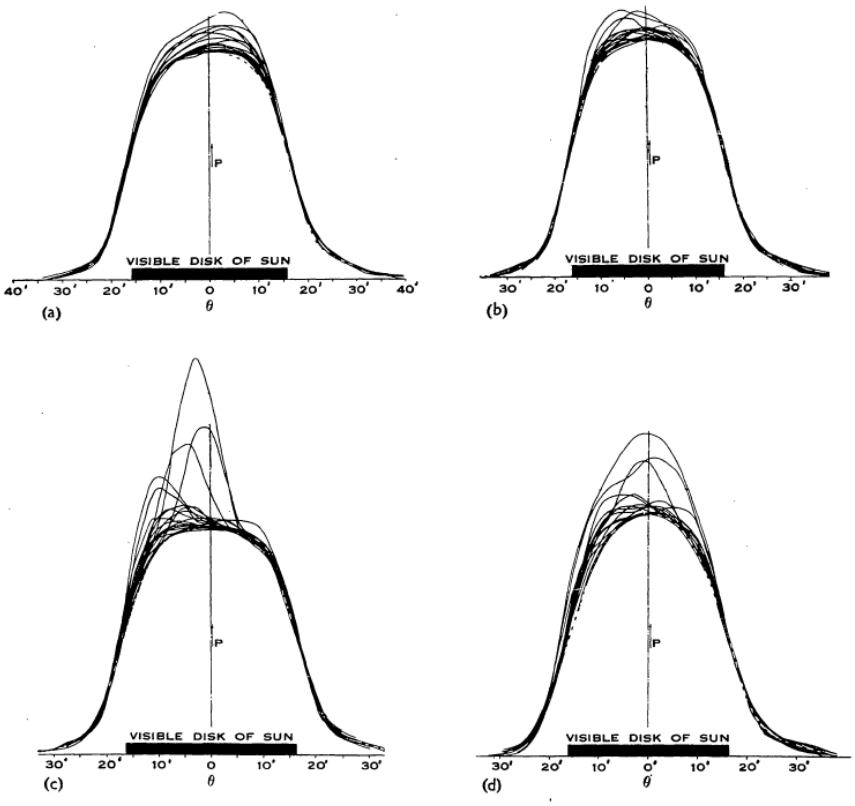

Figure 112: Superimposed one-dimensional brightness distributions at 500 MHz taken between July 1954 and March 1955. Observations were taken from (a) 18 July to 5 August $\phi = 3^{o}$; (b) 9 August to 1 September $\phi = 11.5^{o}$; (c) 15 December to 3 January $\phi = -3^{o}$; (d) 7 February to 4 March $\phi = 26^{o}$; ϕ represents the angle in arc minutes between the Sun's central meridian and the aerial beam (after Swarup and Parthasarathy, 1955b: 490).

Of major interest at the time was the comparison of these results with earlier observations by Stanier at 500 MHz using a two-element interferometer (Stanier, 1950). Stanier's observations, which occurred closer to the maximum of the solar cycle, had not disclosed limb-brightening. Figure 113 shows the comparison of the two different radial distributions detected.

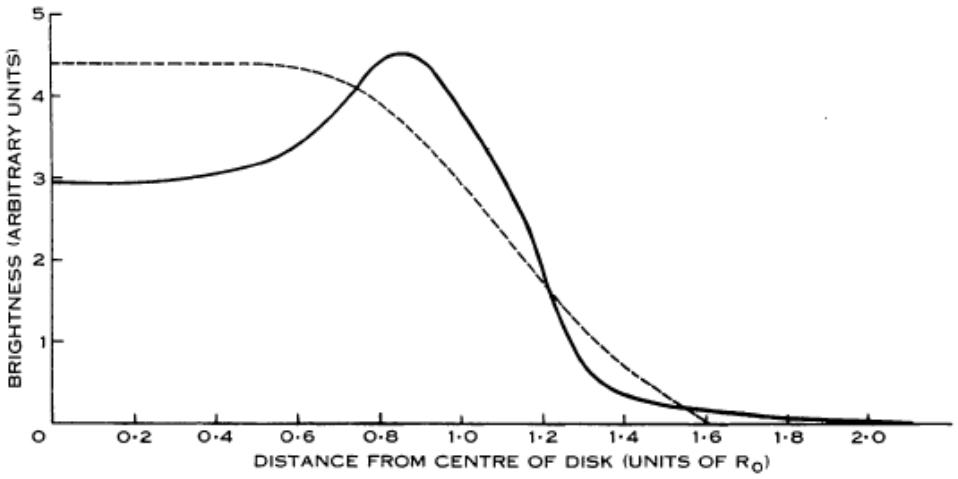

Figure 113: Radial brightness distributions at 500 MHz comparing Stanier's result (dotted) and Swarup and Parthasarathy's observations (after Swarup and Parthasarathy, 1955b: 493).

The difference in the results was suggested by Swarup and Parthasarathy (1955b) to be related to problems with the two element interferometry technique used by Stanier.

Later observations at 500 MHz (O'Brien and Tandberg-Hassen, 1955) using a two-element interferometer also detected limb-brightening, and Swarup and Parthasarathy's results were in good agreement with these. Swarup and Parthasarathy (1955b) also noted that like the higher frequency observations by Christiansen and Warburton, the source emission did not appear to be circularly symmetrical. Although they were observing only with the modified East-West Array, Swarup and Parthasarathy were able to achieve a variety of scan angles by viewing at different times during the day and over a period of eight months. Figure 114 shows the different brightness distributions for the aerial beam positioned at 90° and 64° to the Sun's central meridian. This indicates that the maximum width of the source occurred in the equatorial regions.

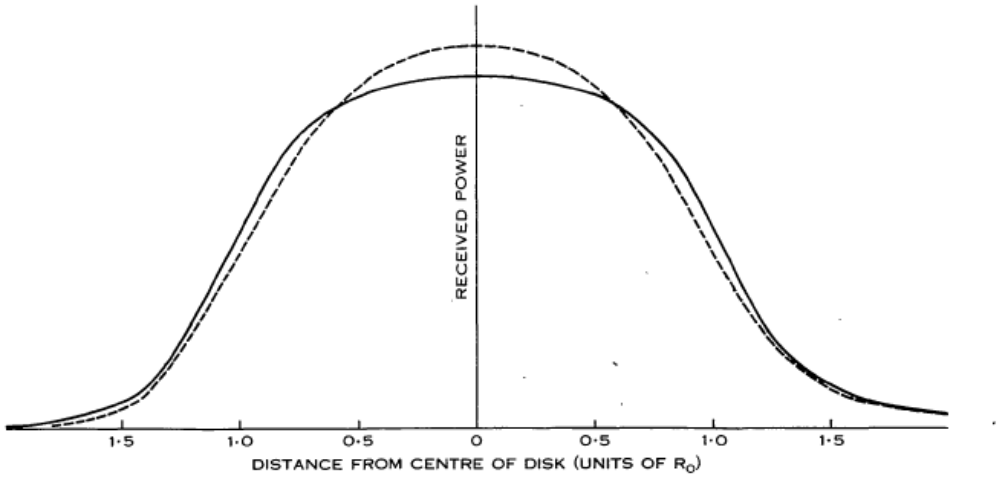

Figure 114: Brightness distributions at 500 MHz for the aerial beam at 90º (solid line) and 64º (dotted line) to the Sun's prime meridian (after Swarup and Parthasarathy, 1955b: 491).

Swarup and Parthasarathy (1955b) calculated that the base apparent temperature of the quiet Sun at 500 MHz was 3.8×10^5 K. This compared to a temperature of 5.4×10^5 K derived by Stanier. By comparison to the previous eclipse observations, they concluded that there was evidence to suggest a change in the base level temperature of the quiet Sun as a result in the decrease in the solar cycle. This is interesting because the conclusion appears to make no reference to the earlier suggestions made by Piddington and Davies (1953b), and later reinforced by the longer-term observations of Christiansen and Warburton (1955a), that this change was not in the base level, but due to the lag in sunspot activity.

In 1957, Christiansen, Warburton and Davies (1957) published the fourth and final paper in their solar series based on observations from the Solar Grating Array. This paper examined the slowly-varying component based on the observations during 1952 and 1953. Part of their analysis concluded that the lag effect first suggested by Piddington and Davies (1953b) was not sufficient to provide the sole explanation of the decline in base temperatures. They concluded that it was likely that both the quiet component and the slowly-varying component varied depending on the solar cycle. They also concluded that the original correlation method proposed by Pawsey and Yabsley (1949) gave results that were quantitatively correct. This analysis, although not published at the time, probably influenced Swarup and Parthasarathy to re-introduce the suggestion of a variation in the level of radiation from the quiet Sun.

Christiansen, Warburton and Davies's paper provided a clear illustration as to why the sunspot area correlation, although strong, was in fact only a partial correlation. This is shown in Figure 115 where three groups are indicated; old sunspot regions, new regions and regions that had reached maximum intensity.

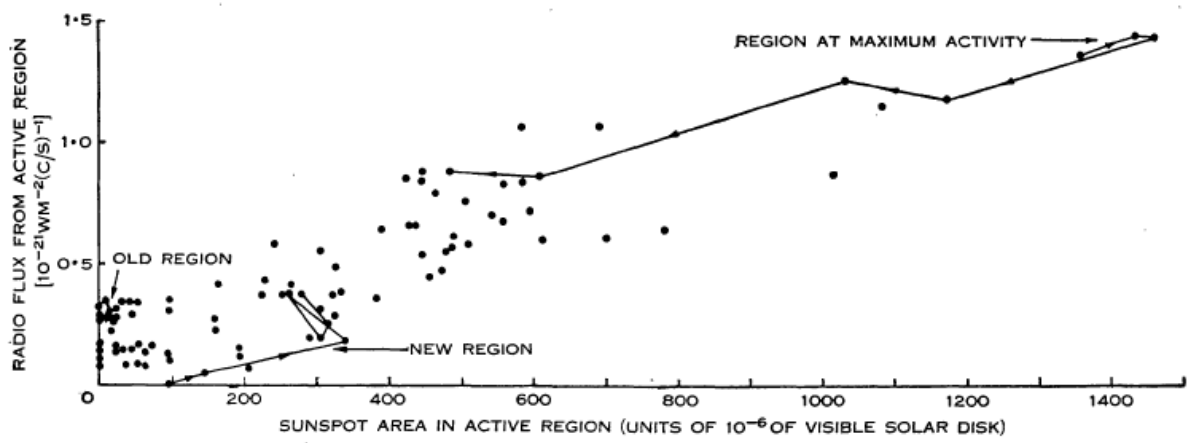

Figure 115: Scatter diagram of sunspot area to radio flux. The day-by-day development of one new and one mature sunspot are shown by line connected points with arrows showing the direction of development (after Christiansen et al., 1957: 511).

The correlation is clearly strongest for areas at maximum intensity. The new region shows a short delay before the radio emission becomes stronger, hence the moderate correlation, and the old fading sunspots show continued radio emission and the weakest correlation.

Christiansen, Warburton and Davies reached the conclusion that the radio emission appeared to be associated with plage faculiare rather than with sunspots themselves. The plage faculiare are the areas in the photosphere and chromosphere where sunspot groups grow and decay due to strong localised magnetic fields. Christiansen, Warburton and Davies based this on comparison of spectroheliograph observations from Mount Stromlo and the Solar Grating Array observations. Figure 116 shows an example of the comparisons where the vertical lines indicate the maximum point of a one-dimensional scan.

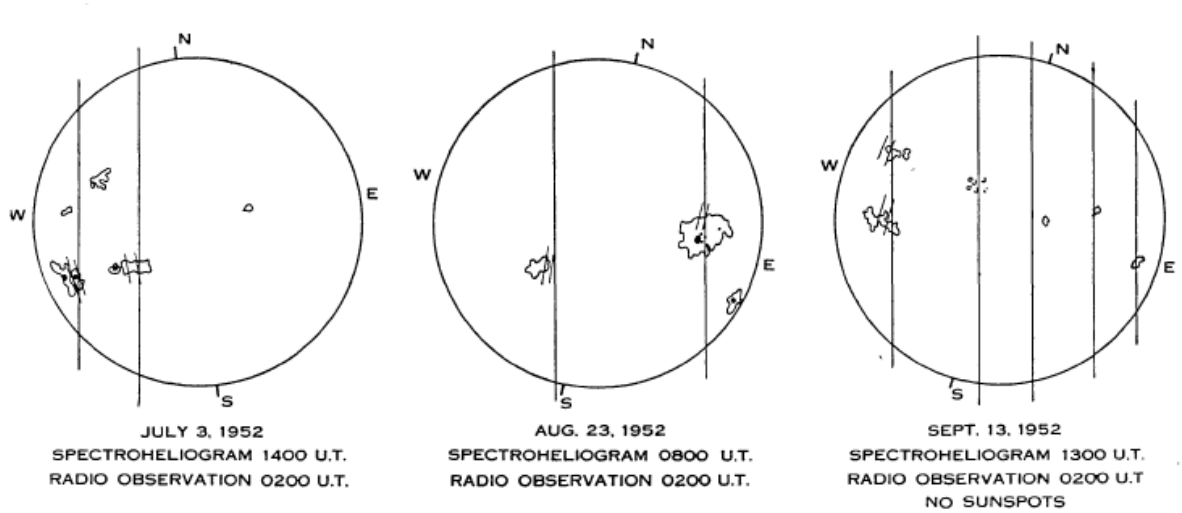

Figure 116: Spectroheliograms showing plague faculiare (Ca *K*) regions with maximum 1,420 MHz emission position lines from one-dimensional scans show as vertical lines (after Christiansen et al., 1957: 506).

A similar conclusion had earlier been reached by Dodson (1954) based on a comparison of her optical observations with Covington's radio observations, and this was discussed with Pawsey following an introductory lecture during the August 1955 IAU symposium on Radio Astronomy at Jodrell Bank (Allen, 1955: 262).

Using an analysis of the relative rates of rotation of the optical and radio sources, Christiansen, Warburton and Davies concluded that the 1,420 MHz radio emission emanated in a region about 24,000 km above the photosphere. They also found a correlation of r = 0.85 between the size of the plages and the sizes of the radio sources and noted that it appeared that the sources behaved like thin disks lying parallel to the photosphere.

In 1958 Swarup and Parthasarathy published their second and final paper on the 500 MHz observations using the modified East-West Grating Array. This paper dealt with their observations of the localised bright regions of radiation during the period July 1954 to March 1955 (Swarup and Parthasarathy, 1958). The paper found similar characteristics to those discussed by Christiansen, Warburton and Davies (1957). The sources were closely correlated with the positions of the chromospheric faculae, they were of the order of 3 to 6 arc minutes in size, and they appeared to be localised to regions approximately 35,000 km above the photosphere. Perhaps the most interesting finding was the observation of some variability in the localised sources. Figure 117 shows an example of the variation in the signal as the Sun passes between two adjacent beams.

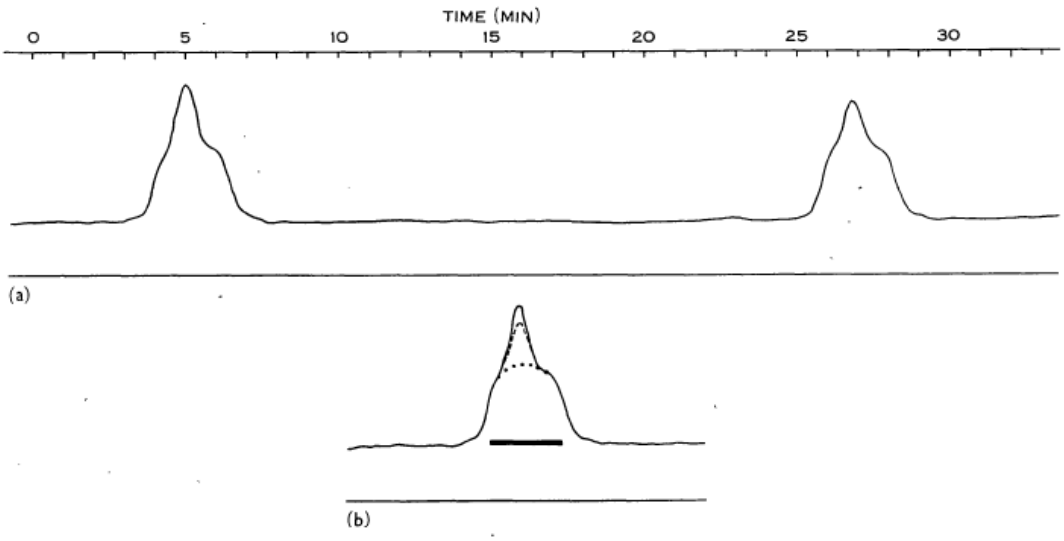

Figure 117: The Sun passing through two adjacent beams (top) and the two responses superimposed (bottom). The dotted line in the bottom graph shows the quiet Sun and the difference in strength of the discrete source in the two beams (after Swarup and Parthasarathy, 1958: 345).

These variations were observed on six occasions and lasted for periods of up to half an hour. This provided strong evidence for the non-thermal origin of some of the energy produced, as it was believed that such a rapid thermal change could not occur to an area the physical size of the source.

Swarup and Parthasarathy's paper was one of the last papers based on observations of solar sources at Potts Hill. By this stage Christiansen had already moved his research to the Fleurs field station using the newly constructed Chris Cross array (Orchiston, 2004c) and the remainder of the original Potts Hill Grating Array was transferred to India.

The final solar research paper from Potts Hill was based on observations of the 8 April 1959 partial solar eclipse (Krishnan and Labrum, 1961). The eclipse was observed both at Potts Hill using the 16-ft × 18-ft Parabola as a high sensitivity total power radiometer and at Fleurs using the Chris-Cross array to help identify areas of enhanced radiation. Figure 118 shows the local circumstances of the eclipse.

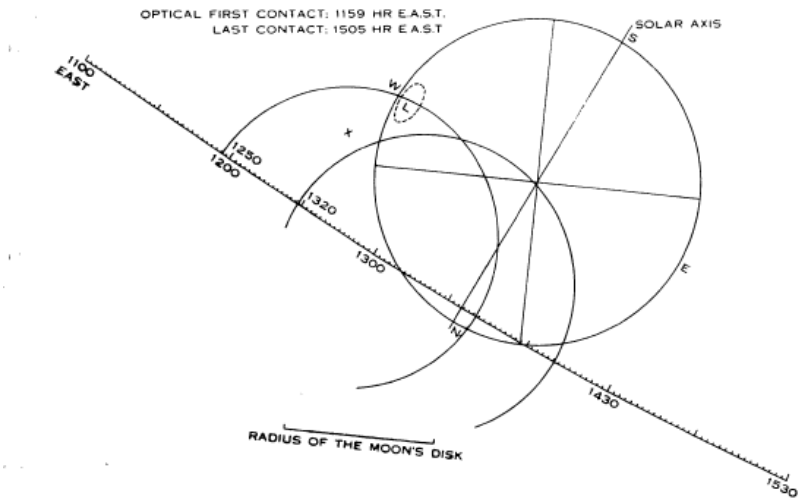

Figure 118: The circumstance of the 8 April 1948 partial solar eclipse as viewed from Potts Hill (after Krishnan and Labrum, 1961: 406).

The receiver used for the eclipse observations was a conventional superheterodyne type preceded by a Dickie switching system. It operated at 1,423 MHz with a bandwidth of 500 KHz. At this frequency its effective beamwidth at the half power points was 2.3º. The theoretical resolution that can be achieved by observing an eclipse is limited only to the diffraction of the Moon's limb and at 1,423 MHz this is ~0.1 arc minutes. During the eclipse the Moon's disk moved across the Sun's disk at ~1 arc second in 4 minutes of time. Therefore, any region on the solar disk with a size greater than 0.25 arc seconds and with more that 1% of the total flux could be resolved. The Chris-Cross was used to determine the location of areas of enhanced radiation on the solar disk during the eclipse so that their effect could be taken into account in obtaining a brightness distribution across the quiet Sun. The resolution of the Chris-Cross at this frequency

was ~4 arc minutes. Figure 119 shows the brightness distribution across the solar disk obtained during the eclipse with the Chris-Cross.

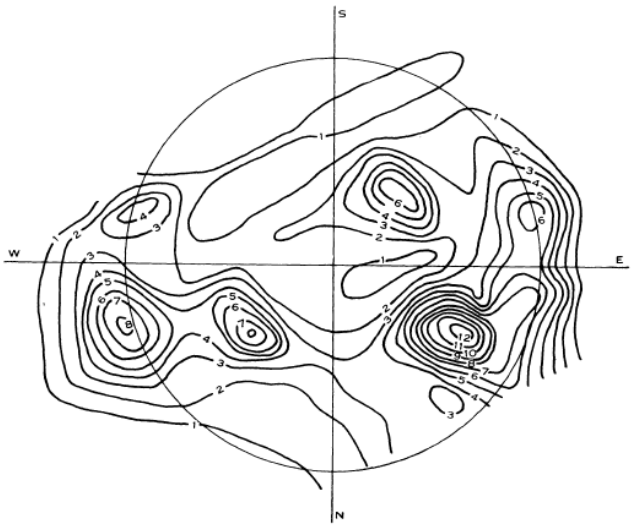

Figure 119: The brightness distribution during the partial solar eclipse of 8 April 1959 as observed by the Chris Cross. The contour spacing unit is 10,000 K, aerial beamwidth ~4 arc minutes (after Krishnan and Labrum, 1961: 407).

The eclipse was successfully observed at Potts Hill (see Figure 120). No calcium spectroheliogram observations were available in Australia at the time, however one was provided by Dobson (now Dobson-Prince) working at the McMath Hulbert Solar Observatory in the U.S. This allowed Krishnan and Labrum to compare the distribution of plage faculaires seen in the K-line of calcium with their radio observations. They found a very close relationship between optical and radio plages, both in their intensity and their overall shape. The eclipse observations provided perhaps the most detailed demonstration of the relationship up until this time and certainly a more convincing set of results than the original work at Potts Hill that had suggested this association (Christiansen et al., 1957).

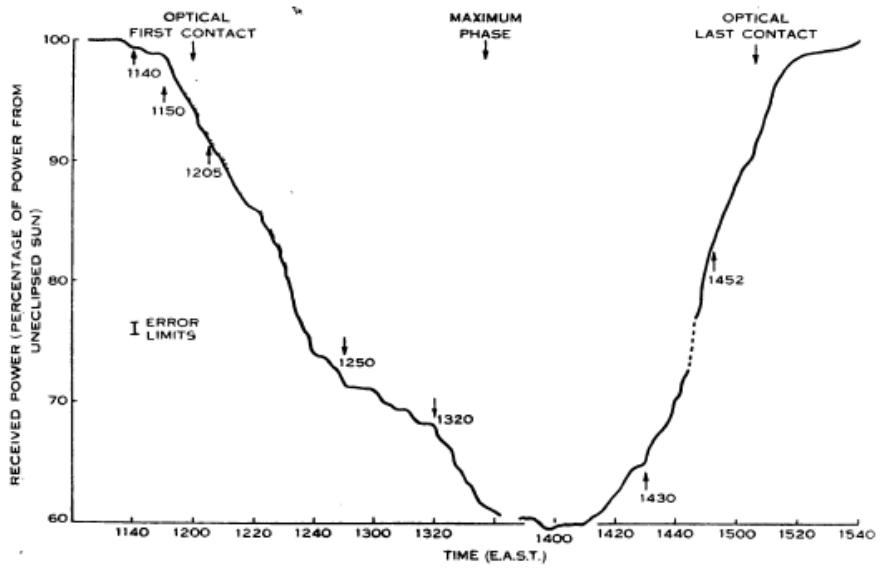

Figure 120: The eclipse curve obtained at Potts Hill for the 8 April 1959 partial solar eclipse (after Krishnan and Labrum, 1961: 408).

Krishnan and Labrum were also able to test a number of quiet Sun models against the eclipse observations. They found that the best fit was achieved by a model based on Christiansen and Warburton's (1955) work for sunspot minimum which showed limb-brightening at the equator, but absent at the poles. After allowing for an overall increase in brightness temperature by a factor of 2 to allow for the sunspot maximum, Krishnan and Labrum found that a stepped-up gradient of limb-brightening (the ear component) provided the best fit. It is likely that the lower resolution of the grating arrays used by Christiansen and Warburton for measurements of limb-brightening would have washed out the steeper gradient and therefore the ear would not appear as pronounced. The higher resolution of the eclipse observation allowed the steeper gradient to be more accurately measured. Figure 121 shows a comparison of the eclipse observations to the distribution model with the enhanced limb-brightening ears.

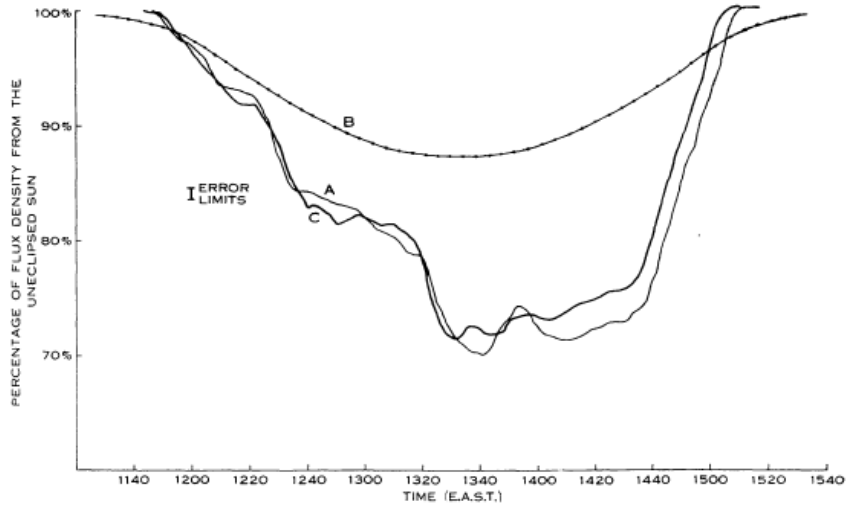

Figure 121: Line-A represents the eclipse observation adjusted for the emissions to lie radially at a height of 70,000 km above the photosphere. A theoretical model based on enhanced ears in the limb-brightening is then used to obtain the quiet Sun component during the eclipse (Line–B). Line-B is then subtracted from the eclipse curve to produce Line-C. The close fit of Line-A and Line-C was taken to indicate that the model with the enhanced ear component of limb-brightening was the best representation of the quiet Sun distribution (after Krishnan and Labrum, 1961: 415).

Figure 122 shows the different quiet Sun models tested against the eclipse observations. The model marked (4) in the diagram gave the best fit to the eclipse observations.

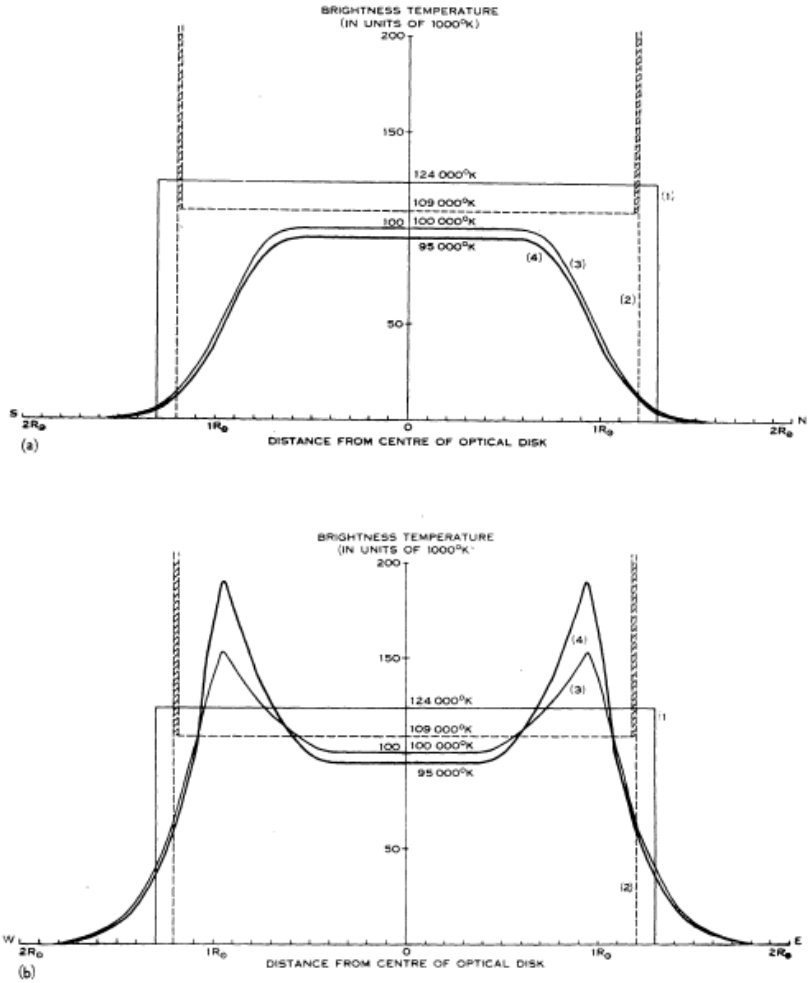

Figure 122: Four different quiet Sun models were tested against the eclipse observations. Model (1) assumes a uniform disk of radius 1.3 times the photospheric radius. Model (2) assumes a uniform disk of radius 1.2 times the photospheric radius containing 75% of the quiet Sun flux with a narrow ring around the limb containing the remaining 25%. Model (3) was based on the Christiansen and Warburton (1955) distribution with temperatures scaled up by a factor of two to account for the sunspot maximum. Model (4) is the same type of distribution as Model (3) but with the temperature gradient in the ear component of limb-brightening scaled up by a factor of 2. The upper graph shows the model distribution along the solar axis and the lower graph across the solar axis (after Krishnan and Labrum, 1961: 417).

Krishnan and Labrum were also able to measure the peak brightness temperatures of the radio plage and found temperatures of the order of 1.5×10^6 K for the larger regions. This indicated that these regions were in the range of normal coronal temperatures reinforcing the hypothesis that the slowly varying component originates in dense regions of the corona that lay above plage faculaires.

These observations were the last published solar observations at Potts Hill. The 1948 partial solar eclipse had been one of the first major research successes and it is fitting that the final observations were also of a solar eclipse some 11 years later.

10.5.1.4. Solar Burst Observations

Before beginning the discussion on the burst observations at Potts Hill, it is worthwhile reviewing the developing classification scheme that was in use in the early 1950s in Australia. For this purpose the classification of solar radio waves from Pawsey and Bracewell (1955) has been used. The basic component, or quiet Sun, and the slowly-varying component have been discussed in the previous Sections. Three other broad classifications were proposed. These are outlined in Table 3.

Table 3: Classification of solar radio sources (after Pawsey and Bracewell, 1955: 150).

	Noise Storm	Unpolarised Burst	
		Outburst	Isolated Burst
Wavelength	1-15 m	1 cm – 15 m	50 cm – 15 m
Polarisation	Strongly Circular	Random	Random
Place of Origin	Small area above sunspot	Small area – rapid movement	Small area
Associated optical features	Large Sunspot	Flare	Unknown
Remarks	With or without numerous bursts	No certain distinction	

Figure 123 provides a useful illustration of the different source classifications by wavelength.

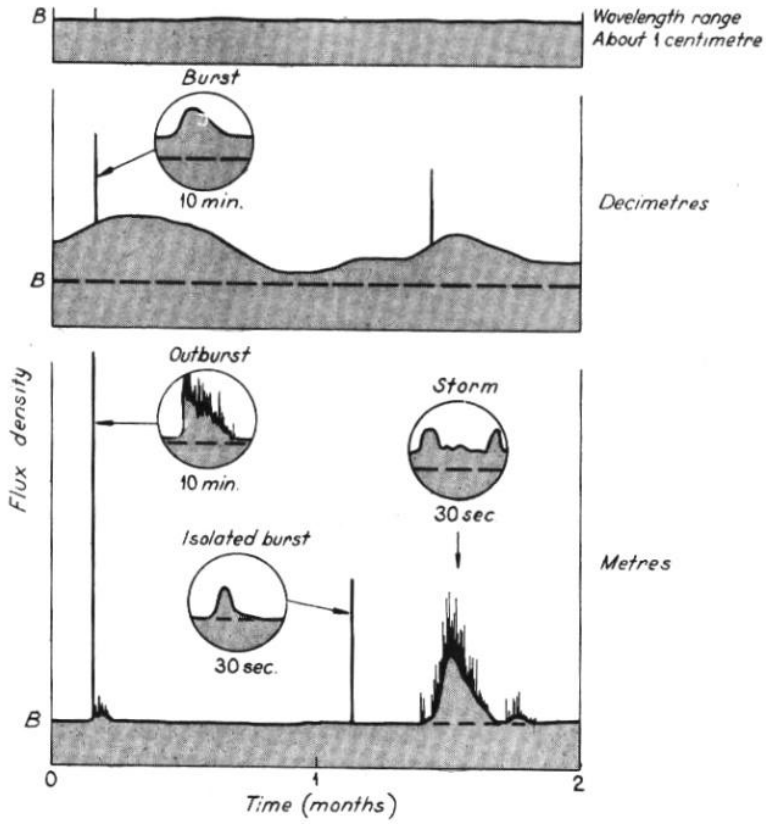

Figure 123: Idealised examples of solar radio sources in three broad frequency bands. The base level (B) increases approximately linearly with wavelength from an apparent temperature of 10^4 ºK at 1 cm to 10^6 at 1 m (after Pawsey and Bracewell, 1955: 147).

The first of the three classifications was Noise Storms. These tended to last for periods of hours to days and were named by Allen (1947) because of their similarity to magnetic storms. Individual bursts during the storm were generally for periods of seconds with irregular wave forms and amplitudes up to several hundred times the background level of radiation. The storms were always associated with large sunspot groups and showed strong circular polarisation.

The second type, Outbursts, were also named by Allen (1947). They were sporadic and infrequent events with durations of minutes and were randomly polarised. They could be of extremely high intensity, with the largest recorded outburst at the time going off the scale at 10^{13} K. This was recorded on 8 March 1947 at 60 MHz (Payne-Scott et al., 1947). In this instance the apparent temperature rose from 10^7 K to 10^{13}+ K in a matter of seconds. At decimetre wavelengths, many bursts occurred at the same time as metre wavelength outbursts and were thought to be part of the same phenomenon. In other cases there was no association. It was also believed that outbursts had an association with solar flares.

Examples of burst and outbursts at 200 MHz are given in Figure 124 based on Allen's original observations.

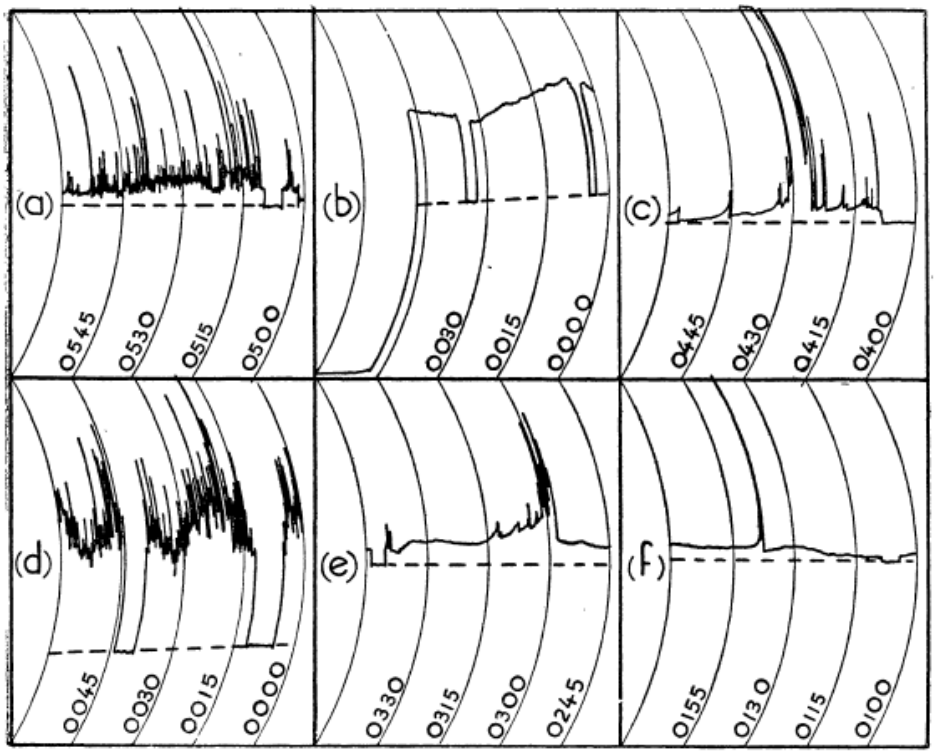

FIG. 1.—*Examples of solar radio-noise recordings. Set noise level is indicated by broken line. Note that timing is from right to left.*

(a) 1946 *September* 14. *Frequent bursts and low noise level.*
(b) 1946 *September* 20. *No bursts and high noise level.*
(c) 1947 *March* 8. *Large outburst.*
(d) 1947 *March* 10. *Frequent bursts and high noise level.*
(e) 1947 *March* 14. *Small outburst.*
(f) 1947 *March* 18. *One burst and fairly quiet.*

Figure 124: Examples of 200 MHz measurement of burst and outbursts (after Allen, 1947: 388).

The third type, Isolated bursts, were named by Pawsey (1950) because they were not associated with any other solar activity. They were generally of short duration (less than 10 seconds), randomly polarised with a moderately-simple waveform and often occurred in groups. They were also believed to have a relatively wide bandwidth of tens of megahertz. Payne-Scott (1949) referred to both outbursts and isolated bursts as 'unpolarised bursts' rather than distinguishing between classes.

While the solar work was underway at Potts Hill, Wild and McCready (1950) examined the spectral characteristics of solar bursts at the Penrith field station between February and June 1949. Based on these observations they proposed a new classification scheme that distinguished between the spectral characteristics of the bursts over time. This scheme would ultimately become the accepted nomenclature for solar bursts e.g. Type I, Type II, Type III (and later expanded to include IV and V). Type I bursts were characterised by having a narrowband width, with short-lived duration, and could occur in large numbers during noise storms. They were generally circularly polarised and were believed to be associated with sunspots. Type II bursts were characterised by a slow drift in frequency from high to low and appeared to

be associated with the sporadic outbursts and solar flare events. They were thought to be associated with Allen's outbursts. Type III events were characterised by a very rapid change in frequency from high to low lasting in the order of seconds and were believed to be equivalent to the 'isolated outbursts'. They were reasonably common and sometimes occurred in groups. Other sporadic burst events had a diverse range of spectral characteristics that fell outside of these broad classifications and it would be some years before further classifications were proposed. The original classifications and descriptions were published in a series of four papers (Wild, 1950a,b, 1951; Wild and McCready, 1950). Examination of the spectral characteristics and classification of the solar bursts became the major focus for Wild's group. A new field station was established at Dapto specifically for this pursuit and became operational in August 1952 (Orchiston and Slee, 2005a).

The solar burst research at Potts Hill was less concerned with spectral characteristics and more with the accurate location of the events and their association with other characteristics. For this reason Pawsey's classification is used in the following descriptions rather than the 'Type' nomenclature.

The first published records of solar burst observations from Potts Hill were included with Minnett and Labrum's 9,428 MHz observations of the partial solar eclipse of 1 November 1948 (1950). They noted that bursts were very rare at this short wavelength, occurring on only five occasions in 230 hours of observations. Intensities varied from 6 to 30 percent increases in base temperatures. Two of the bursts occurred at the same time as stronger decimetre bursts that were monitored independently. One of the bursts was associated with an observed radio fadeout. The radio fadeouts were believed to be caused by the arrival of intense ultraviolet radiation in the ionosphere as a result of a solar flare.

On 17 and 21-22 February 1950 two extremely large radio-frequency solar outbursts were observed across all of the frequencies being monitored at Potts Hill. This ranged from 62 MHz using a Yagi array, 98 MHz using the swept lobe interferometer, 600 MHz and 1,200 MHz using the 16-ft×18-ft ex-Georges Heights Paraboloid, 3,000 MHz using the 68-in Parabola and finally, 9,400 MHz using the ex-Search Light 44-in Parabola. In additional, 200 MHz observations were made using the 4-element Yagi at Mount Stromlo. Figure 125 shows the power flux levels recorded at the different frequencies for observations on both dates.

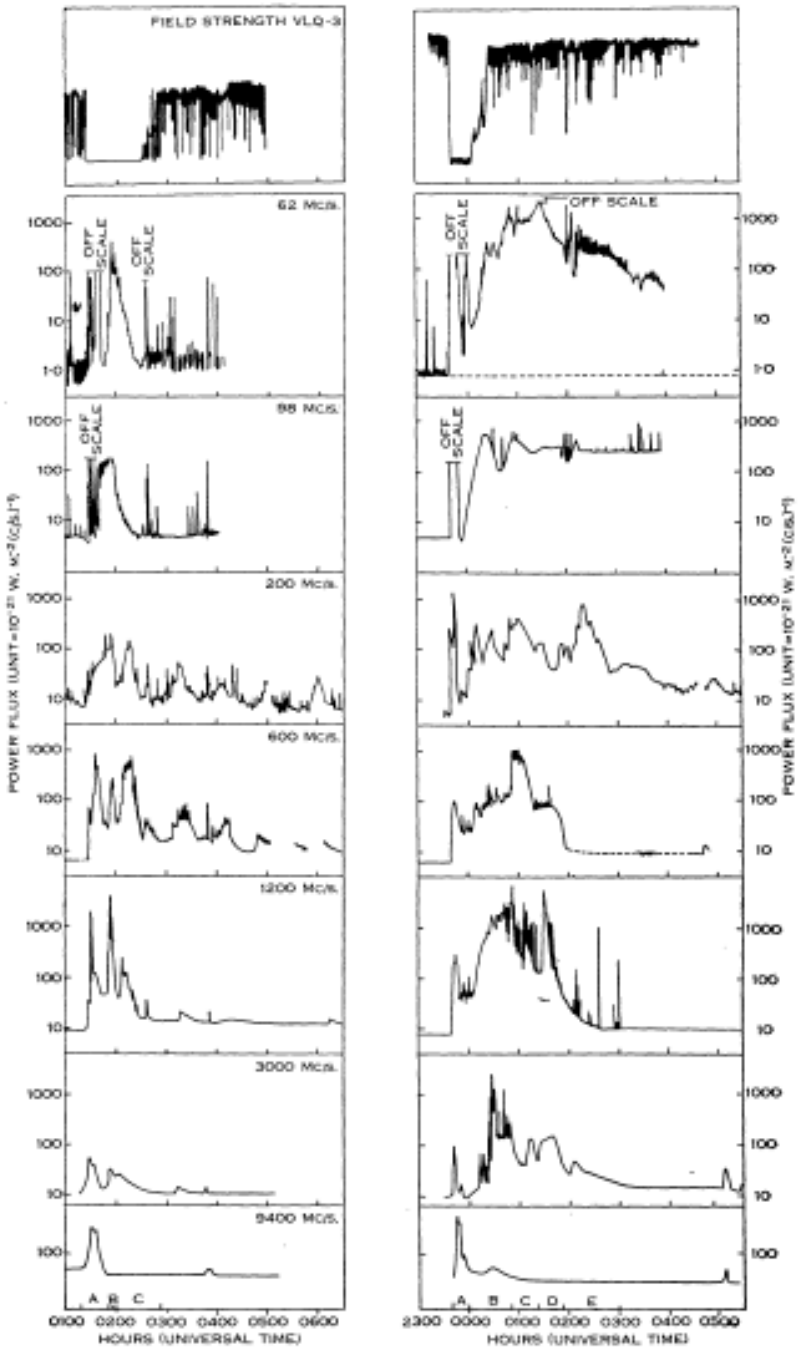

Figure 125: Power flux records for the seven frequencies observed on 17 (left) and 21-22 (right) February 1950. The top record is of the field strength for the radio station VLQ-3 from Brisbane, measured at Sydney. The 200 MHz record is from Mt Stromlo (after Christiansen et al., 1951: 53).

These observations were supplemented by a range of other data and included measurement of the short-wave radio fade out in Sydney of the Brisbane radio station VLQ-3 broadcasting at 9.6 MHz, sunspot and solar flare observations from Mount Stromlo, flare observations from Cater Observatory in Wellington, New Zealand, and from Kadaikanal Observatory in India, and magnetogram records from the Watheroo Magnetic Observatory in Western Australia. The combined observations were published in 1951

(Christiansen et al.). This demonstrates the increasingly cooperative approach being undertaken with other solar astronomy groups both domestic and international. Figure 126 shows a schematic of the start times of the outbursts as well as the radio fadeout and magnetic crochet measurement.

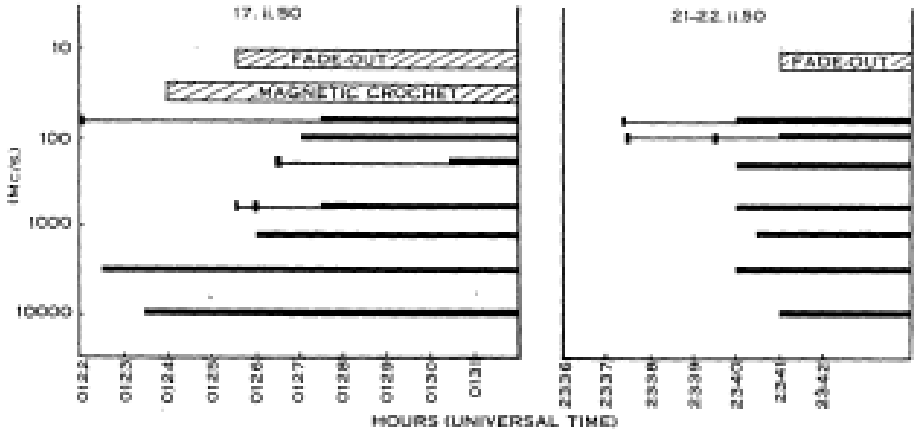

Figure 126: Schematic of the start time of the outbursts at the different frequencies, together with the radio fade out and magnetic crochet. February 17th (left) and 21-22nd (right) (after Christiansen et al., 1951: 57).

While generally similar, the two outbursts showed some distinct differences. On 17 February, the outburst was first received at higher frequencies, while the second outburst appeared almost simultaneously at all frequencies. No magnetic crochet was observed for the second outburst, although a magnetic storm was observed 35 hours after the second burst and was clearly linked to the outburst. Circular polarisation was observed in both cases with the low frequencies having a change in sense while the higher frequencies retained a fixed sense. In both cases flare activity was associated with the outburst and the radio fadeout.

Payne-Scott and Little were able to use the swept-lobe interferometer to determine the position and movement of the outbursts at 98 MHz. The first outburst occurred very close to the position of an observed flare and then slowly tracked eastward over a period of 30 minutes to a position 10 arc minutes to the east of the Sun's limb (Figure 127).

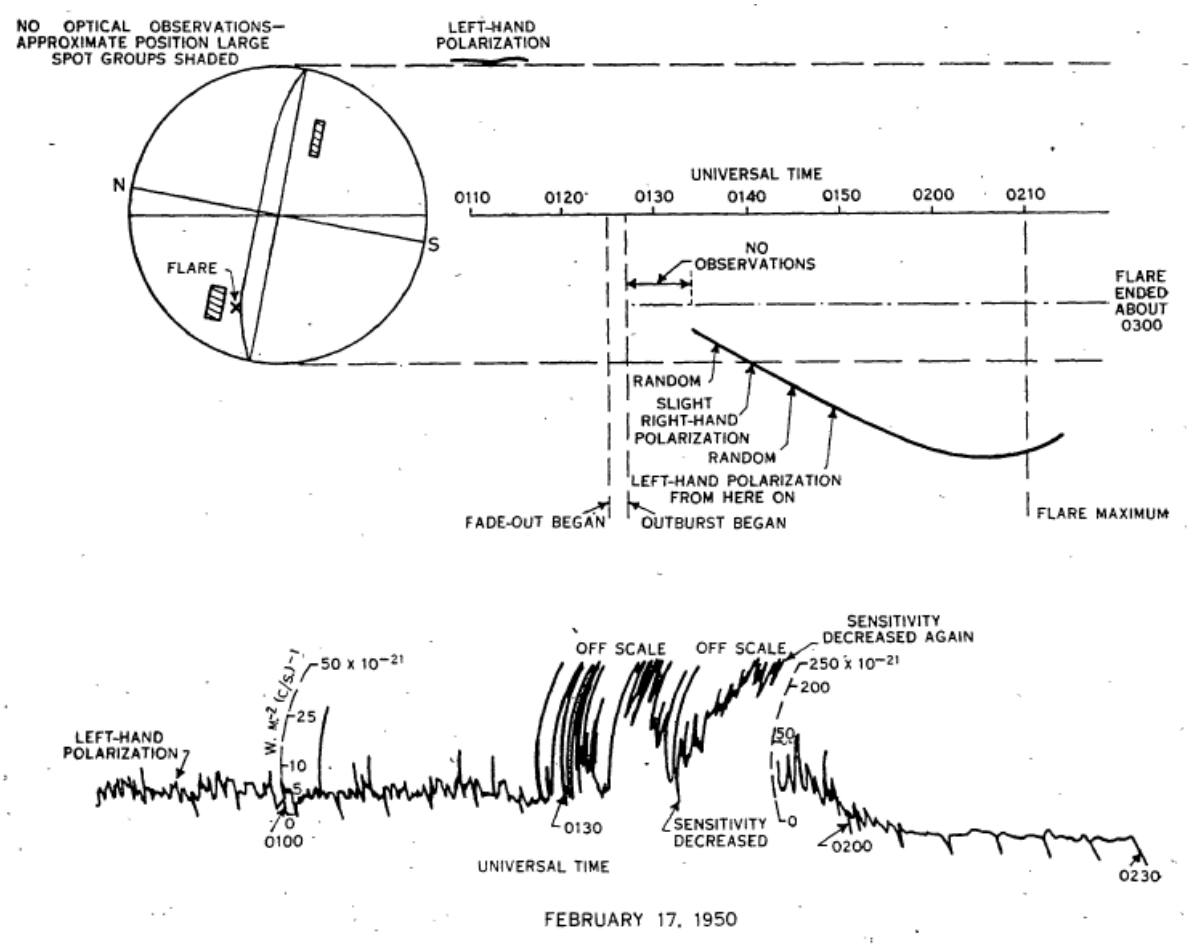

Figure 127: The outburst of 17 February 1950, showing the flare position on the solar disk, the outburst position movement and polarisation measurements. The lower chart shows the overall emission measurement at 98 MHz with timing marks indicated by the downward ticks (after Payne-Scott and Little, 1952).

An initial report on the 17 February 1950 outburst was published in a short article in *The Observatory* together with description of the swept-lobe interferometer (Bracewell, 1950).

The outburst recording shown in this paper (Figure 128) makes an interesting comparison with Figure 127. This version, although lacking the total flux charts, makes much clearer the initial one-dimensional positional strip measurement obtained from the swept-lobe interferometer against which the flare position is compared. The position movement also appears to have been considerably smoothed in the final analysis.

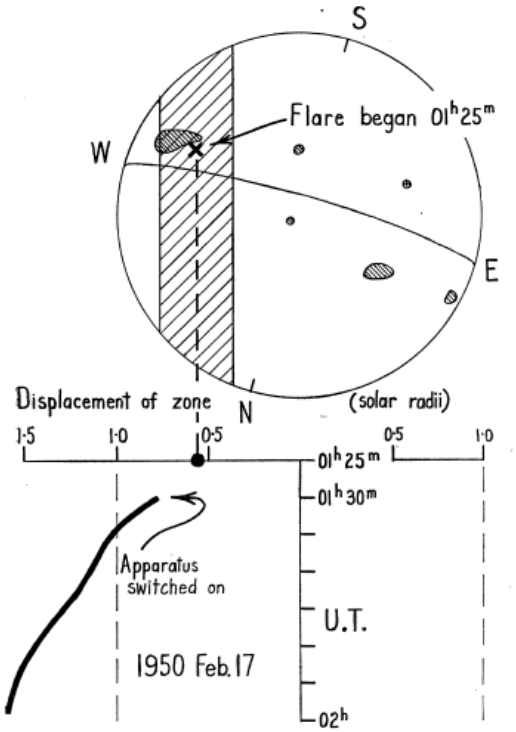

Figure 128: The earlier published version of the outburst of February 17, 1950 (after Bracewell, 1950: 186).

For the second outburst, position measurements only began after the outburst had been underway for approximately 27 minutes. At this time the source position was still close to an observed flare. Over the next 40 minutes it tracked out to the western limb of the Sun and then returned to the position of the flare after a period of some rapid oscillations between the limb and the flare (Figure 129).

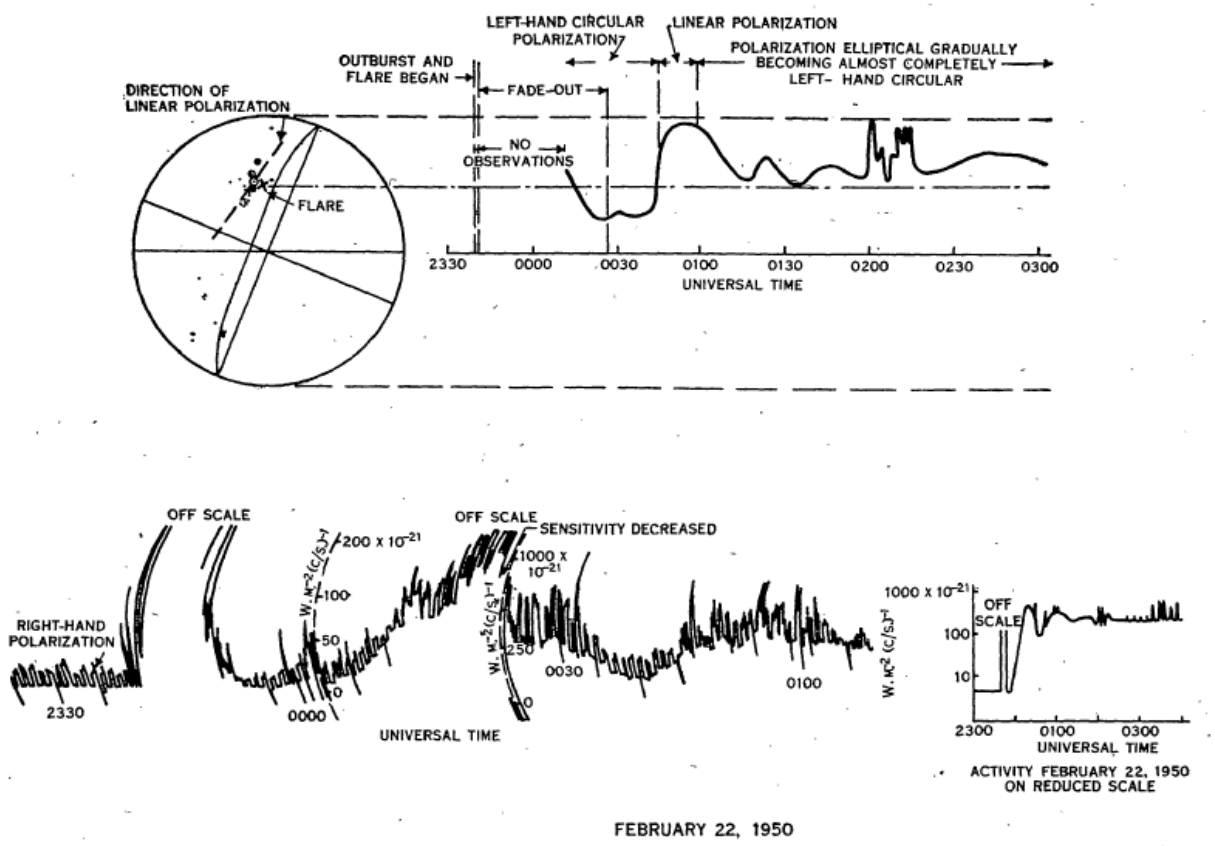

Figure 129: The outburst of 22 February 1950, showing flare position on the solar disk, the outburst position movement and polarisation measurements. The lower chart shows overall emission measurements at 98 MHz with timing marks indicated by the downward ticks (after Payne-Scott and Little, 1952: 35).

These measurements provided a clear indication that the outbursts were associated with solar flares and appeared to show movement of the source outward through the solar atmosphere. In today's terms these outburst would be classified as Type II bursts.

A further four outbursts were observed by Payne-Scott and Little and together with those of the 17 and 21-22 February 1950 made a total of six outbursts for which one-dimensional accurate positions and polarisation measurements were determined. Five of the events clearly showed an outward movement interpreted as the passage of an exciting agent through the solar corona. The most likely exciting agent was the corpuscular stream assumed to be responsible for terrestrial magnetic storms. The position measurements suggested that the origin of the outbursts was approximately 2×10^5 km above the photosphere and that they travelled outward at velocities ranging from 500 to 3000 km/sec. These velocity estimates were higher than those deduced by Wild from measurements of the frequency spectra of outbursts assuming a given electron density for the corona (Wild, 1950a: 406). However, if a higher electron density for the corona was assumed, then the results were in general agreement. One of the outbursts appeared to exhibit a downward motion (Figure 130). This was interpreted as the stream of corpuscles falling back into the Sun after first being ejected without the production of an initial outburst.

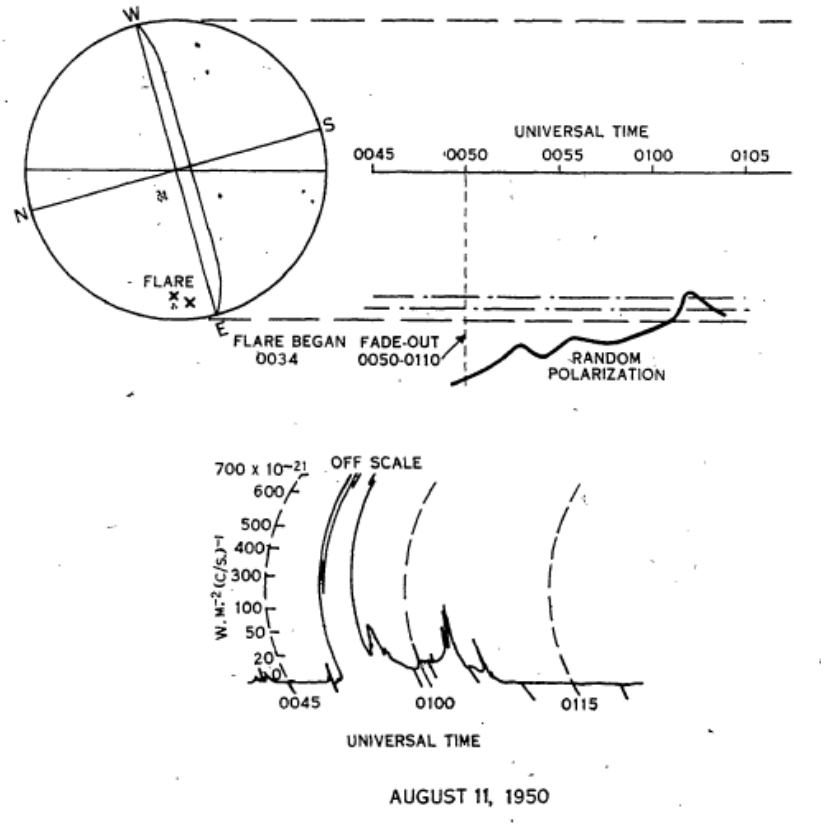

Figure 130: The 11 August 1950 outburst showing the inward movement of the outburst source (after Payne-Scott and Little, 1952: 34).

Polarisation measurements generally showed random polarisation in the early stages of the outburst, often followed by a second increase showing elliptical (mainly circular) polarisation. On two occasions linear polarisation was observed in the late stages. Payne-Scott and Little (1952) noted that the sense of polarisation followed the broad pattern that had been observed for noise storms whereby there appeared to be a relationship between the direction of polarisation based on the hemisphere of origination and the polarity of the largest sunspot in the group.

The reader should bear in mind that in interpreting these source position drift diagrams the paths shown are projections of a 3-dimensional movement onto the solar disc and corona.

While outbursts were known to be associated with chromospheric flares, up to this point no clear association had been made with other catastrophic optical events such as solar prominences. In the period 24 - 26 February 1953 three bursts were observed on the full range of frequencies being covered by daily observations at Potts Hill. The first burst occurred prior to a prominence erupting. The second burst occurred coincident with a prominence eruption that Davies also observed with the spectroheliograph that was in use at Potts Hill in support of the Solar Grating Array observations (Davies, 2005: 95). The prominence occurred on the northeast limb of the Sun and erupted to a height of 3-4 arc minutes above the

limb. The third, and most intense burst, occurred as the prominence material was streaming back toward the Sun. No flare activity was evident during the period. The results of these observations were published in *Nature* (Davies, 1953) alongside observations of the same event at 100 MHz from the Kadaikanal Observatory in India (Das and Sethumadhavan, 1953).

From May 1949 to July 1950 Payne-Scott and Little carried out a systematic investigation of solar bursts using the swept-lobe interferometer. During this period they observed thirty noise storms, six of which were examined in detail. Figure 131 shows position lines from one of the storm sources shown on sunspot sketches from Mount Stromlo.

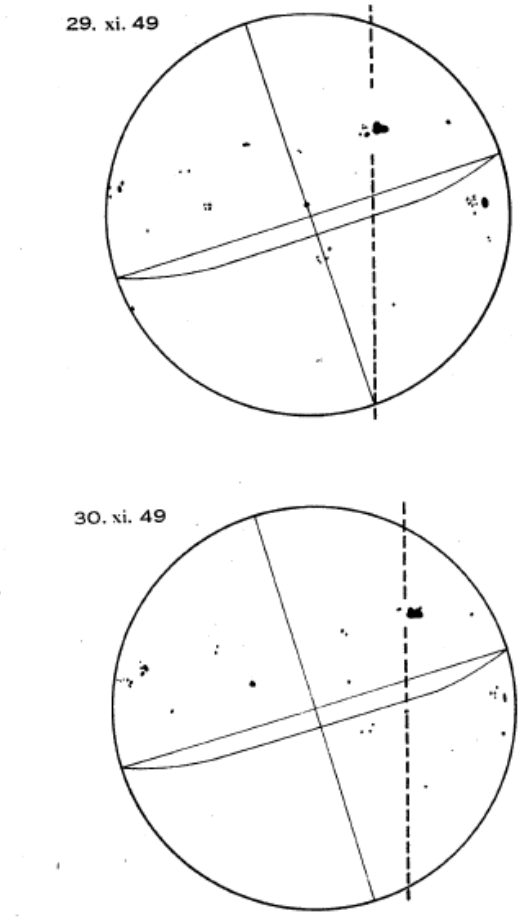

Figure 131: Storm source position lines from the swept-lobe interferometer shown on sunspot sketches from Mount Stromlo (after Payne-Scott and Little, 1951: 514).

The six noise storms showed a very strong correlation with the largest sunspots within sunspot groups. Drawing on the records of the Mount Wilson Observatory in the U.S., Payne-Scott and Little were able to show that there appeared to be a threshold of sunspot size (around 300 millionths of the solar area) of the largest sunspot in a group after which storms could occur. Figure 132 shows the scatter diagram of sunspot

group area compared to the area of the largest sunspot. This is overlaid with the observations of radio noise storms.

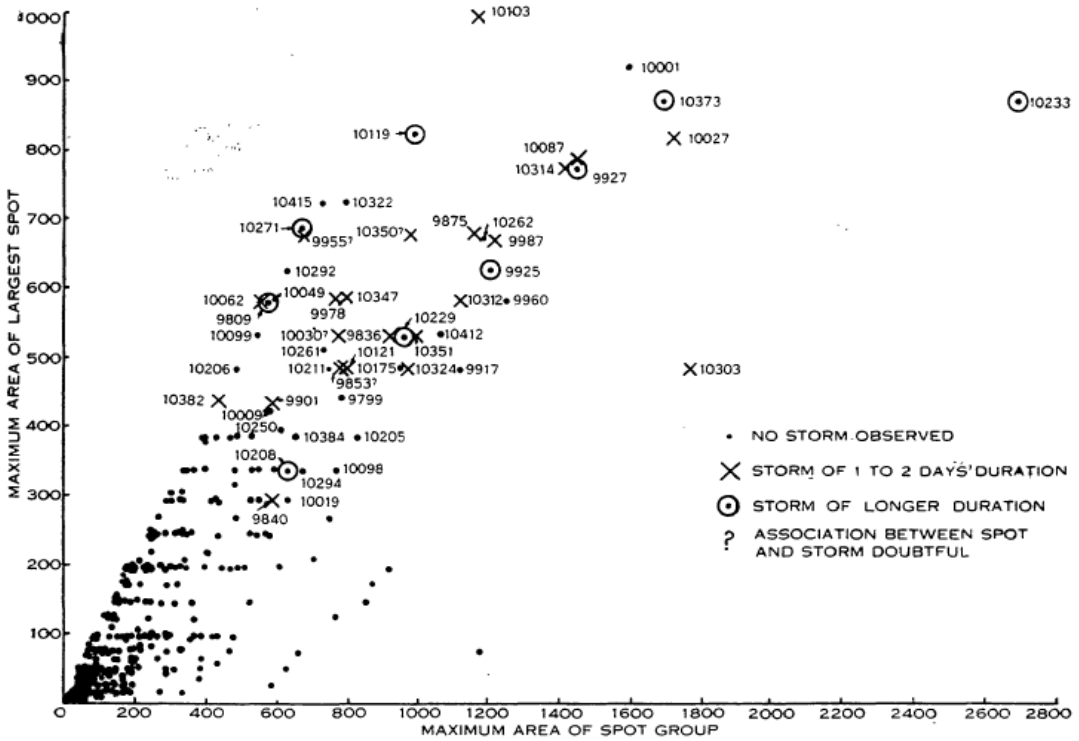

Figure 132: Scatter diagram of sunspot groups from Mount Wilson Observatory May 1949 to July 1950 overlayed with Noise Storm observations (after Payne-Scott and Little, 1951: 512).

Circular polarisation was evident in all of the noise storms and was a clear indication that magnetic fields associated with the largest sunspots were an important factor in the production of the noise storms. The observed sense of polarisation indicated a fairly simple sunspot dipole model could have been in operation, with a south seeking magnetic pole associated with right-hand polarisation and a north seeking pole with left-hand polarisation. This was, however, complicated by a predominance of right-hand polarisation in the observations.

One of the most interesting aspects of the high positional resolution observations was that it allowed for the testing of the height of the origin of the storm source in the corona. Using Smerd's model (1950b), Payne-Scott and Little constructed a model comparison of a 100 MHz source radiating above the locus of return directly above a sunspot. This model is shown in Figure 133.

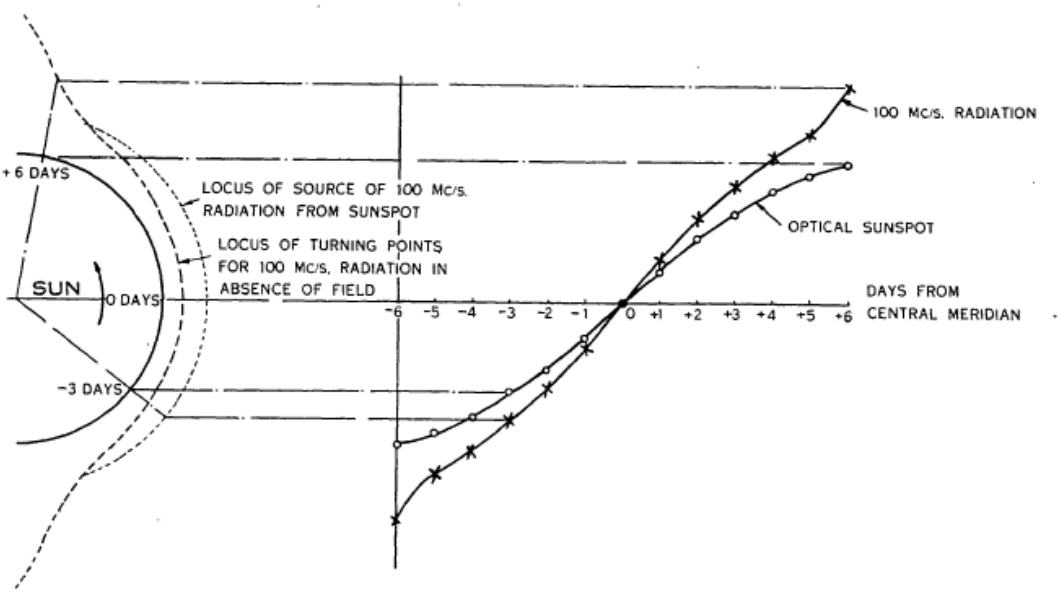

Figure 133: Model showing the relation between the apparent positions of a 100 MHz source and the associated sunspot group, assuming the source is in the corona (after Payne-Scott and Little, 1951: 522).

The model was compared to the actual observations of source positions relative to the sunspot groups and is show as part of the observational summaries in Figure 134 (lower sections of the graphs). Strong agreement was evident and this was further enhanced if a higher density of the corona was assumed. This observation and their analysis of outbursts indicated that a higher coronal density may have been present than was the assumed standard value at the time.

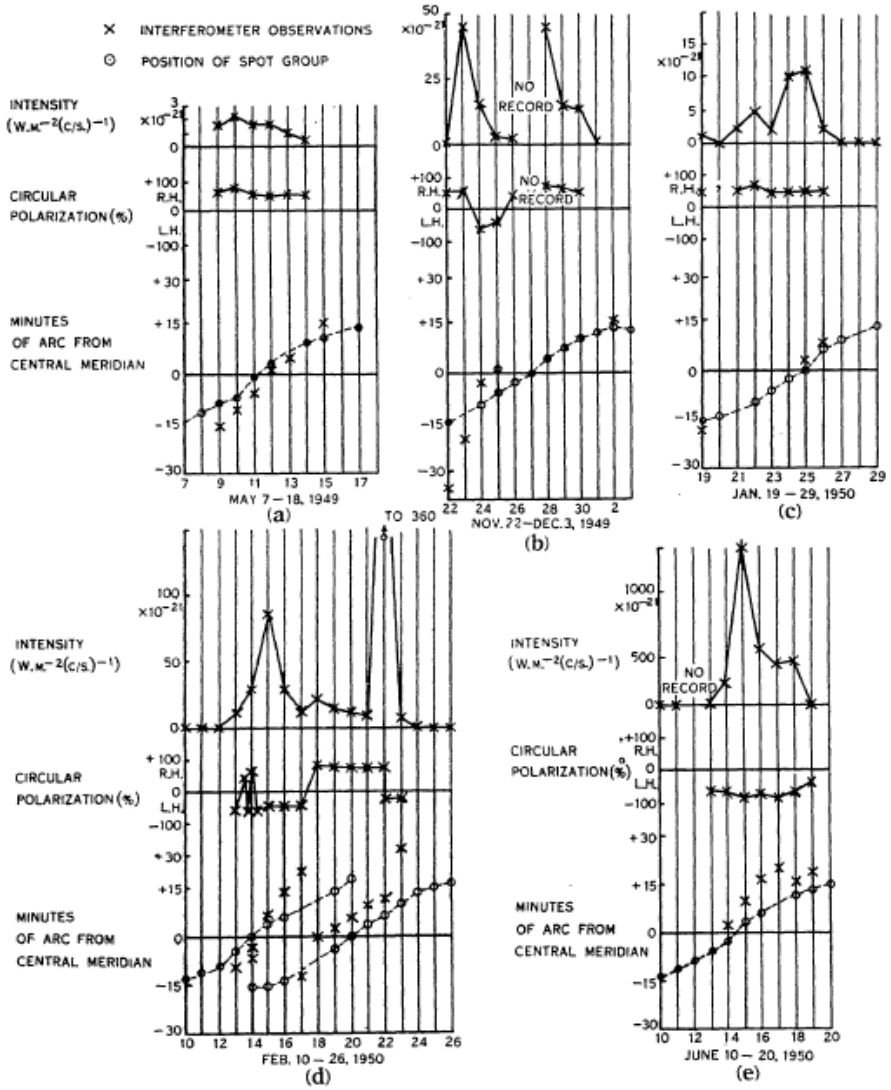

Figure 134: Observation summaries of the six noise storms observed in detail using the swept-lobe interferometer. Note graph (d) contains two storm records (after Payne-Scott and Little, 1951: 516).

These observations also ruled out theoretical models that proposed an origin of the source of radiation low in the solar atmosphere. They also provided further strong evidence for a non-thermal mechanism for the radiation.

Unfortunately further work by Payne-Scott was curtailed in a very untimely manner by her departure from the Radiophysics Division as discussed in section 10.3.10.

The final published research based on the ongoing daily solar observation program at Potts Hill was an analysis of solar radio bursts over a period of 18 months from January 1950 to June 1951 (Davies, 1954). Piddington and Davies had earlier tabulated data based on the daily records at 200, 600, 1,200, 3,000 and 9,400 MHz in an internal report. These were later extended to include the 62 and 98 MHz records. With

the exception of the 200 MHz records which came from Mount Stromlo, all of the records were based on observations made at Potts Hill. Piddington was interested in tabulating the data to support his theoretical work on the origin of the solar corona (Davies, 2005: 94).

Davies used the tabulated data to perform an analysis of some 400 bursts that were observed during the period and looked at their association with other solar events and with terrestrial magnetic crochets and radio fadeouts. The data for the magnetic crochet comparisons were drawn from the Toolangi Magnetic Observatory located near Melbourne, from the quarterly reports of the *Journal of Geophysical Research* and from the 1950 *Bulletin of International Association of Terrestrial Magnetism and Electricity*. The radio fadeout data were derived from 18 MHz measurements of galactic radiation made at the Hornsby Valley field station. It is interesting to note that these were the same records that contained the detection of Jovian radio bursts that remained unnoticed until the records were re-examined (Shain, 1956) in light of the Jupiter emission discovery in the US (Burke and Franklin, 1955). The solar flare and sunspot information were based on the *Quarterly Bulletin* of the International Astronomy Union and the *Monthly Bulletin* of the Tokyo Observatory. An example of a radio burst observation from the available records is given in Figure 135.

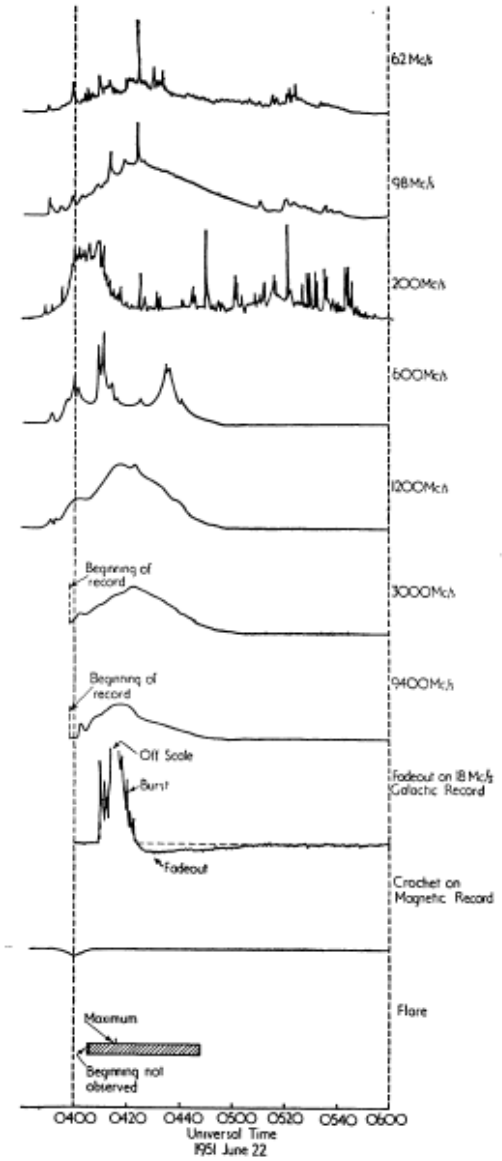

Figure 135: Example of the seven radio frequency records together with fadeout, magnetic crochet and optical solar flare records taken on 22 June 1951 (after Davies, 1954: 77).

The main aim of this analysis was to study the correlation of the radio bursts with other phenomena, therefore no attempt was made to classify burst types or examine the physical origins of the bursts. Given that the broadest definition of a burst, being any clear-cut solar radio emission rising above the daily level, was used, the analysis included all types of bursts without distinction. The broad characteristics of the bursts were described together with relationships between bursts at different frequencies. One of these features was the linear decrease in the occurrence of bursts per hour as frequency increased, as shown in Figure 136.